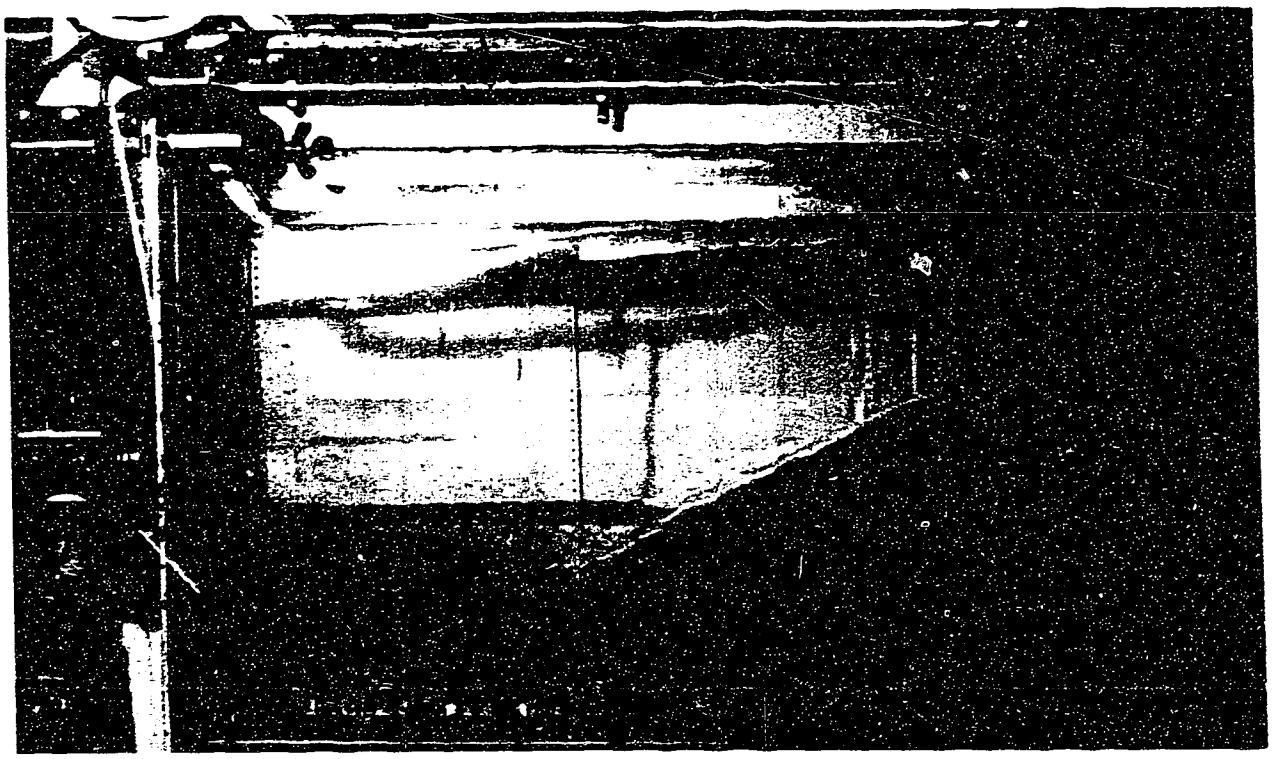

PLATE 1 SCOURED BED

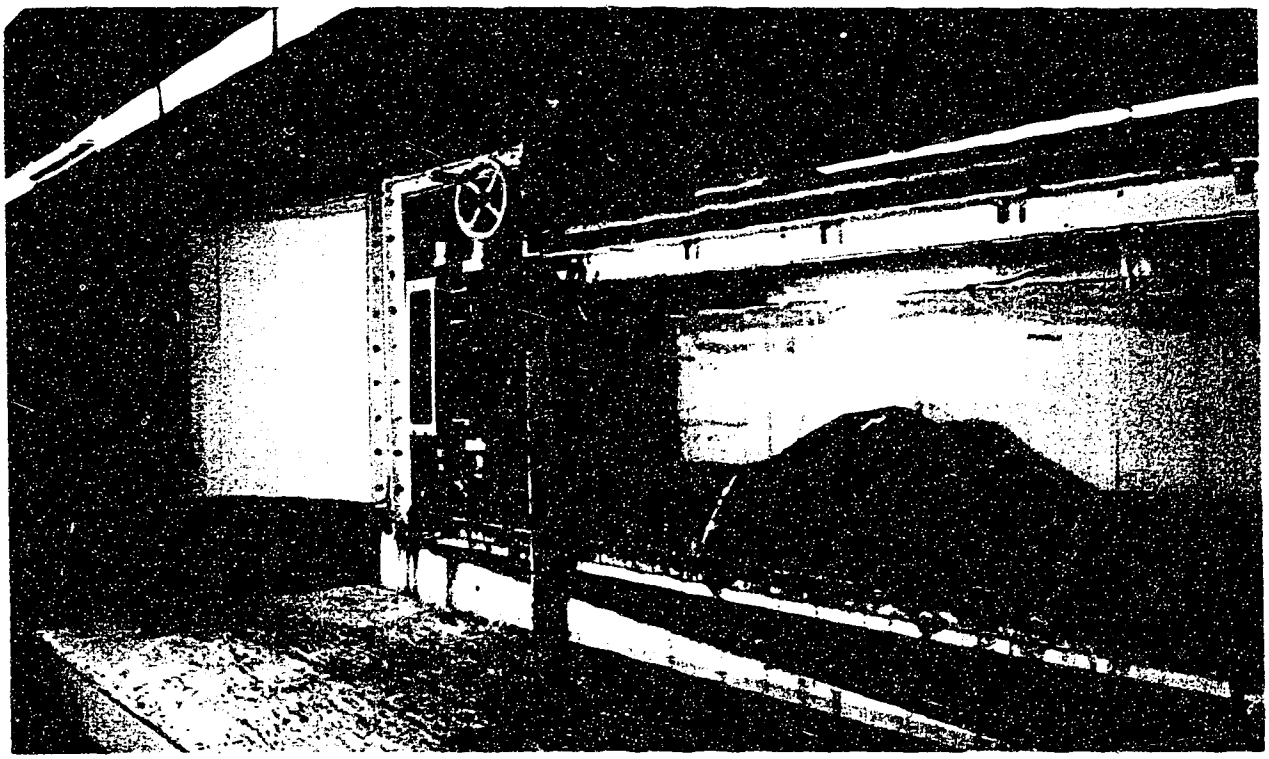

PLATE 2 TEST LOCATION

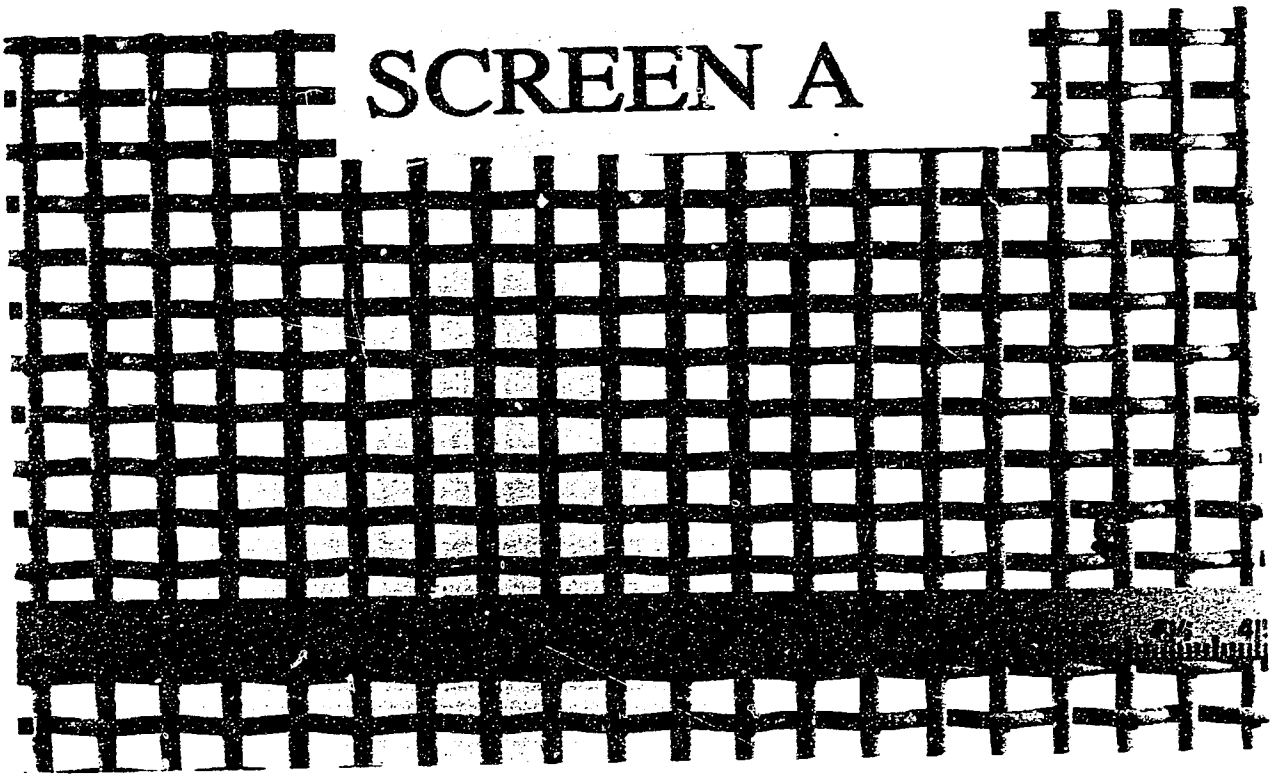

PLATE 3 SCREEN A

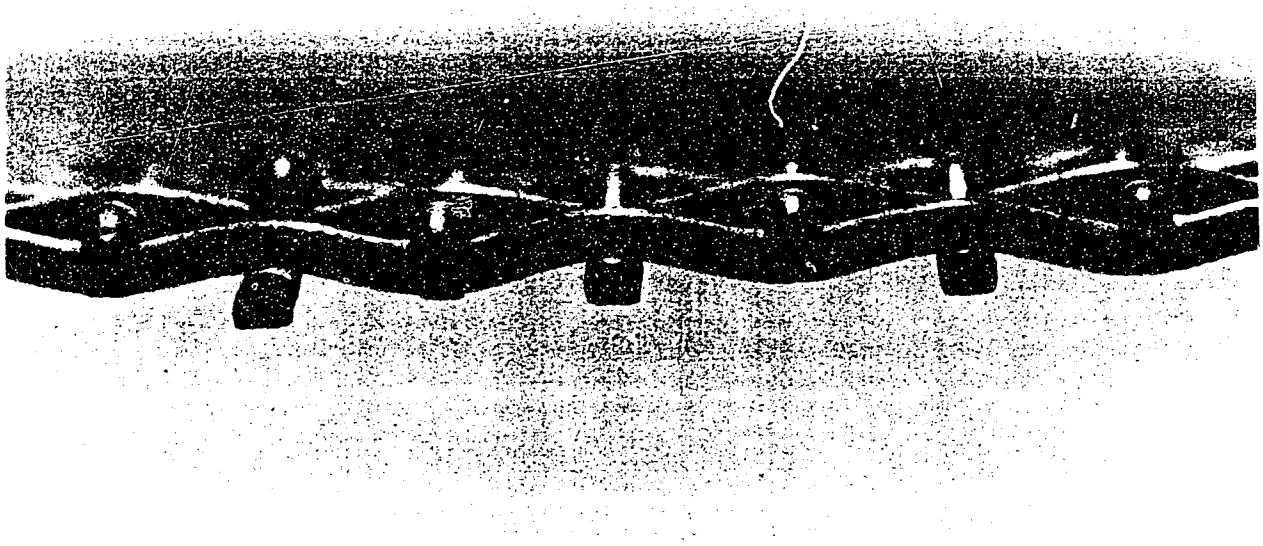

PLATE 4 SIDE VIEW OF SCREEN A

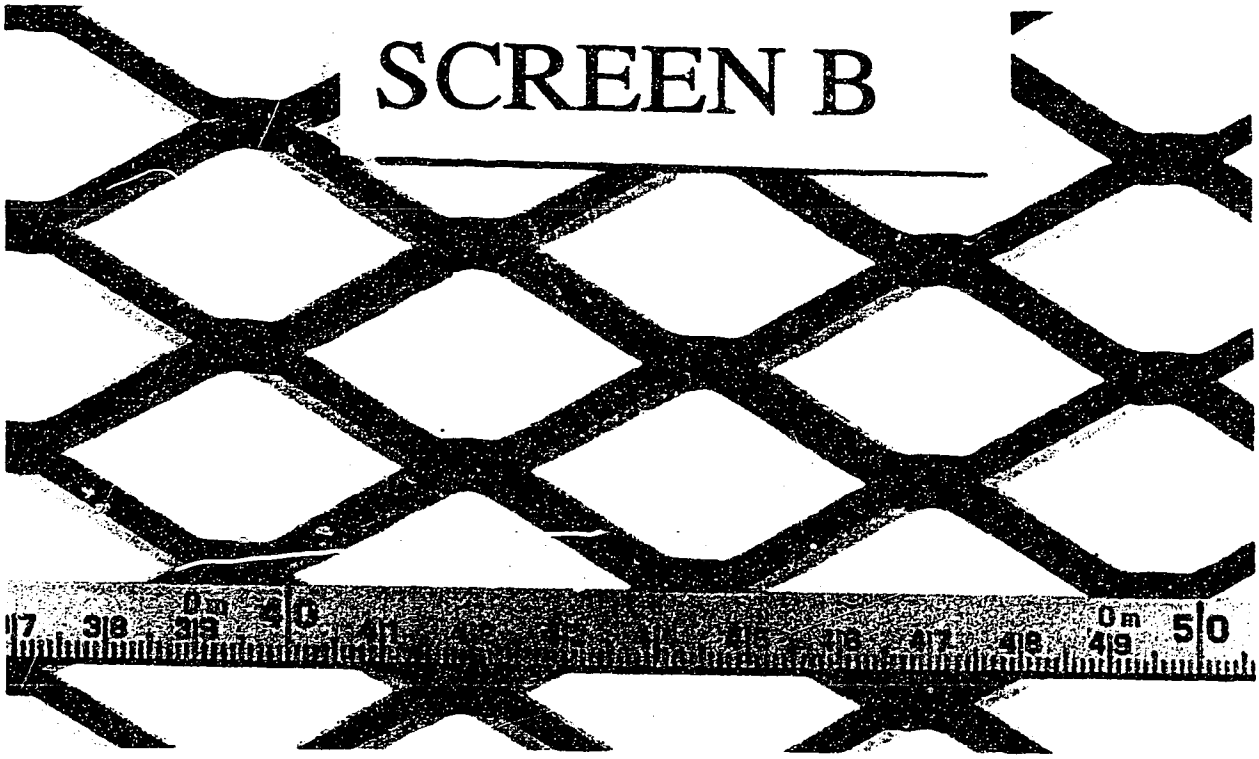

PLATE 5 SCREEN B

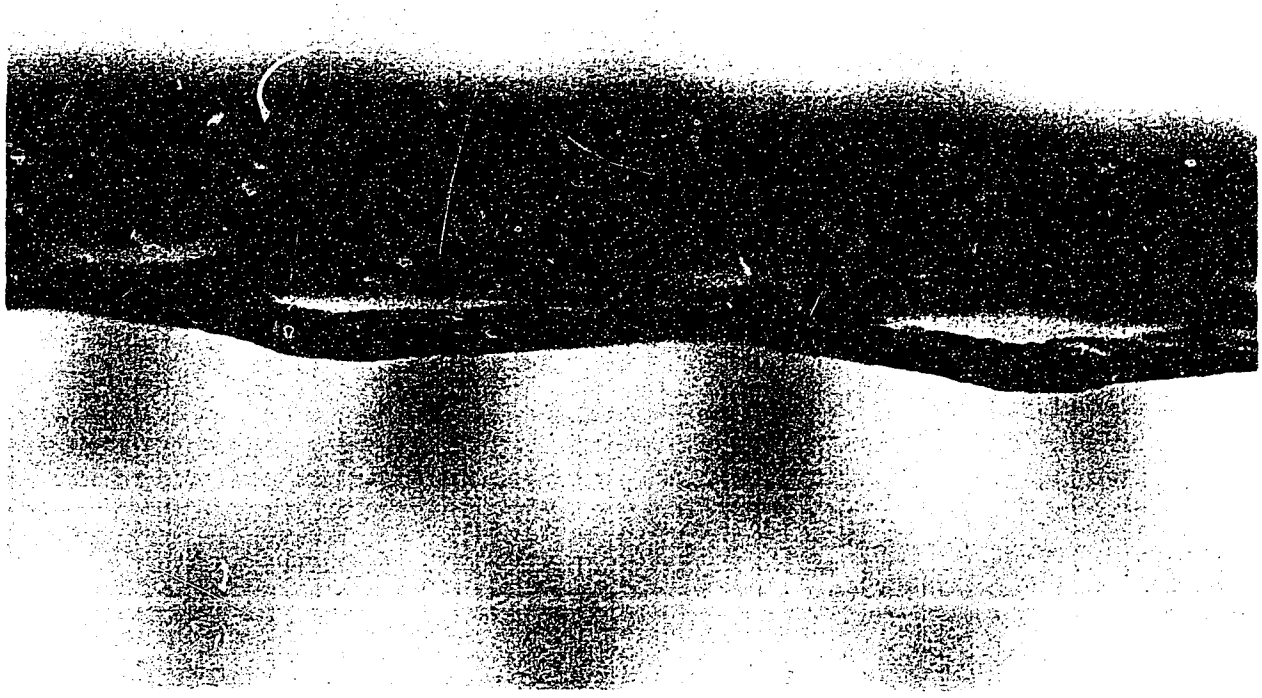

PLATE 6 SIDE VIEW OF SCREEN B

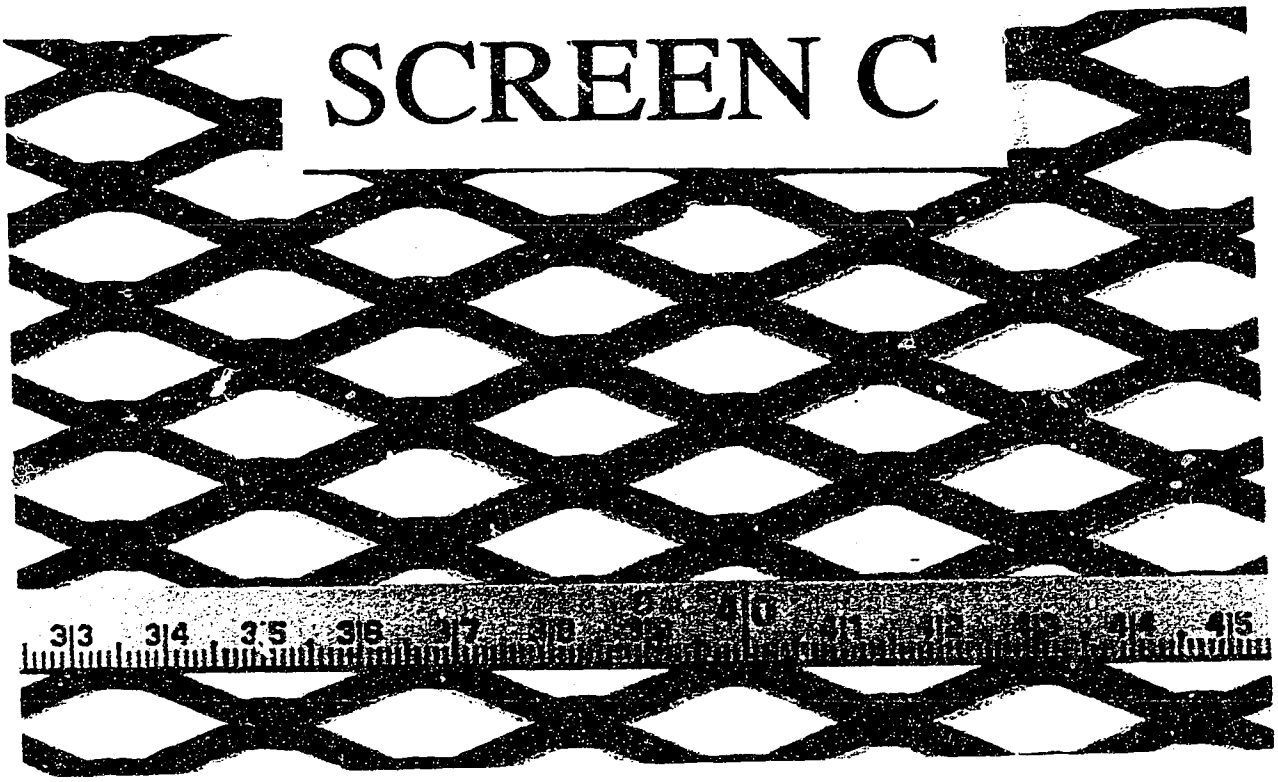

PLATE 7 SCREEN C

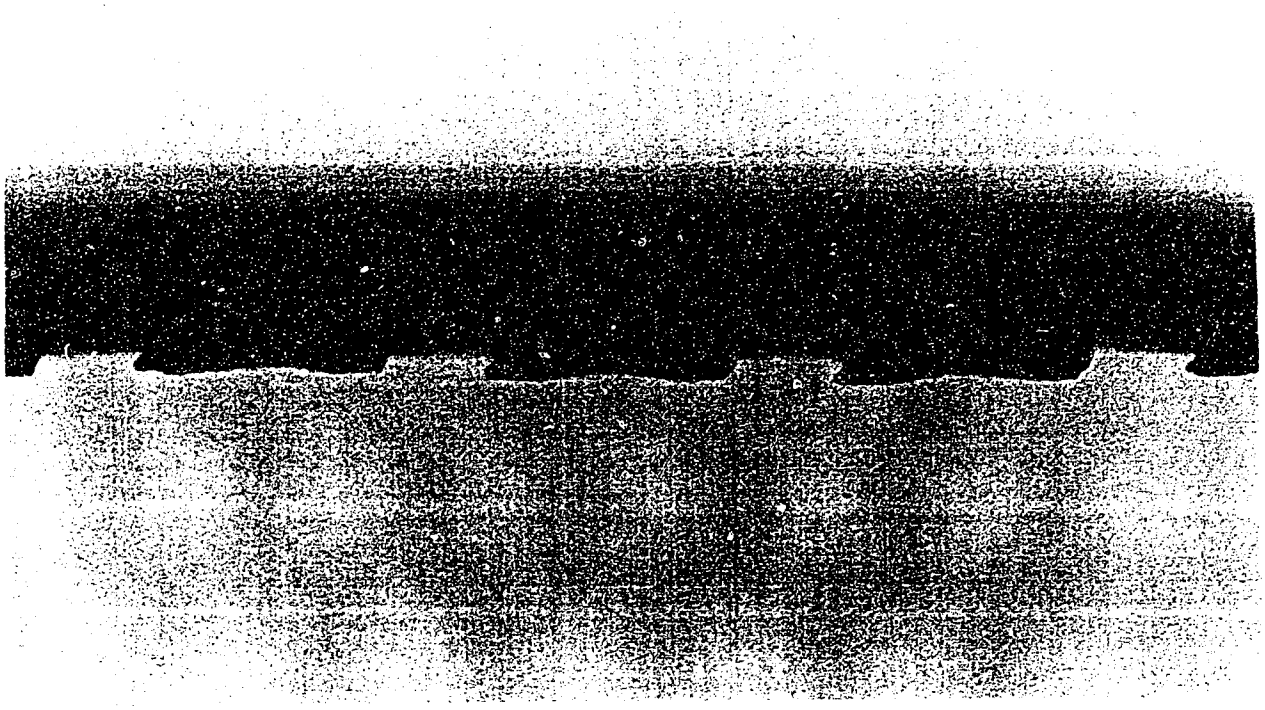

PLATE 8 SIDE VIEW OF SCREEN C (SIDE 1)

THE UNIVERSITY OF ALBERTA

FACULTY OF GRADUATE STUDIES AND RESEARCH

The undersigned certify that they have read and recommend to the Faculty of Graduate Studies and Research, for acceptance, a thesis entitled A METHOD FOR REDUCING SCOUR BELOW VERTICAL GATES submitted by OLUFEMI O. ADERIBIGBE in partial fulfillment of the requirements for the degree of MASTER OF SCIENCE

.....

Supervisor

John Shaw

F.E. Hicks

Date 26 Aug 91

ABSTRACT

A method for the reduction in scour below vertical gates is presented. In this method, a screen is placed on the erodible bed immediately downstream of the gate. The presence of the screen appears to divert the high velocities from the erodible bed, thereby reducing the amount of scour. Experiments were carried out with three sand sizes and three screens of different design, that is, nine combinations of sand and screen.

Experimental results, obtained at asymptotic state, on the characteristics of the eroded bed were analyzed using dimensional analysis of the basic variables involved. Similarity of erosion profiles was checked for each of the screens used and a comparison was made. The variations of the characteristic lengths of the eroded bed profile in terms of gate opening with densimetric particle Froude number and dimensionless screen size were investigated. Scour reduction ratios for quantifying the reductions in the characteristic lengths of the eroded bed profile were defined and evaluated and recommendations on further study and analysis are suggested.

ACKNOWLEDGEMENTS

The author would like to express his sincere gratitude to Dr. N. Rajaratnam for suggesting the topic of this study and for his guidance and encouragement throughout the work.

The technical assistance provided by S. Lovell and M. Jasek in the laboratory is sincerely and gratefully acknowledged.

My gratitude also goes to the Association of Universities and Colleges of Canada for providing me with a Postgraduate Scholarship award.

TABLE OF CONTENTS

LIST OF TABLES

LIST OF FIGURES

LIST OF PLATES

LIST OF SYMBOLS

A	Screen hole area
b_o	Gate opening
d	Size of bed material
F_o	Densimetric particle Froude number
f	Function (with suffixes)
g	Acceleration due to gravity
l	any characteristic length
l_s	length scale for screen hole
l_x	Screen hole length in the direction of flow
l_y	Screen hole length in the transverse direction of flow
NSFC	Non-Statistically fitted curve
R	Regression coefficient
SFC	Statistically fitted curve
TW	Tailwater depth
U_o	Jet exit velocity
X	Longitudinal distance from gate
X_c	Value of X at the peak of the ridge
X_e	Value of X at the end of the ridge
X_m	Value of X at maximum erosion point
X_o	Value of X at the end of scour hole
∞	Suffix to denote asymptotic state
α	Dimensionless screen hole size
ε	Depth of erosion below original bed level
ε_m	Maximum value of ε

ΔH Difference between reservoir and tail water elevation

$\Delta \varepsilon$ Height of ridge

$\Delta \rho$ Difference between mass densities of bed material and flow

ϕ Parameter representing screen design

η_1 Maximum scour reduction ratio

η_2 Reduction ratio for maximum scour location

η_3 Ridge height reduction ratio

η_4 Reduction ratio for ridge location

ν Coefficient of kinematic viscosity of fluid

ρ Mass density of fluid

1. INTRODUCTION AND LITERATURE REVIEW

1.1 Introduction

In hydraulic engineering, the safe design of many hydraulic structures depends on the prediction and control of erosion. Some examples of erosion problems are erosion downstream of a spillway, erosion below vertical gates and erosion around bridge piers. The study of erosion has therefore received much attention during the past couple of decades. Erosion, which can be simply defined as the detachment and removal of rock particles from their environment, can refer to soil erosion, beach erosion or erosion of a river bank. The term scour is used for a localized erosion process and this applies to this study.

Most of the studies on scour have been carried out using noncohesive sediments. Erosion of cohesive sediments is more difficult to study because the breaking of the chemical bonds between particles is not very well understood and flow quickly becomes opaque due to the suspended colloidal material which makes observations difficult. The study of local scour involves sediment transport and a complex flow pattern which may have vortices or jets. These make the physics of the problem complex and an empirical approach has to be used at present to make any progress.

Erosion of noncohesive sediments by plane turbulent submerged wall jets is one problem that has been studied extensively. Chatterjee and Ghosh (1980), Rajaratnam (1981), Farhoudi and Smith (1985) and Narayanan and Hassan (1985) are some of the recent investigators. This study takes a step further and attempts to look at the effect of protecting the bed from scouring by covering it with a screen and also looks at the characteristic features of the scoured bed in the asymptotic state.

One way of preventing scouring is to build an apron. This can be expensive and the effects of uplift pressures must be checked if the flow involves a hydraulic jump. Installing a protective screen may still permit some scouring, however this method is cheap, easy to install and maintain and there will be no uplift pressure.

The effects of protective screens on loose beds subjected to plane turbulent submerged wall jets were investigated by the following procedure. Three screens of different opening shapes and sizes and three different sizes of sand were used for the experiments. These produced nine combinations of sand and screen. Experiments were carried out for each combination and the results were analyzed to obtain characteristics features of the scoured bed. Dimensional analysis was used to obtain dimensionless parameters and some plots were made. The results were then compared to a previous

study by Rajaratnam (1981) on erosion by plane turbulent submerged wall jets without a protective screen.

1.2 Literature Review

The study of erosion by plane wall turbulent jets has been approached in two ways. Some investigators have concentrated more on the flow patterns and the bed shear stress distributions, others on the characteristic features of the scoured bed. Results from these two approaches have helped in understanding this problem better and serve as a prerequisite to further study.

The pioneering investigation was by Rouse (1940) who studied the scour of a bed of noncohesive sediment by a vertical jet. Other early investigators such as Doddiah, D., Albertson, M., and Thomas, R. (1953) investigated scour by solid and hollow vertical jets. Laursen (1952) and Tarapore (1956) studied scour by horizontal jets. Some of the recent investigators have been mentioned earlier and no published work on screen protection for jet caused scour was found. A review of some of the recent investigations is presented next and classified according to the approach to the problem.

1.2.1 Flow Characteristic Approach

i) Chatterjee and Ghosh (1980)

An experimental investigation on a submerged horizontal jet flowing over a partly rigid apron to an erodible bed was

carried out to obtain empirical relationships describing the velocity distribution within the boundary layer at the location of maximum scour and also the boundary layer growth with distance. An expression for the relationship of shear stress at the location of maximum scour with time was also developed. Using Karman's integral equation, an expression for critical shear stress at the asymptotic state was found and this compared well with that of the conventional Shield's criteria when a gravel bed was used but poorly when a sand bed was used.

ii) Narayanan and Hassan (1985)

This study was on local scour downstream of an apron. Mean velocity profiles in rigid models simulating the shape of the scour hole were measured. These were found to be similar above the line of maximum velocity but not below. An expression describing the decay of the maximum velocity in the scour hole was developed and a semi-empirical theory was presented based on measured velocity profiles.

iii) Ali and Lim (1986)

Experimental results were presented for localized scour caused by two and three dimensional turbulent wall jets, in mostly shallow tail water depths. Correlations were developed for the maximum depth and volume of scour holes. Center line bed profiles were found to be similar for all jet sizes, tail water depths and scouring times. They also found that the

velocity profiles in the boundary layer for the section up to that of maximum scour were similar irrespective of the period of scouring action. Reasonable agreement was also obtained between measured and calculated velocities obtained from Rossinskii's analytical method.

1.2.2 Bed Characteristic Approach

i) Rajaratnam (1981)

Rajaratnam (1981) presented the results of an experimental study on erosion caused by submerged plane wall jets of air and water on beds of sand and polystyrene. It was noted that the maximum depth of scour or any other significant length scale of the erosion process has a linear relationship with the logarithm of time measured from the start of the erosion process. The characteristic lengths were found to eventually reach an asymptotic state. The asymptotic erosion profiles were found to be similar and the characteristic lengths mainly functions of densimetric particle Froude number.

ii) Rajaratnam and Macdougall (1981)

Here the jet was unsubmerged and the tail water was approximately equal to the jet thickness. It was discovered that there was no formation of a ridge after the scour hole. The material removed from the scour hole was transported by the flow out of the test section of the flume into the sand trap. The asymptotic erosion profiles were also found to be

similar and the characteristic lengths mainly functions of densimetric particle Froude number.

iii) Farhoudi and Smith (1985)

Farhoudi and Smith (1985) studied the development of local scour holes downstream of a hydraulic jump using three geometrically similar models. A correlation was found to exist among the characteristic length parameters of the scour hole that made it possible to use one of these parameters to describe the scour hole geometry. An equation to predict the volume of sediment removed from the scour hole at any time given the maximum depth of scour was derived.

iv) Uyumaz (1987)

Uyumaz (1987) investigated scour created in noncohesive soils when water flows simultaneously over and under the gate. From the experimental data, it was found that the final depth of scour is smaller when compared to the cases of flow only under or over the gate for the same discharge. An empirical equation for the final depth of scour was derived.

v) Johnston (1989)

The development of a scour hole by a plane jet entering shallow tail water conditions was studied. It was found, unlike in the deeply submerged case, that an asymptotic state might not be reached. Three different scour hole regimes were defined. For the first and the second regimes, it was

observed that the jet was permanently attached to the bed and the free surface respectively while for the third, the jet was periodically oscillating between the bed and the free surface boundary. The bed jet and the surface jet regimes occurred for deeply and shallowly submerged jets respectively.

2. EXPERIMENTAL INVESTIGATION

2.1 Apparatus

The experimental study was performed using a recirculating rectangular flume. It is 0.31m wide, 0.65m deep and 5.5m long. Water was pumped from the sump and discharged through a butterfly valve into a reservoir. Short circular pipes and a foam were placed in a short channel connecting the reservoir to the flume to reduce secondary currents. Water entered the flume under a gate provided with a curved guiding vane to produce a uniform jet. The gate opening was 22.8mm and was the same for all the experimental runs. The flume contained a sand bed that was 0.31m wide, 0.16m deep and 0.68m long immediately downstream of the gate. It was covered with a screen that was flush with the bed level of the incoming jet and a sand trap was built after the sand bed. The tail water depth was adjusted by a gate at the end of the flume. The scoured bed profile was measured using a staff gauge with a vernier reading to the nearest one hundredth of a centimeter. Figure 1a shows the sectional view of the experimental arrangement. The scoured bed and the test location can be seen in Plates 1 and 2 respectively.

Three different sizes of almost uniform sand were used. The sieve analysis results are shown in Figure 2. The sands

were named Sand 1, Sand 2 and Sand 3 and their median sizes (d_{50}) in millimeters are 1.29, 2.26 and 2.42 respectively. The mean sizes in millimeters were calculated and respectively are 1.29, 2.27 and 2.45. These are very close to the median sizes.

Three screens of different design were used and designated as Screen A, Screen B and Screen C. The screen design is comprised of: the shape of the screen hole; the void ratio, which is defined as the screen hole area per unit screen area; the cross section of the metal strip forming the screen; and lastly, its formation, which could be flat or woven. Screens B and C are flat and have diamond shaped holes whereas Screen A is woven and has square holes. The cross section of the metal strip forming the screen for Screen A is circular, for Screen B, it is fairly rectangular and for Screen C, it is a five sided irregular polygon (see Figure 1b). The length of the hole in the direction of flow is refereed to as l_x and in the transverse direction as l_y. The possible length scales for the screens are given in Table 1. The screens can be seen in Plates 3 to 8 in Appendix B.

2.2 Experimental Procedure

2.2.1 General

First, the sand bed was made as horizontal as possible using the staff gauge with a vernier and then it was covered with a screen. The pump was then turned on and the butterfly

valve outside the reservoir was opened slightly to allow water to trickle into the flume. When the flume was full and water started to flow over the tail water gate into the sump, the butterfly valve was then opened to the desired point. The jet was checked for deep submergence, by making sure that the water surface level downstream of the gate was essentially horizontal. The pump was then shut off when the scoured bed reached an asymptotic state and the water in the flume was allowed to drain off. Three longitudinal bed profiles were taken, one at the center line of the flume and the other two at 80mm left and 80mm right of this line. The average of these profiles was taken as the scoured bed profile. The exit jet velocity was calculated by the expression,

$$U_o = \sqrt{2g\Delta H} \qquad (1)$$

where U_o = exit jet velocity

g = acceleration due to gravity

ΔH = difference between reservoir and tail water elevation.

This equation, which has been found to work well for this flume, was derived from energy equation assuming negligible velocity head in the reservoir and losses

2.2.2 Preliminary Runs

A few preliminary runs were carried out to determine an

estimate of the time required for the scoured bed to reach an asymptotic state. It was found that within the range of exit jet velocity expected for the test runs, an average of ten hours would be required to bring the scoured bed to an asymptotic state. The criteria adopted were to make sure that the maximum depth of scour did not increase nor change position for the last hour.

The effect of the screen was tested by carrying out two experiments with the same conditions but one was with a screen. Sand 1 and Screen A were used. The exit jet velocity was 1.89m/s, tail water depth was 0.31m and experimental time was four hours. The results showed a big difference between the maximum scoured depths as can be seen in Figure 3.

The other set of preliminary experiments was to find out if the two sides of each of the screens would produce the same scour profile when facing upwards. The same scour profile was produced by the two sides of Screen A and Screen B, but not for Screen C. Figure 4 shows the results for the two sides (Sides 1 and 2) of Screen C under the same conditions. The cross sections of the metal strip forming this screen for the two sides are shown in Figure 1b. Side 2 was chosen for the experiments since the scour profile produced by it looks similar to those of Screens A and B, however, Side 1 would be better for practical application.

2.2.3 Test Runs

Nine combinations of sand and screen were experimented on. For each combination, the water discharge was varied and the gate opening was unaltered for all the combinations. This resulted in a total of ninety-five experimental runs and their full details are given in Appendix A. The dimensionless tail water depth, which can be defined as the ratio of tail water depth to gate opening (TW/b_o), ranged from 14.61 to 16.71 and the exit jet velocity (U_o) ranged from 0.66m/s to 2.19m/s. Most experiments were run for a period more than 10 hours. Three or four characters were used for easy identification of each experiment. For example, experiment 2A10 stands for the tenth experiment using the combination of Sand 2 and Screen A, that is, combination 2A.

2.3 Observations

Physical observation of the erosion process is time consuming, unable to provide complete description of the complex processes taking place, but it is a good way of understanding the phenomenon better. At the beginning of the experiment, the jet comes out under the gate and for a very short time, before any significant erosion, the jet behaves like a classical wall jet. The shear stress distribution on the erodible bed can be approximated to be equal to that of the classical wall jet. The bed shear stress is inversely proportional to the distance from the gate and this is the reason for having a higher erosion rate closer to the gate.

The first few eroded particles come from the surface layer of the bed and are transported as bed load far downstream. A scour hole starts to develop close to the gate after a while and the sediments from this form a ridge downstream but not as far as the resting place of the first few eroded particles. The classical wall jet theory is no longer useful at this stage. The erosion process continues with the eroded particles from the scour hole being transported on the uphill slope of the ridge. When they reach the peak of the ridge, most of them roll down the downhill slope and some are sent flying into the flow and finally settle on the downhill slope or further downstream. The growth rates of the scour hole and ridge appear to vary inversely with time. After many hours, an asymptotic state is reached when the scoured bed experiences no significant bed movement and bed shear stresses then have their critical values. It was difficult to obtain an asymptotic state in some experiments with high velocity jets. A continuous cyclic process was responsible for this. It starts with a gradual transport of sediments out of the scour hole. When the sediments get to a level about the original bed layer, there is great difficulty in transporting them along the uphill slope of the ridge. After a while, they are suddenly thrown into suspension and get caught in the backward flow towards the gate. The flow becomes heavy with suspended sediment and most of them settle on the downward slope of the scour hole. The cycle then repeats itself.

It is known at this point that the screen in some way reduces the magnitude of the flow velocity at the bed resulting in a lower erosion rate and hence a smaller scour hole. The complete physics of the velocity reduction by the screen is however yet to be fully understood. It was noticed that the bigger the screen holes, the less effective the screen is.

In most of the experiments, the scour holes were well formed and the ridges were mostly asymmetrical and flattened. The asymmetrical shape was due to secondary currents which were difficult to eliminate and high velocity jets were responsible for their flatness. When a high velocity jet is used, the ridge could grow high as a result of significant scour and become much less submerged. A time comes when the flow over it produces enough shear stress to flatten its peak. The ridge can not grow any further and a limiting growth point is reached. Few ridges were well formed and these occurred when the screen with the biggest hole, Screen B, was used. Secondary currents were weak in these cases because low discharges were needed to cause significant erosion. Remarks were given to all the scoured bed profiles and these can be checked in Appendix A. *G* was used for Good, *P* for Poor, *F* for Fair, *S* for Scour and *R* for Ridge. For example, a scoured bed profile with a *GSPR* remark means Good Scour Poor Ridge.

Table 1

Length Scales for Screens' Holes

Screen	lx (mm)	ly (mm)	Area, A (mm^2)	√A (mm)	Void Ratio, %	ly/lx Ratio
A	5.1	5.1	26.01	5.1	48	1
B	21	40	493.5	22.2	72.9	1.9
C	8.1	23.1	113.5	10.7	55.4	2.85

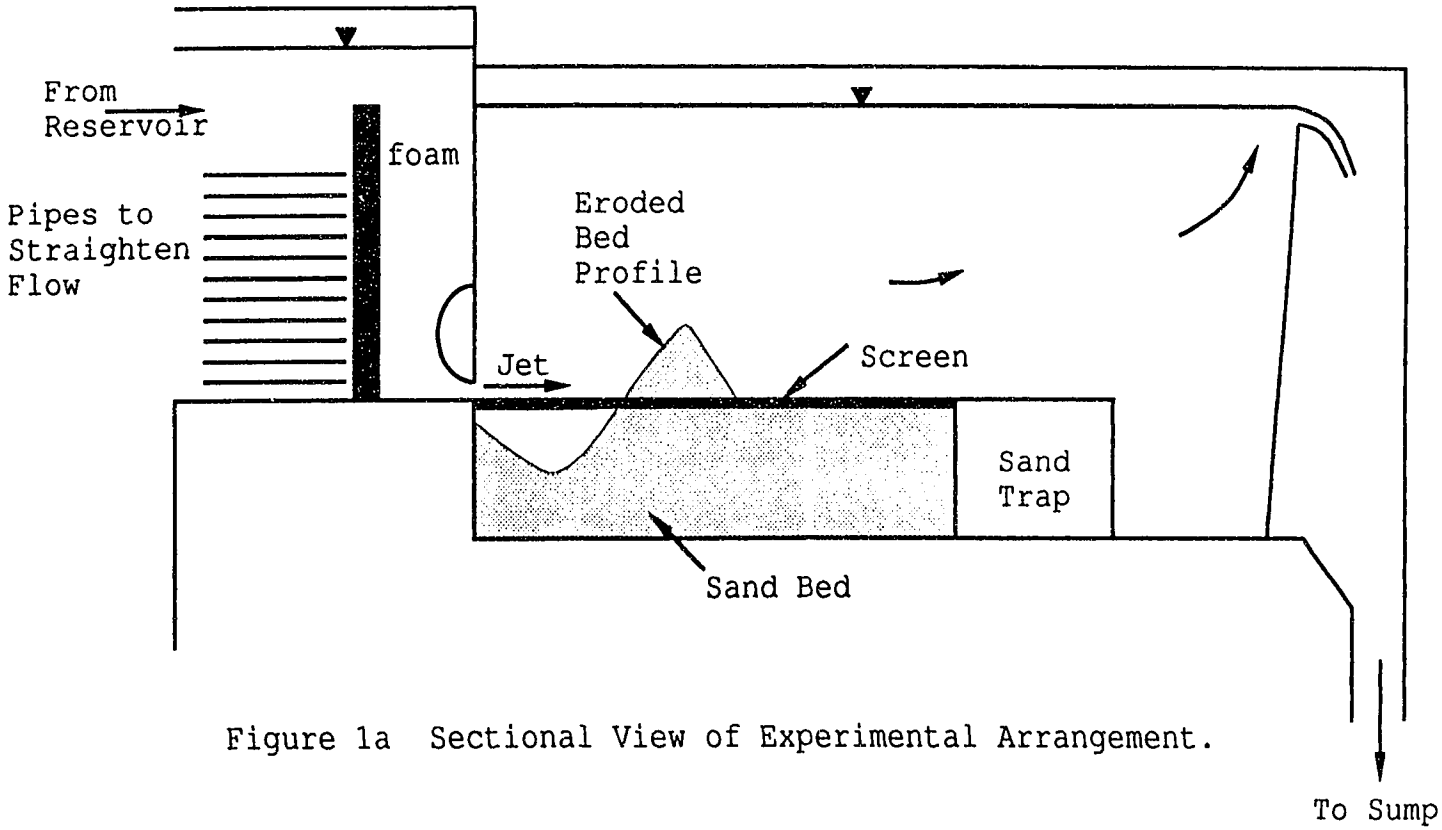

Figure 1a Sectional View of Experimental Arrangement.

Figure 1b Cross Sectional View of the Metal Strip forming the Screen

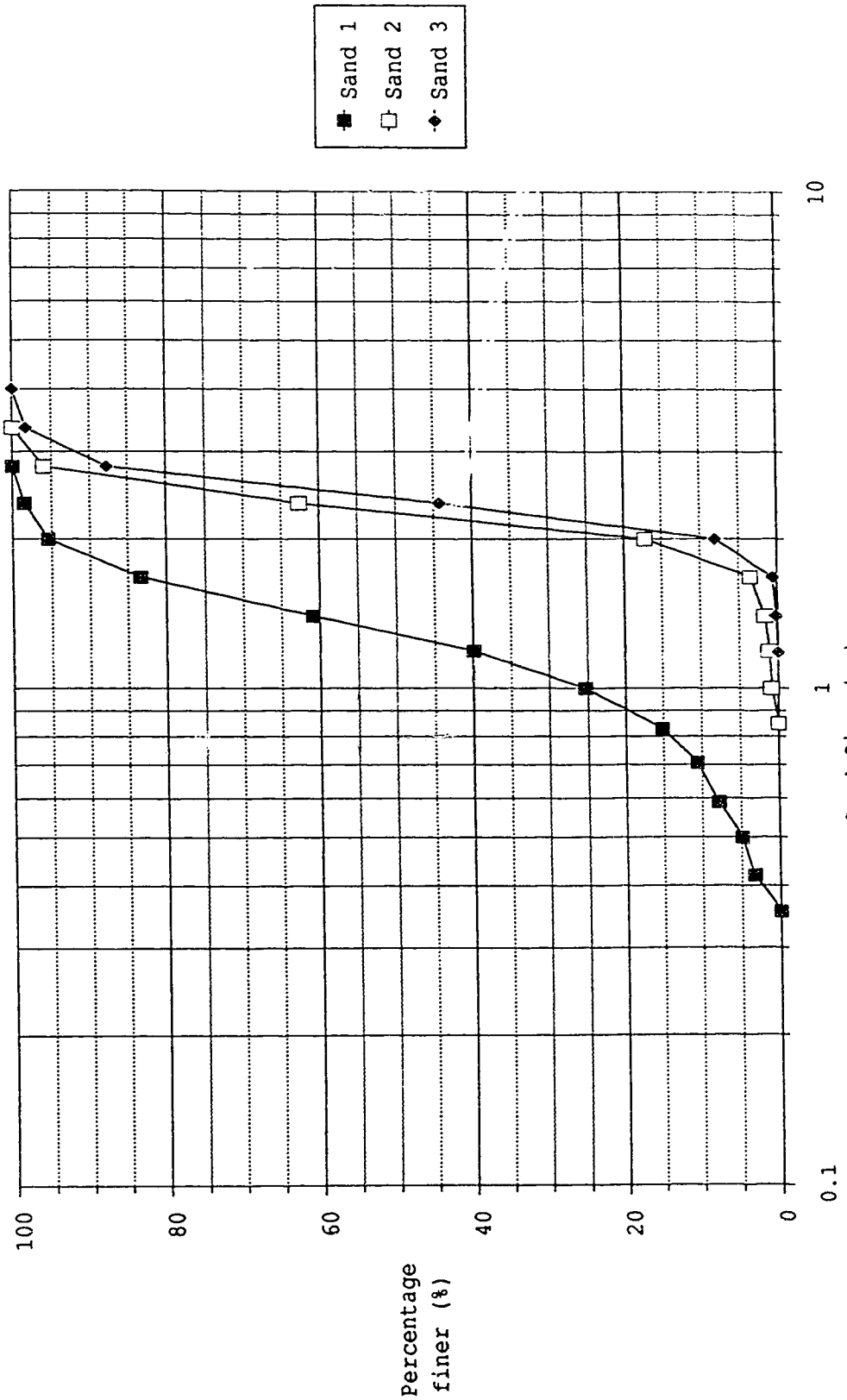

Figure 2 Sieve Analysis Plot

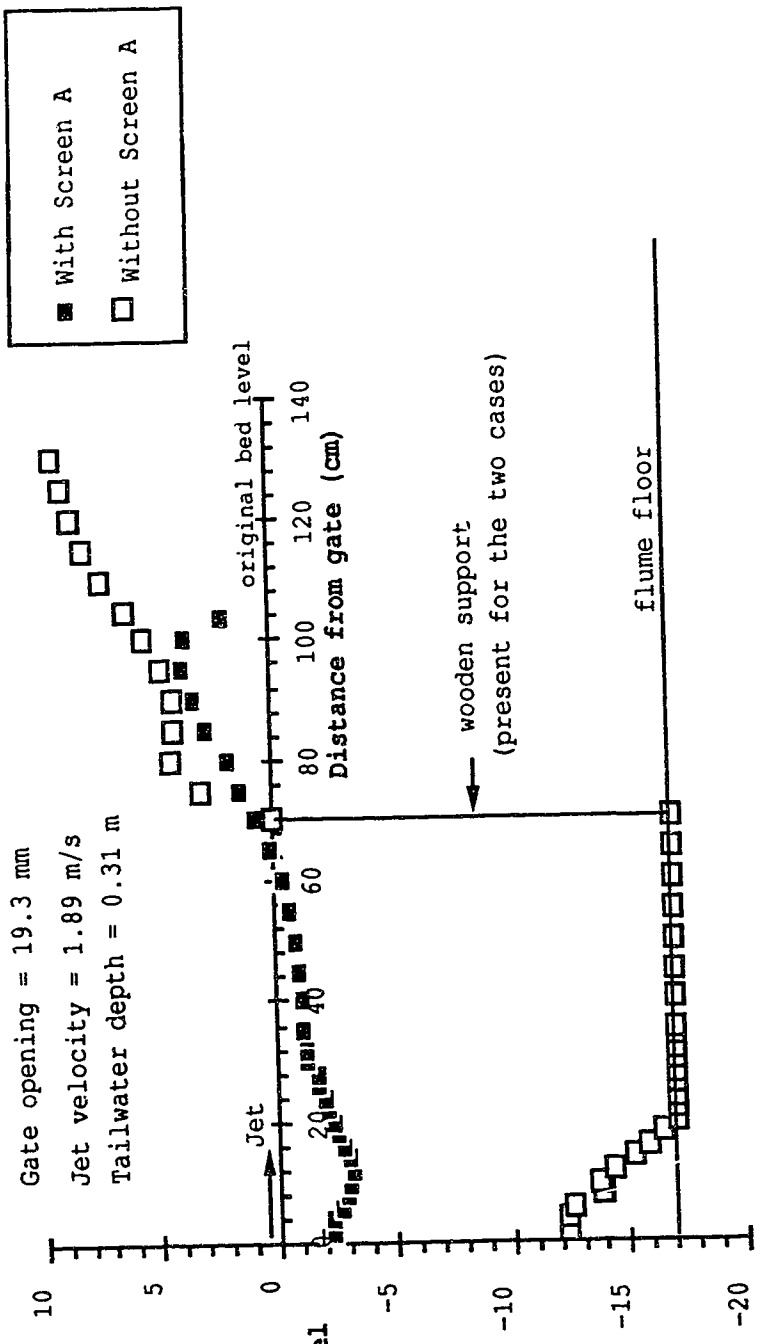

Figure 3 Eroded Bed Profile with and without Screen

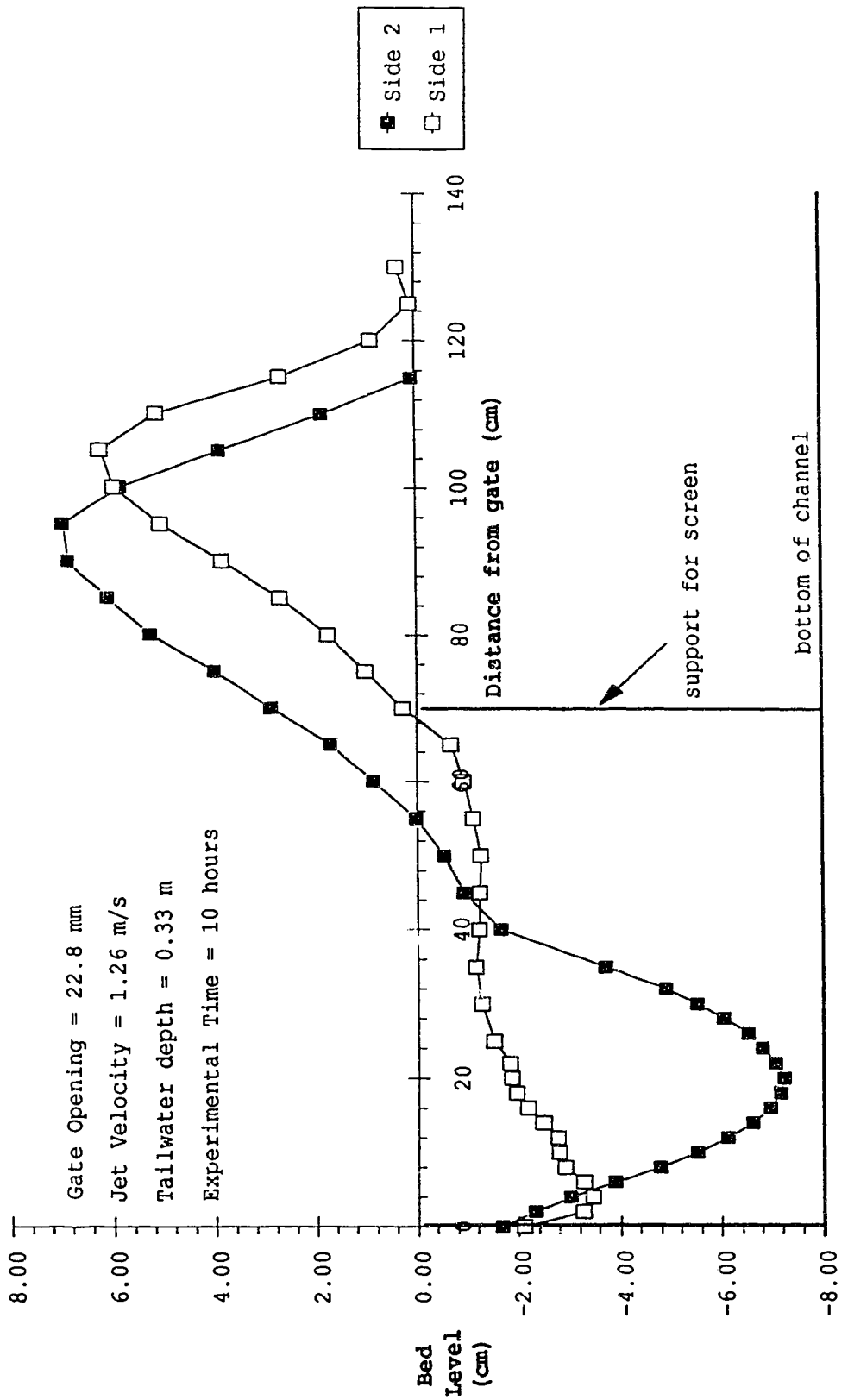

Figure 4 Effect of the Two Sides of Screen C on Scour Depth

3. ANALYSIS AND DISCUSSION OF RESULTS.

3.1 Dimensional Analysis

Dimensional analysis is a useful tool for combining the various parameters involved in this complex problem into a dimensionless form. These parameters have to define the flow, the erodible bed and the screen. In the asymptotic state, the scoured bed profile can be defined by some characteristic lengths such as the maximum depth of erosion $\varepsilon_{m\infty}$, its location from the gate $x_{m\infty}$, ridge height $\Delta\varepsilon_{\infty}$ and its location $x_{C\infty}$. Figure 5 shows an eroded bed profile.

Any of these characteristic lengths, represented by l_{∞}, can be expressed as a function of the following parameters, provided the jet is deeply submerged.

$$l_{\infty} = f_1 \left(\vartheta , \rho , g\Delta\rho , U_o , b_o , d , l_s , \phi \right) \qquad (2)$$

where l_{∞} = any asymptotic characteristic length

υ = kinematic viscosity

ρ = density of fluid

$\Delta\rho$ = difference between mass densities of bed material and fluid

b_o = gate opening

d = size of bed material

l_s = length scale for screen hole

ϕ = parameter representing screen design

Equation (2) can be rewritten using the Pi-Theorem in terms of six dimensionless combinations.

$$\frac{l_\infty}{b_o} = f_2 \left(\frac{U_o}{\sqrt{g\frac{\Delta\rho}{\rho}d}}, \frac{U_o b_o}{\vartheta}, \frac{b_o}{d}, \frac{l_s}{d}, \phi \right) \tag{3}$$

It has been shown that the effect of viscosity on the growth of jets is small if the jet Reynolds number, $U_o b_o/\upsilon$, is greater than a few thousand (Rajaratnam 1976). Reynolds number is therefore not important in this study and this approximation can only be erroneous if applied to a thin layer close to the bed. The term b_o/d can only be important when it is very small (Rajaratnam 1981). The b_o/d values used in this study are 9.42, 10.09 and 17.67 and it has been considered safe to neglect this term.

Equation (3) is therefore reduced to

$$\frac{l_\infty}{b_o} = f_3 \left(F_o = \frac{U_o}{\sqrt{g\frac{\Delta\rho}{\rho}d}}, \alpha = \frac{l_s}{d}, \phi \right) \tag{4}$$

where F_o = densimetric particle Froude number

α = dimensionless screen size

Possible values of α for all combinations of sand and screen are given in Table 2. Some relationships between the dimensionless terms have been studied and presented in this chapter. Evaluating the value for ϕ will be quite demanding and this has not been attempted in this study.

3.2. Similarity of erosion profiles

The erosion profiles were tested for similarity using X_o and $\varepsilon_{m\infty}$ as the horizontal and vertical length scale respectively. Some of the erosion profiles were made dimensionless and categorized according to the screen used. Figures 6,7 and 8 show the dimensionless scoured bed profiles obtained using Screen A, Screen B and Screen C respectively.

From Screen A's results, it can be noticed that there is some scatter and a non-statistically fitted line has been drawn to estimate the best fit. A close look at the scour hole region shows that profiles of low densimetric particle Froude number tend to lag and vice versa. In the ridge region, there is more scatter and profiles of low densimetric particle Froude number tend to lead and vice versa when the uphill slope section is considered. This can not be said of the downhill slope section and this may be due to the asymmetrical ridges formed. The ratio of $(\Delta\varepsilon/\varepsilon_m)_\infty$ was found to be 0.95 and $(X_e/X_o)_\infty$ to be 2.35. Results from Screen B are presented in Figure 7 and the dimensionless profiles fit very well with little scatter. The densimetric particle Froude

number is therefore not a factor in this case. The ratio of $(\Delta\varepsilon/\varepsilon_m)_\infty$ is 1.13 and $(X_e/X_o)_\infty$ is 2.2. Screen C's results are presented in Figure 8 and the same comments from Screen A's results are applicable here. The fitted curve for the dimensionless profile is however different. The ratio of $(\Delta\varepsilon/\varepsilon_m)_\infty$ is 1.03 and $(X_e/X_o)_\infty$ is 2.15. Figure 9 shows the comparison of the fitted curves obtained with the three screens. The scour hole profile from Screen B fits fairly well with the sine curve. The profiles are different from each other and this suggests that the profile is dependent on the screen used. The profiles from Screen A and Screen C are slightly dependent on F_o whereas this is not the case for Screen B. It is evident that the screen is a much more important factor in determining the profile than the densimetric particle Froude number. The average ratio of $(\Delta\varepsilon/\varepsilon_m)_\infty$ is 1.01 for most experiments and $(X_e/X_o)_\infty$ is approximately 2.2.

Similarity of the profiles was further tested by checking the dependance of $(X_c/X_m)_\infty$ on F_o. Figure 10 shows the results for the three screens. It can be seen that the results from Screen B are within a narrow $(X_c/X_m)_\infty$ range, that is, they are almost independent of F_o. A mean $(X_c/X_m)_\infty$ value was found to be 3.2. Results from Screens A and C are dependent on F_o and they finally attain values of about 3.6 and 4.6 respectively at high F_o values.

3.3 Variation of Characteristic Lengths

3.3.1 Maximum Scour, $\varepsilon_{m\infty}$

The dimensionless maximum scour, $\varepsilon_{m\infty}/b_o$, was plotted against the densimetric particle Froude number, F_o, and the resulting graphs are presented in Figures 11 to 17. Two sand sizes, d_{50} and d_{65} were used in the analysis to find out if one of them would produce a better correlation. The results from Screen A are presented in Figures 11 and 12. It can be seen that the curves are parallel and each curve stands for a particular sand size or α value. The uppermost curve, for combination 3A, is for the biggest sand size and for a given value of F_o, this curve gives the highest $\varepsilon_{m\infty}/b_o$ value and not the lowest as would have been expected. Given the same conditions, that is, exit jet velocity and tail water depth, a sand bed with the smallest sand size should produce the biggest scour. This is noticeable in the experimental results (Appendix A). A way of interpreting Figures 11 and 12, is to obtain F_o values for each of the three sand sizes by using a fixed value for U_o. After obtaining the corresponding values of $\varepsilon_{m\infty}/b_o$ for the F_o values, it will be noticed that the bed with the smallest sand size has the highest $\varepsilon_{m\infty}/b_o$ value. The use of d_{65} for sand size did not really improve the correlation obtained for d_{50}. The same kind of curves were obtained but were shifted a little backwards. Screen B produced a different kind of behavior. All the data from the different sand sizes can be fitted with one curve. This curve is therefore independent of sand size or α as can be seen in

Figures 13 and 14. The effect of d_{65} is the same as in Screen A. All the data obtained using Screen C can also be fitted into a curve which tends towards an asymptotic $\varepsilon_{m\infty}/b_o$ value of 3.6 as shown in Figures 15 and 16. Sand size, d_{65}, has the same effect as above. The results from all the screens are shown in Figure 17 for comparison. The curves for 1A,2A,3A and 1B,2B,3B appear to be parallel. The curve for 1C,2C and 3C has a different behavior and the screen design is definitely responsible for this.

3.3.2 Location of Maximum Scour, $x_{m\infty}$

The relationship of maximum scour location in terms of b_o with F_o was studied and the resulting plots are Figures 18 to 21. Figure 18 shows the results obtained from Screen A. The data would be poorly fitted by one curve, so each combination has been fitted with a curve just as in the analysis of maximum scour. Combination 1A has the worst fit. These curves are also parallel. Figure 19 presents Screen B's results. Although, the data are a little scattered, they can still be fitted with a curve. This curve is independent of sand size and $x_{m\infty}/b_o$ was found to be proportional to F_o. Results obtained from Screen C can also be fitted with a single curve as shown in Figure 20. This is similar to that obtained in the maximum scour analysis. The fitted curve tends to an asymptotic value of 10.4. A comparison of results is made in Figure 21. The curves are similar to those in the maximum scour analysis (Figure 17) and the same comments

apply here.

3.3.3 Height of Ridge, $\Delta\varepsilon_\infty$

The ridges were not well formed in most of the experiments except for the experiments involving Screen B. As mentioned earlier, secondary flow was responsible for this and could be coupled with excessive shear stress over the ridge which would lead to flattening and spreading of the ridge further downstream. The results of the analysis are not as successful as those for maximum scour and have been presented in Figures 22 to 25. The results from Screen A are shown in Figure 22. The data from the sand sizes can be fitted with one curve. The relationship is fairly linear initially ($F_o < 8$) and then tends towards an asymptotic $\Delta\varepsilon_\infty/b_o$ value of about 3.1. This could be taken as the limiting growth value for the ridge. Figure 23 presents the results from Screen B. The data are scattered and the linear fitted line is a poor fit. Because the ridges produced with the screen were mostly well formed, it is safe to say that limiting growth was not attained. Also when compared to Screen A's results, where limiting growth starts around an F_o value of 10, nearly all of the data from Screen B are below this value. Results from Screen C are presented in Figure 24 and are similar to those from Screen A. In this case, the curve tends to an asymptotic value of about 3.2 and limiting growth begins close to an F_o value of 9. A comparison of results is shown in Figure 25. It can be seen that for a

given F_o value the screen with the biggest hole (Screen B), produces the biggest ridge and vice versa.

3.3.4 Location of Ridge, $X_{c\infty}$

The relationship of this length scale in terms of b_o with F_o was also studied and the results are presented in Figures 26 to 29. These results are also not so good due to the poor formation of the ridges. The ridges produced by Screen A were the most flattened. Figure 26 shows the results and no meaningful relationship can be deduced. Most of the ridges lie within a $x_{c\infty}/b_o$ value of 35 and 39.6. The results from Screen B are presented in Figure 27. Though there is some scatter, the fitted line is good and independent of sand size. There is some scatter for Screen C's results as can be seen in Figure 28. A comparison of the screens' results is made in Figure 29.

3.3.5 Length Scale for Screen Hole, l_s

The length scale for the screen hole can be chosen as l_x, l_y or $\sqrt{A}$ where A is the screen hole area. Since the scouring process is essentially a two dimensional problem, the length scale of the screen hole in the transverse direction of flow, l_y, becomes relatively unimportant. The dimensionless screen size, α, can then be chosen as l_x/d_{50} or $\sqrt{A}/d_{50}$. For Screen A these values are the same since the screen holes are squares. If l_y/l_x ratio is too small or big, it will not be appropriate to use $\sqrt{A}/d_{50}$. The values of l_y/l_x

ratio for the screens' holes, which are considered to be moderate, are given in Table 1 and $\sqrt{A}/d_{50}$ has been chosen as α in this study. From the scour hole analysis, the results from Screens B and C are independent of sand size or α. Results from Screen A are dependent, so the relationships between dimensionless maximum scour, $\varepsilon_{m\infty}/b_o$, and α and dimensionless maximum scour location, $x_{m\infty}/b_o$, and α for different F_o values are presented in Figures 30 and 31 respectively. In these figures, combination 3A (largest sand size and smallest screen size) gives the highest maximum scour and the farthest maximum scour location. A similar behavior was experienced in the maximum scour analysis and the same reason applies here.

3.4 Scour Reduction Ratios

An attempt has been made to find expressions for quantifying the reductions in the characteristic lengths of the eroded bed profile due to a protective screen. The reductions have been expressed as ratios and are defined by the following equations.

Reduction in maximum scour,

$$\eta_1 = \frac{\left(\frac{\varepsilon_{m\infty}}{b_o}\right)_{(screen)}}{\left(\frac{\varepsilon_{m\infty}}{b_o}\right)_{(no\ screen)}} \qquad (5)$$

Reduction in maximum scour location,

$$\eta_2 = \frac{\left(\frac{X_{m\infty}}{b_o}\right)_{(screen)}}{\left(\frac{X_{m\infty}}{b_o}\right)_{(no\ screen)}} \tag{6}$$

Reduction in ridge height,

$$\eta_3 = \frac{\left(\frac{\Delta\varepsilon_{\infty}}{b_o}\right)_{(screen)}}{\left(\frac{\Delta\varepsilon_{\infty}}{b_o}\right)_{(no\ screen)}} \tag{7}$$

Reduction in ridge location,

$$\eta_4 = \frac{\left(\frac{X_{c\infty}}{b_o}\right)_{(screen)}}{\left(\frac{X_{c\infty}}{b_o}\right)_{(no\ screen)}} \tag{8}$$

The value of η can only range from zero to one. A value close to zero means very good protection and when close to one, it means very poor protection. To evaluate η from the equations above, the curves for the variations of the characteristic lengths of the eroded bed profile with densimetric particle Froude number (without screen) were obtained from Rajaratnam (1981). Polynomial equations were obtained for these curves and the curves from this study to

allow easy calculation of η for different F_o values. Figure 32 shows the variation of η_1 with F_o. For Screens B and C, the results are independent of α, but the results from Screen A are not and a mean curve has been drawn to represent them. The value of η_1 tends asymptotically towards a value of about 0.12 at high F_o values for Screens A and C, and for Screen B, a value of about 0.24. Figure 34 shows that η_2 tends asymptotically to 0.29 for Screen B and roughly 0.2 for Screens A and C. The variation of η_3 with F_o is shown in Figure 36. η_3 also tends asymptotically to a value of 0.29 for Screen B and around 0.1 for Screens A and C. Figure 38 shows the variation of η_4 with F_o. η_4 tends asymptotically to 0.34 for Screen B and 0.28 for Screen C. The variations of η_1, η_2, η_3 and η_4 with $\sqrt{A}/d_{50}$ for different F_o values are shown in Figures 33, 35, 37 and 39 respectively. From these figures, it can be seen that the relationships are less dependent on F_o at high F_o values.

Table 2

Possible values of α

Screen	Sand 1			Sand 2			Sand 3		
	lx/d50	ly/d50	√A/d50	lx/d50	ly/d50	√A/d50	lx/d50	ly/d50	√A/d50
A	3.95	3.95	3.95	2.26	2.26	2.26	2.11	2.11	2.11
B	16.28	31.01	17.21	9.29	17.7	9.82	8.68	16.53	9.17
C	6.28	17.91	8.29	3.58	10.22	4.73	3.34	9.55	4.42

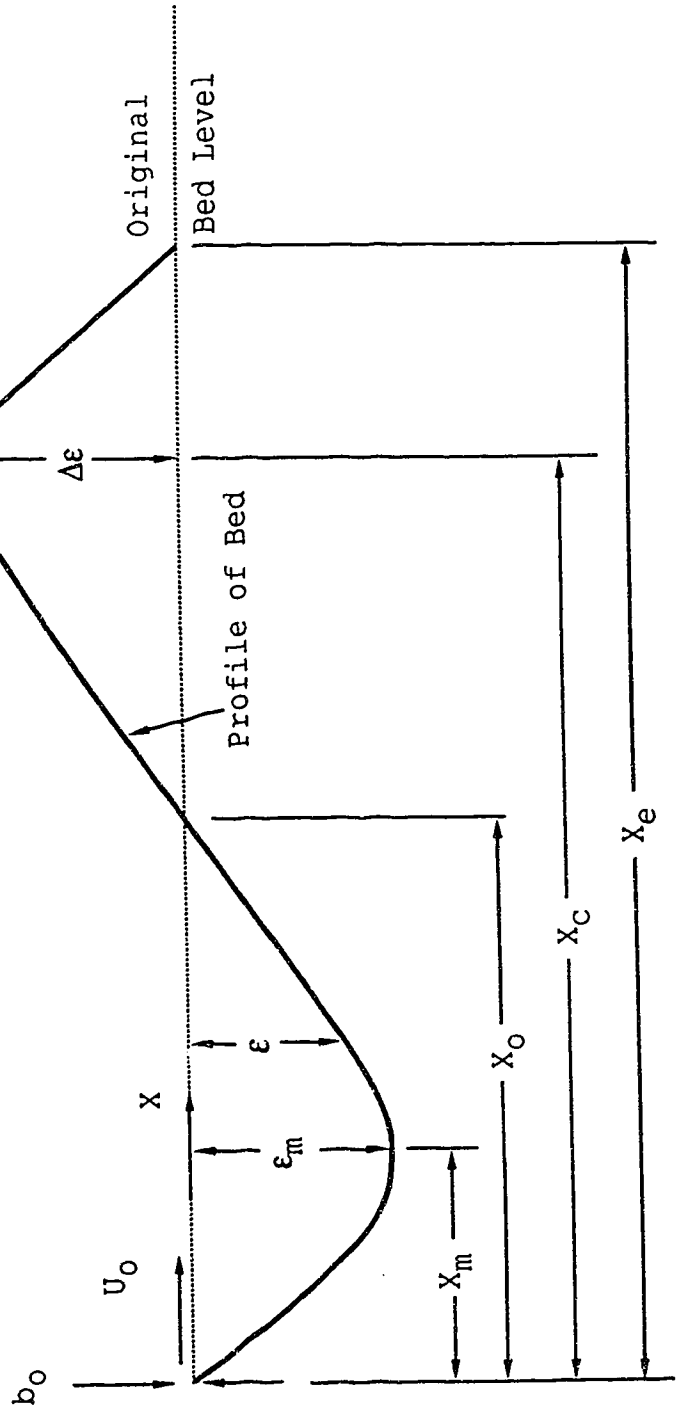

Figure 5 Profile of an Eroded Bed

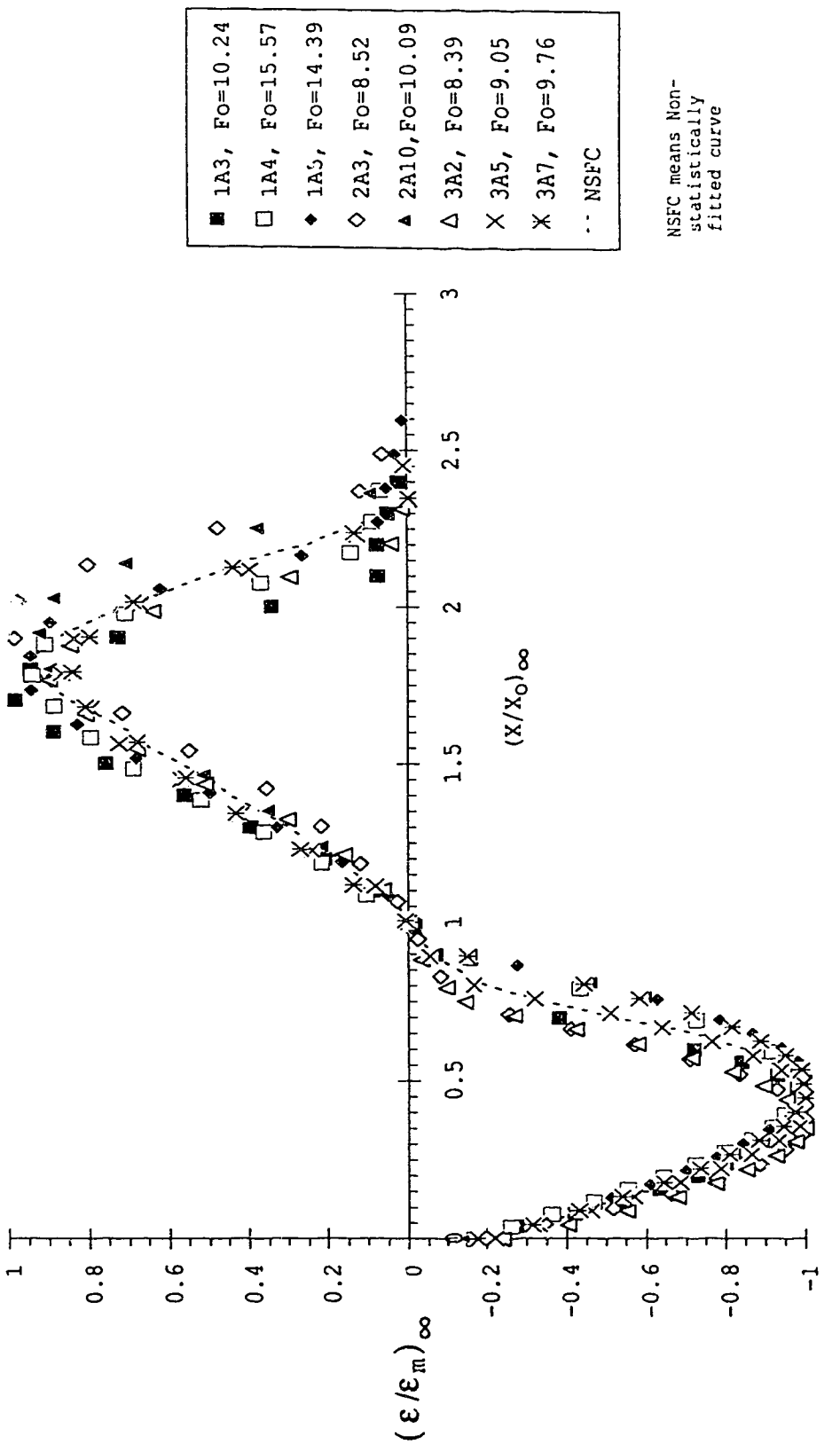

Figure 6 Similarity of Erosion Profile Using Screen A

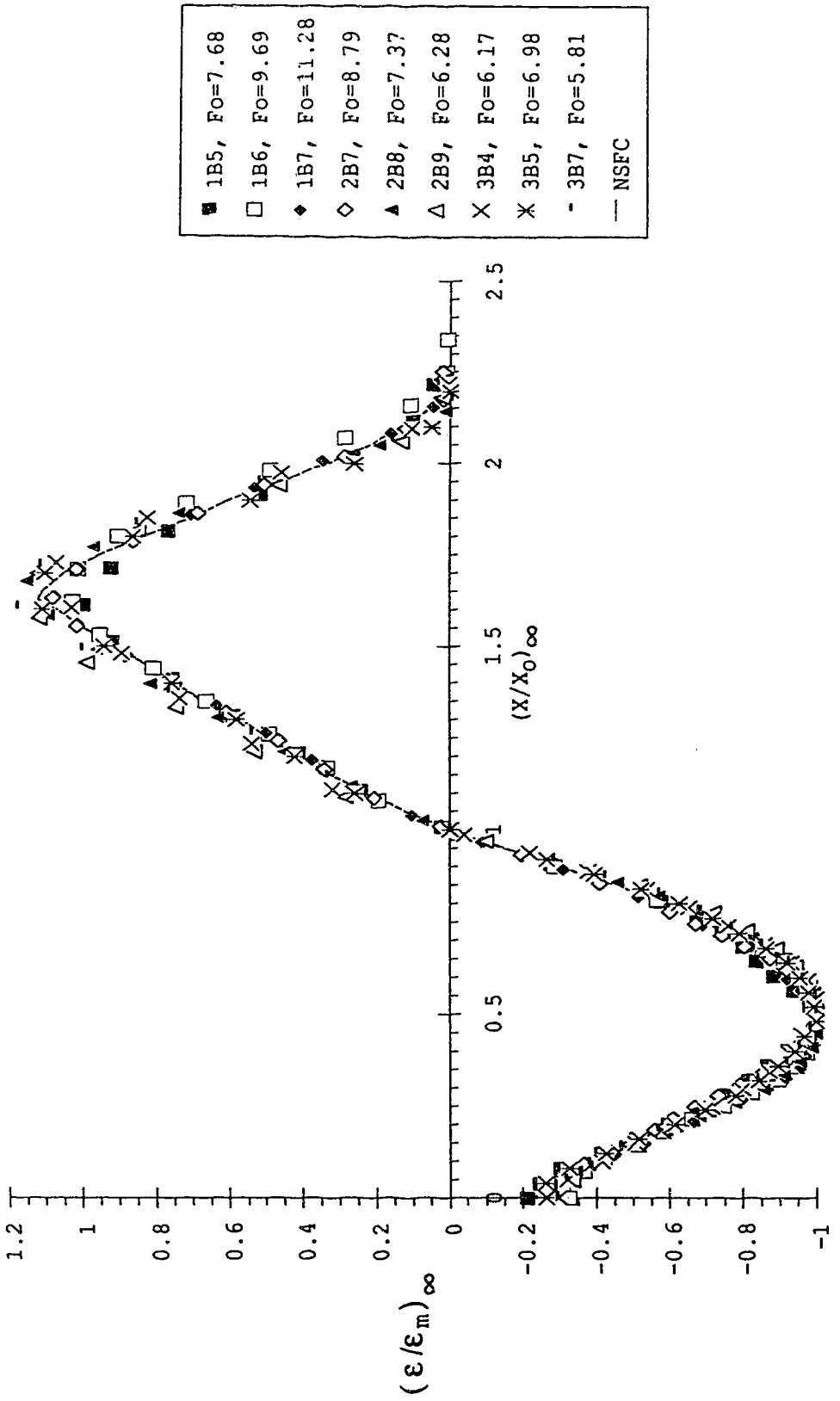

Figure 7 Similarity of Erosion Profile Using Screen B

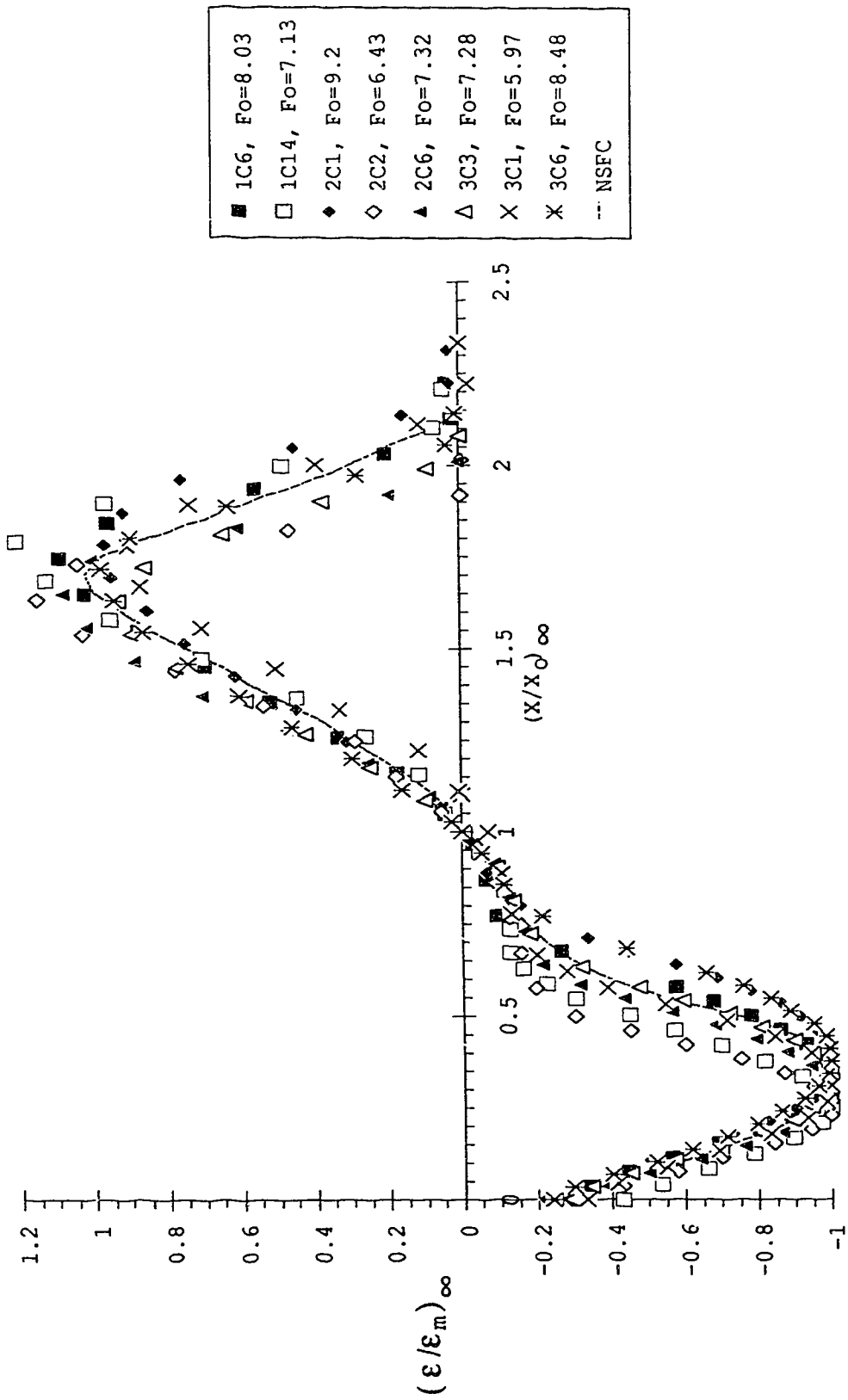

Figure 8 Similarity of Erosion Profile Using Screen C

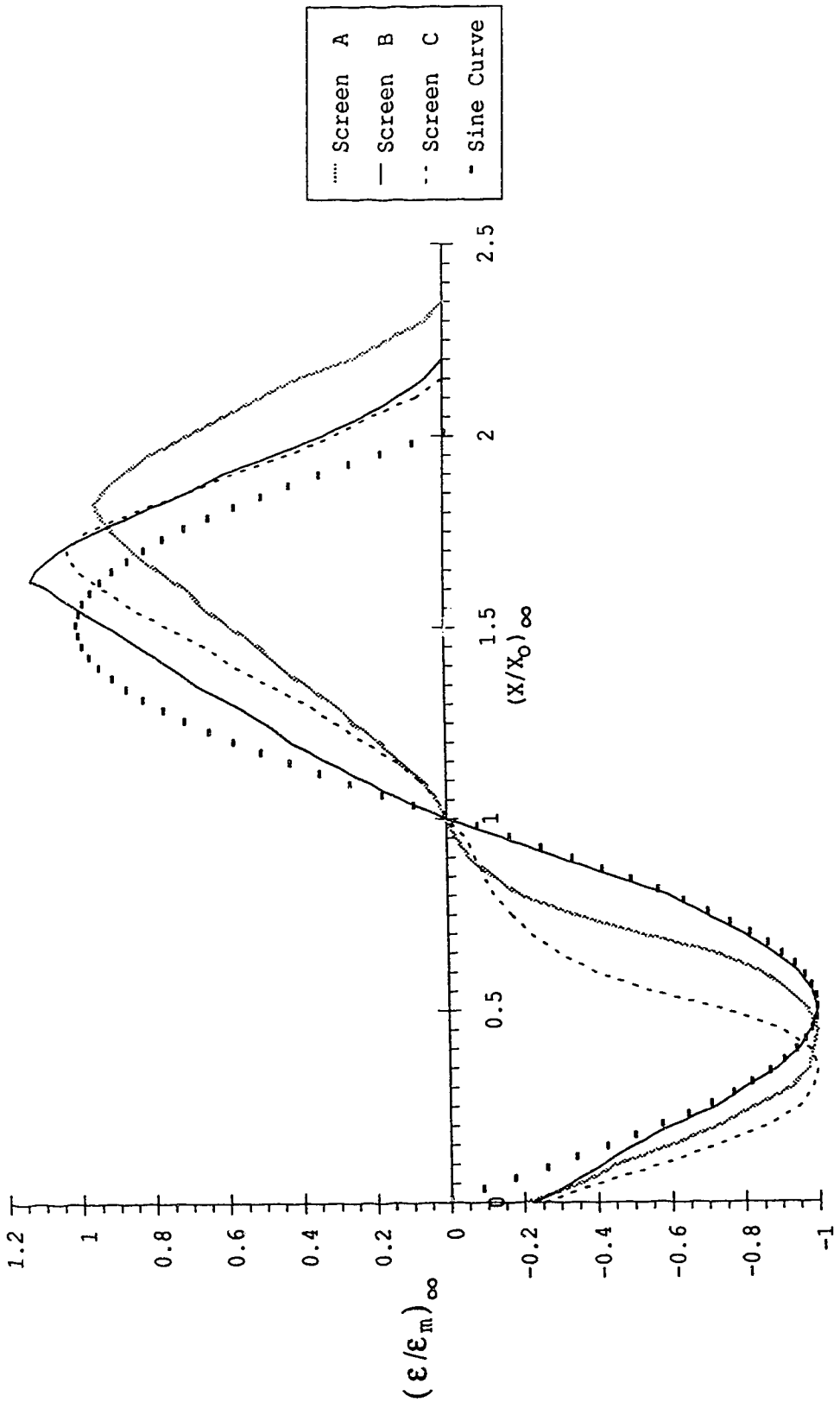

Figure 9 Comparison of Similarity of Erosion Profiles

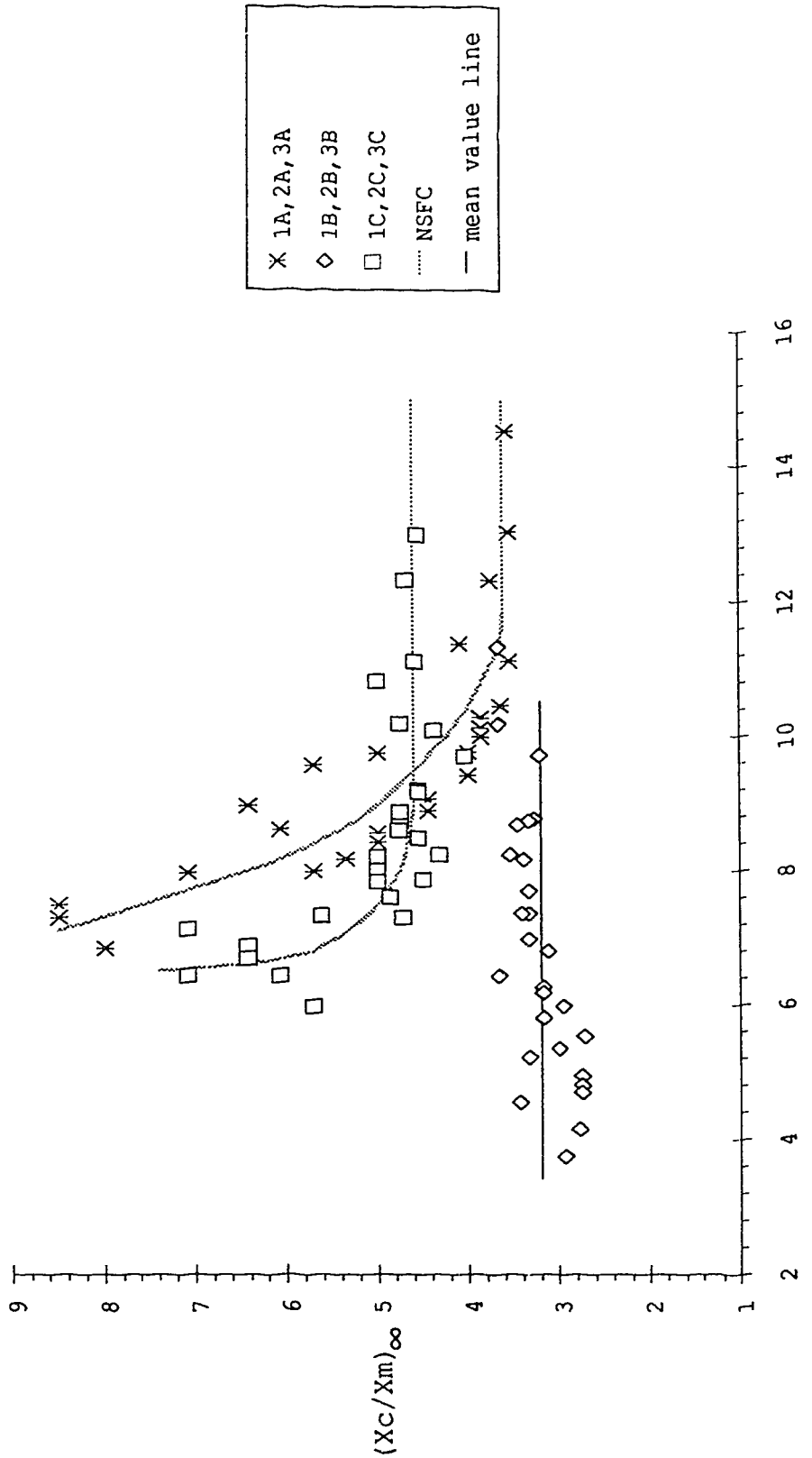

Figure 10 Variation of Ratio of Ridge Location to Maximum Scour Location with

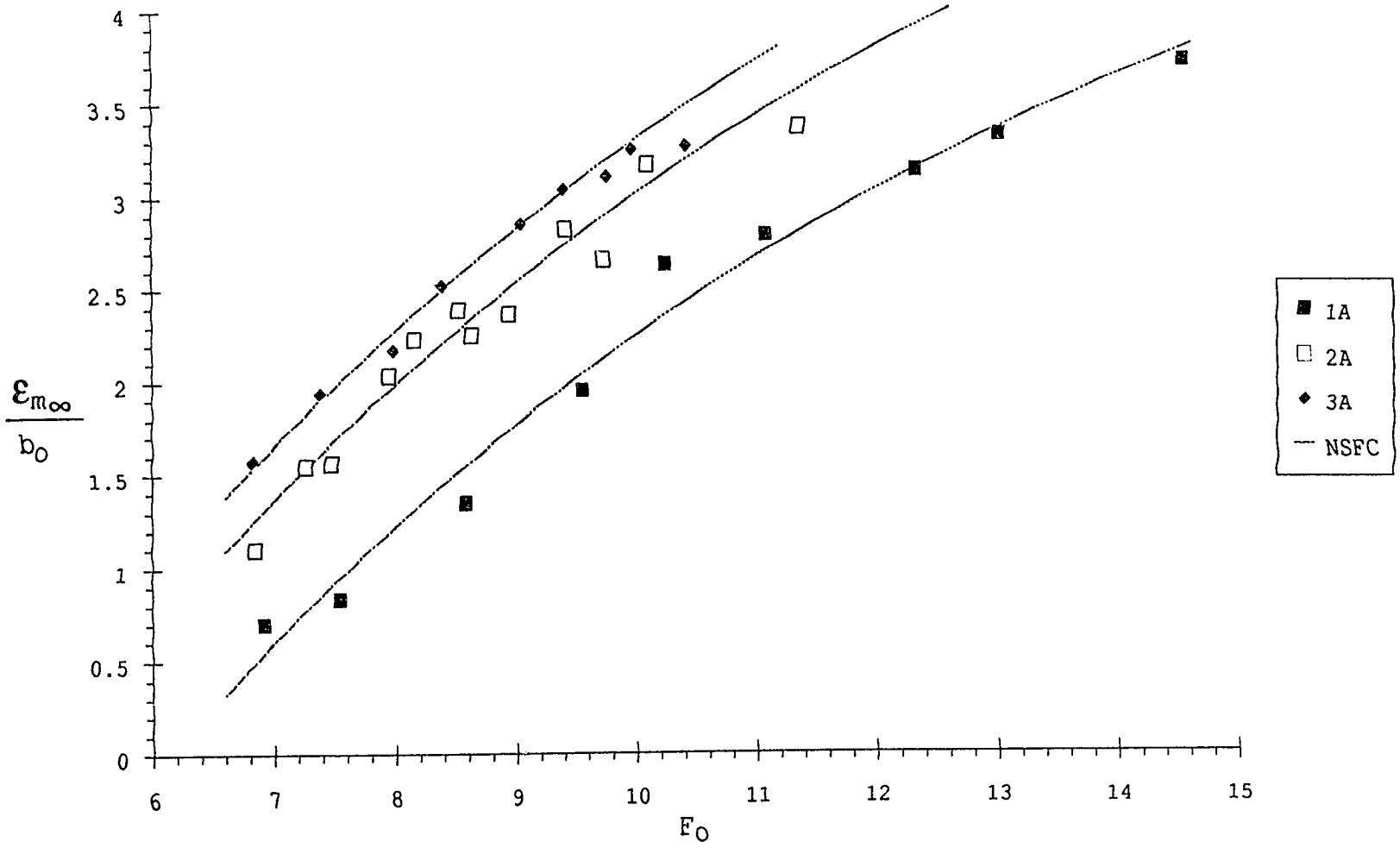

Figure 11 Screen A: Variation of Maximum Scour with Fo (using d50)

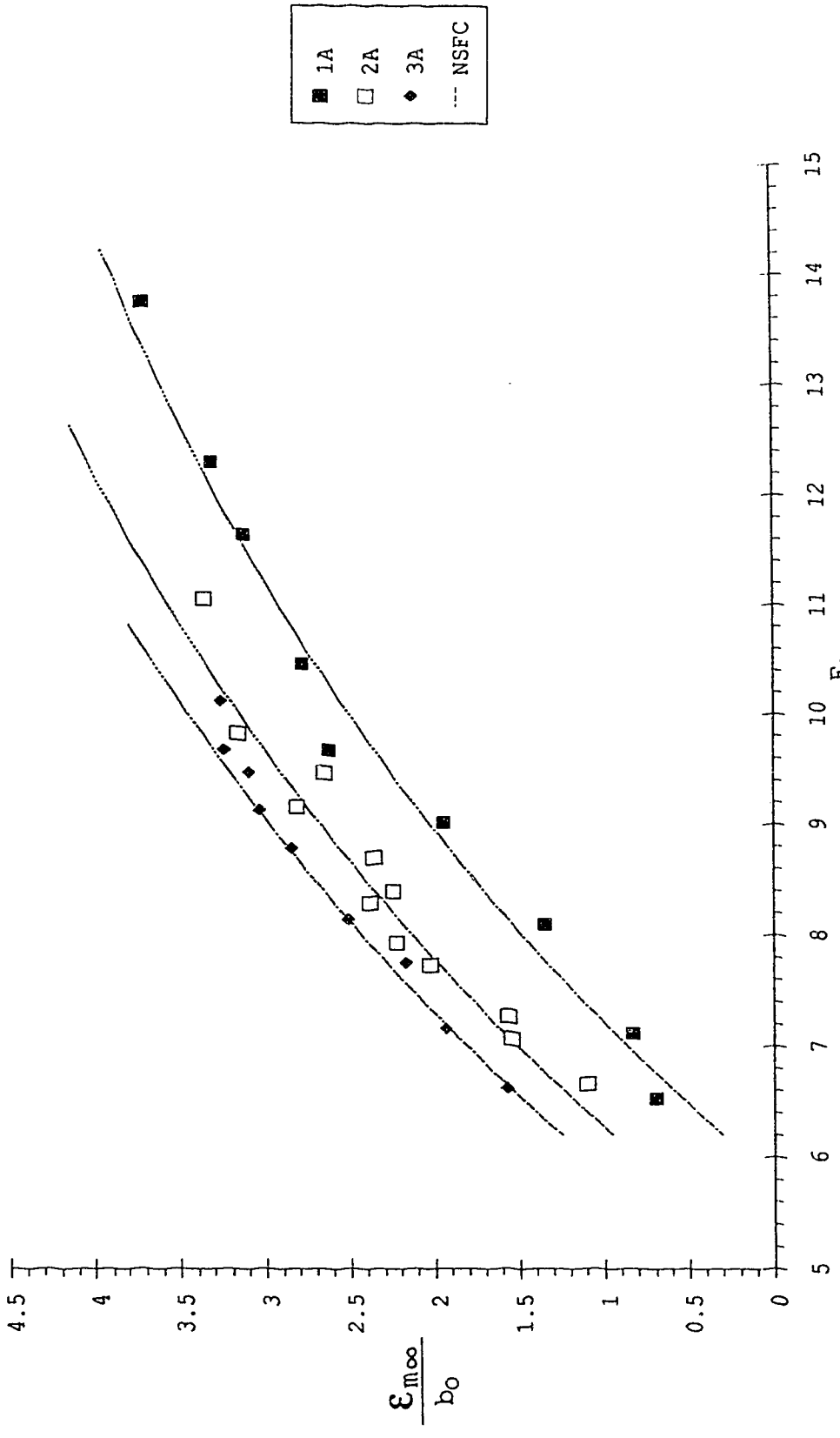

Figure 12 Screen A: Variation of Maximum Scour with Fo (using d65)

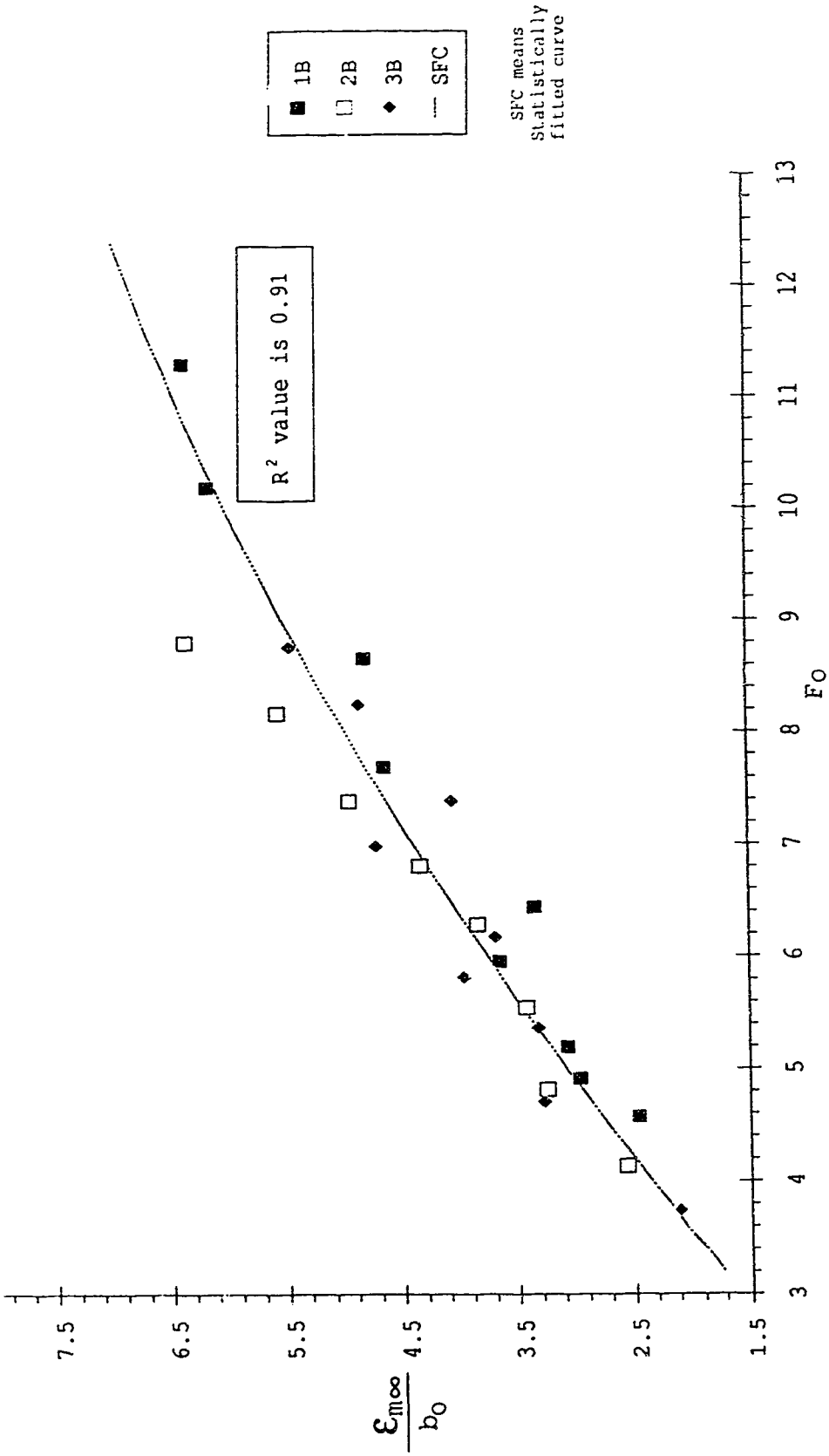

Figure 13 Screen B: Variation of Maximum Scour with Fo (using d50)

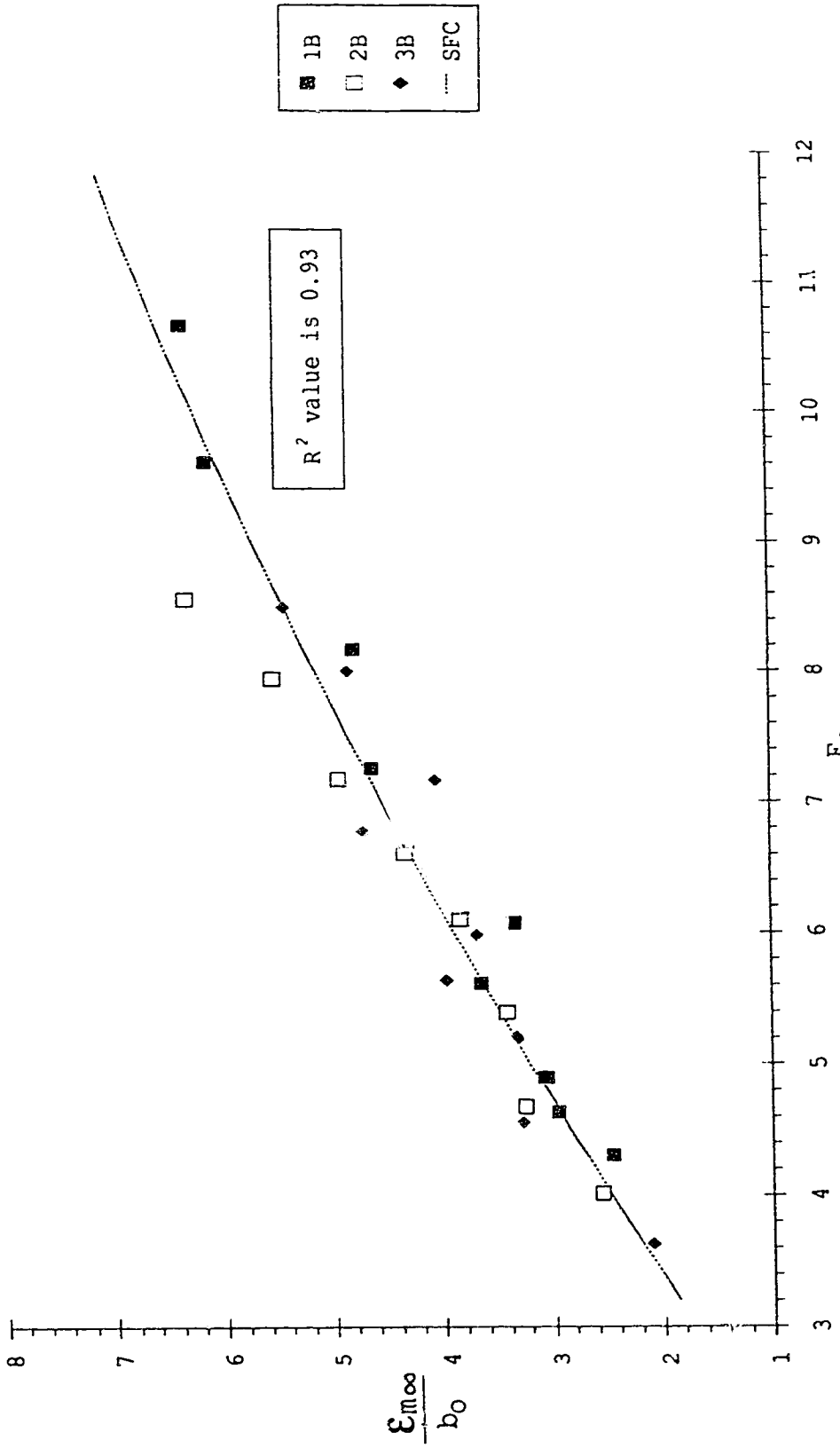

Figure 14 Screen B: Variation of Maximum Scour with Fo (using d65)

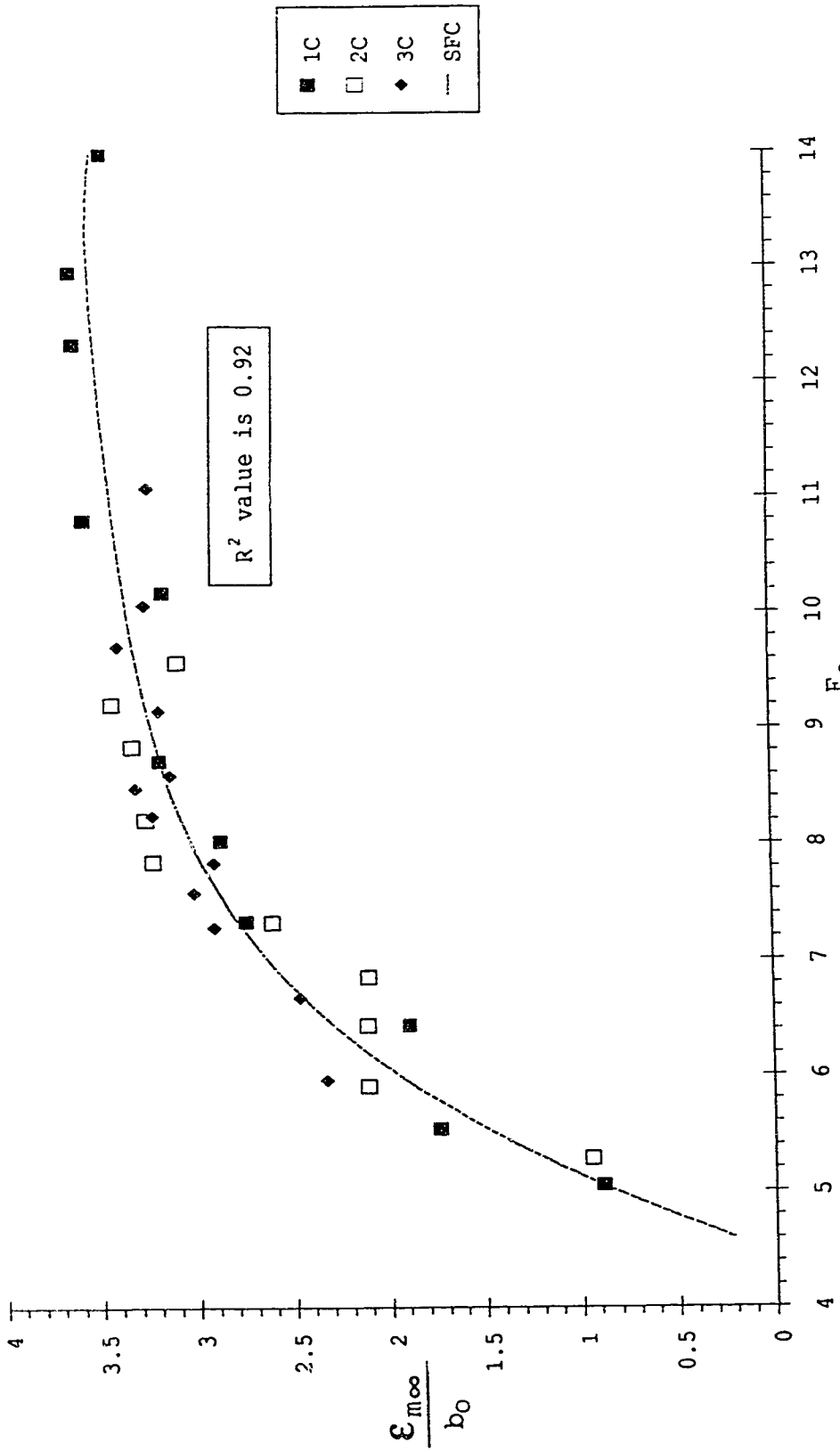

Figure 15 Screen C: Variation of Maximum Scour with Fo (using d50)

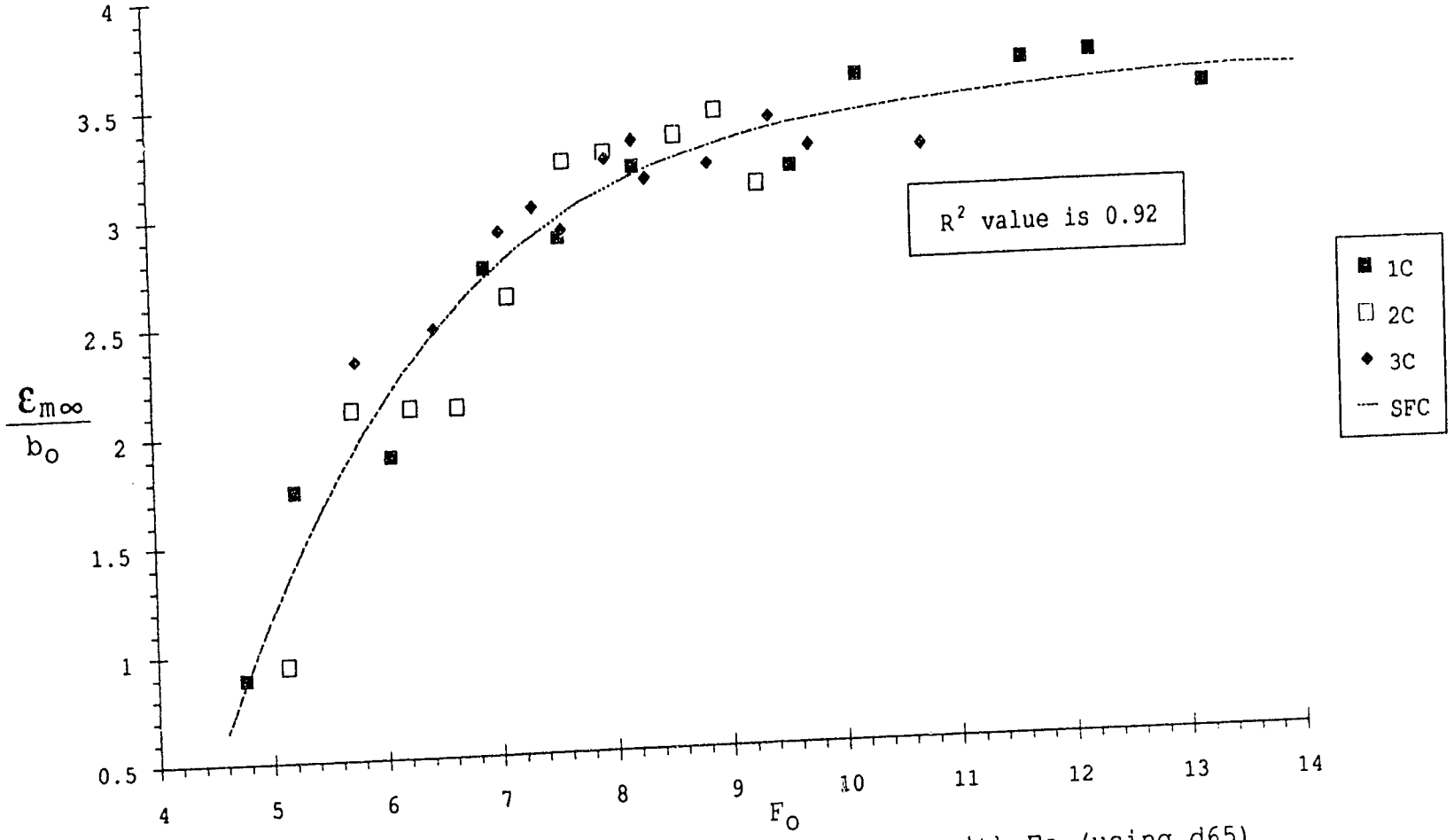

Figure 1 Screen C: Variation of Maximum Scour with Fo (using d65)

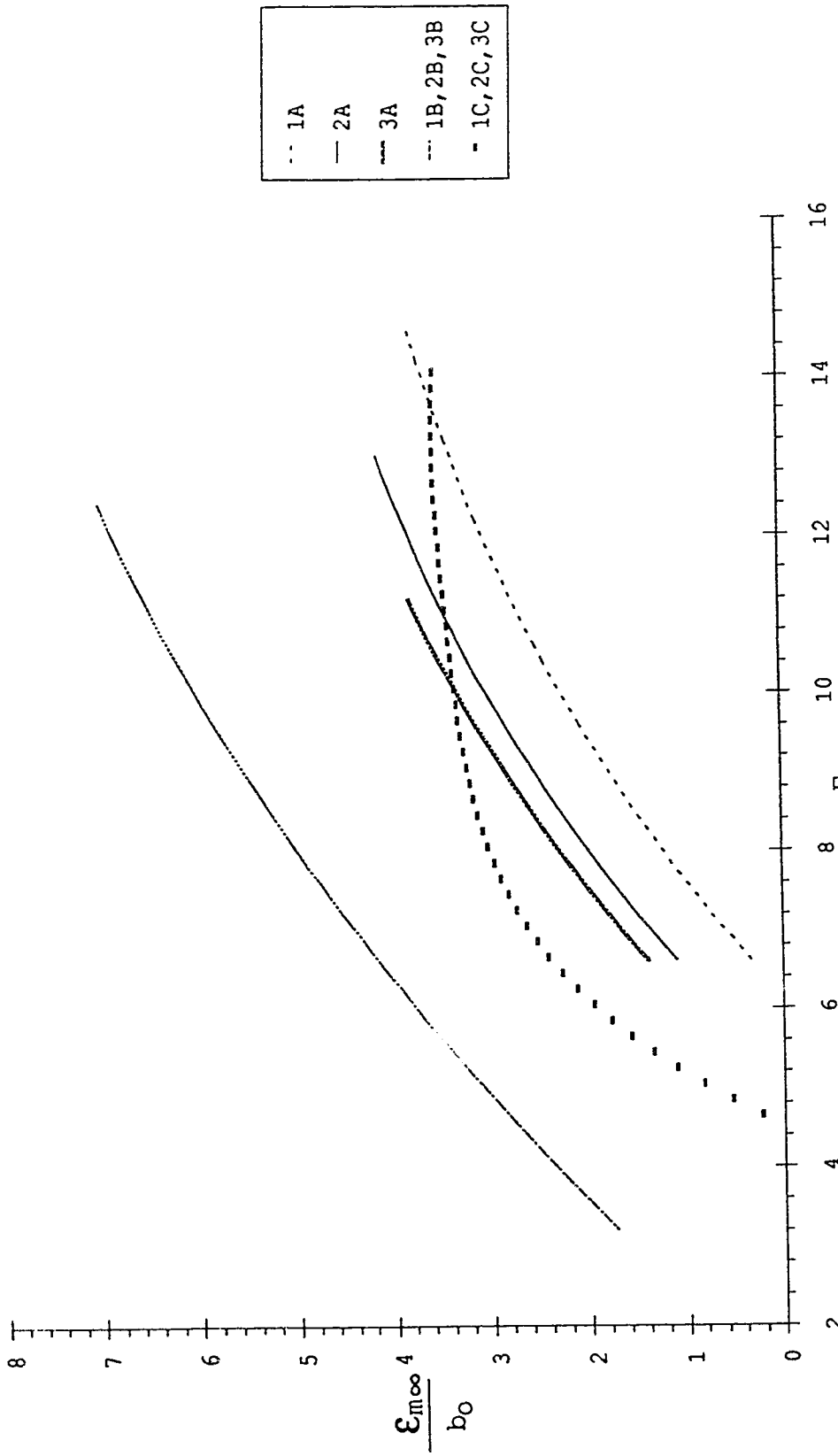

Figure 17 Variation of Maximum Scour with Fo (using d50) for all Screens

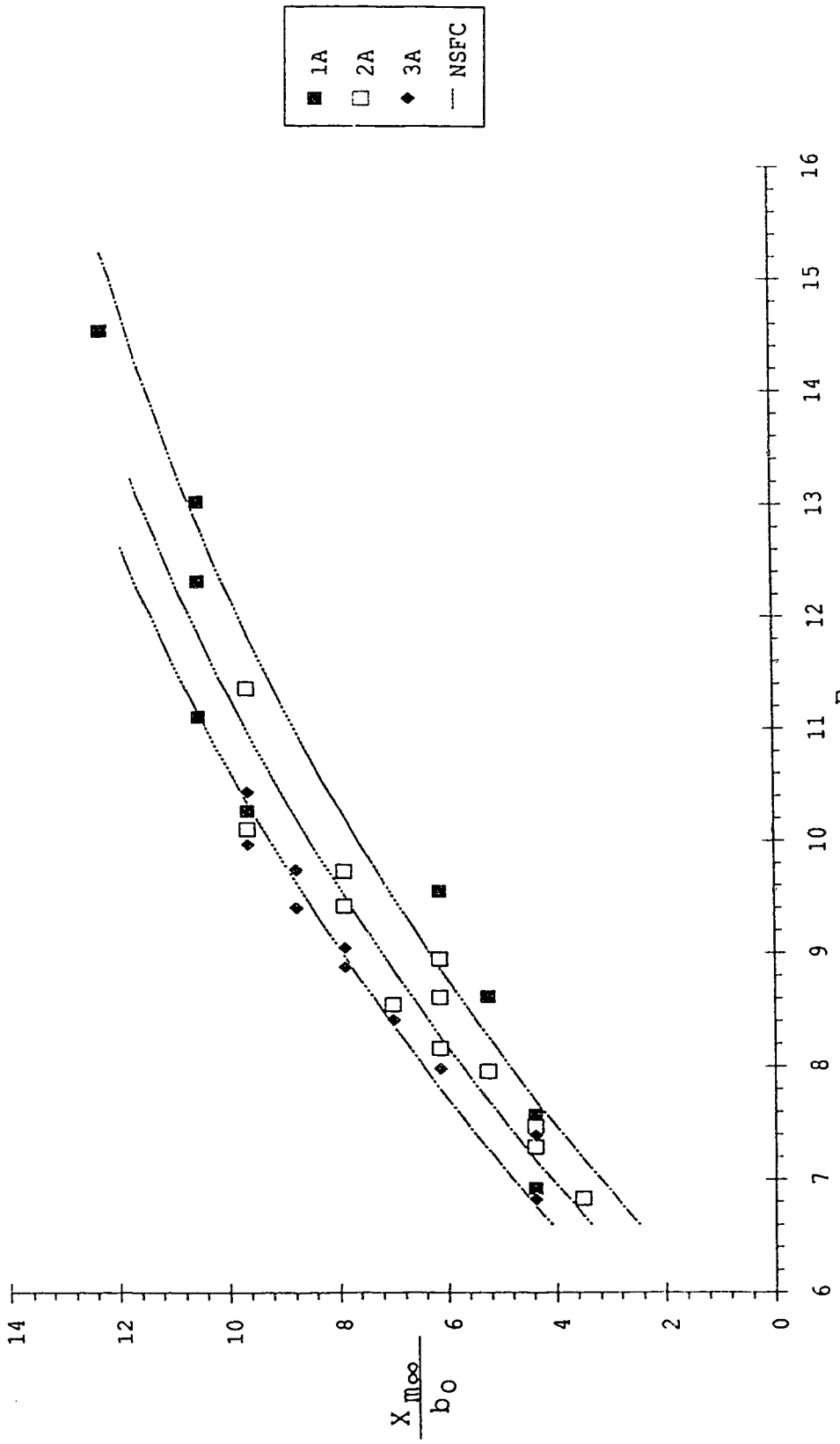

Figure 18 Screen A: Variation of Location of Maximum Scour with Fo

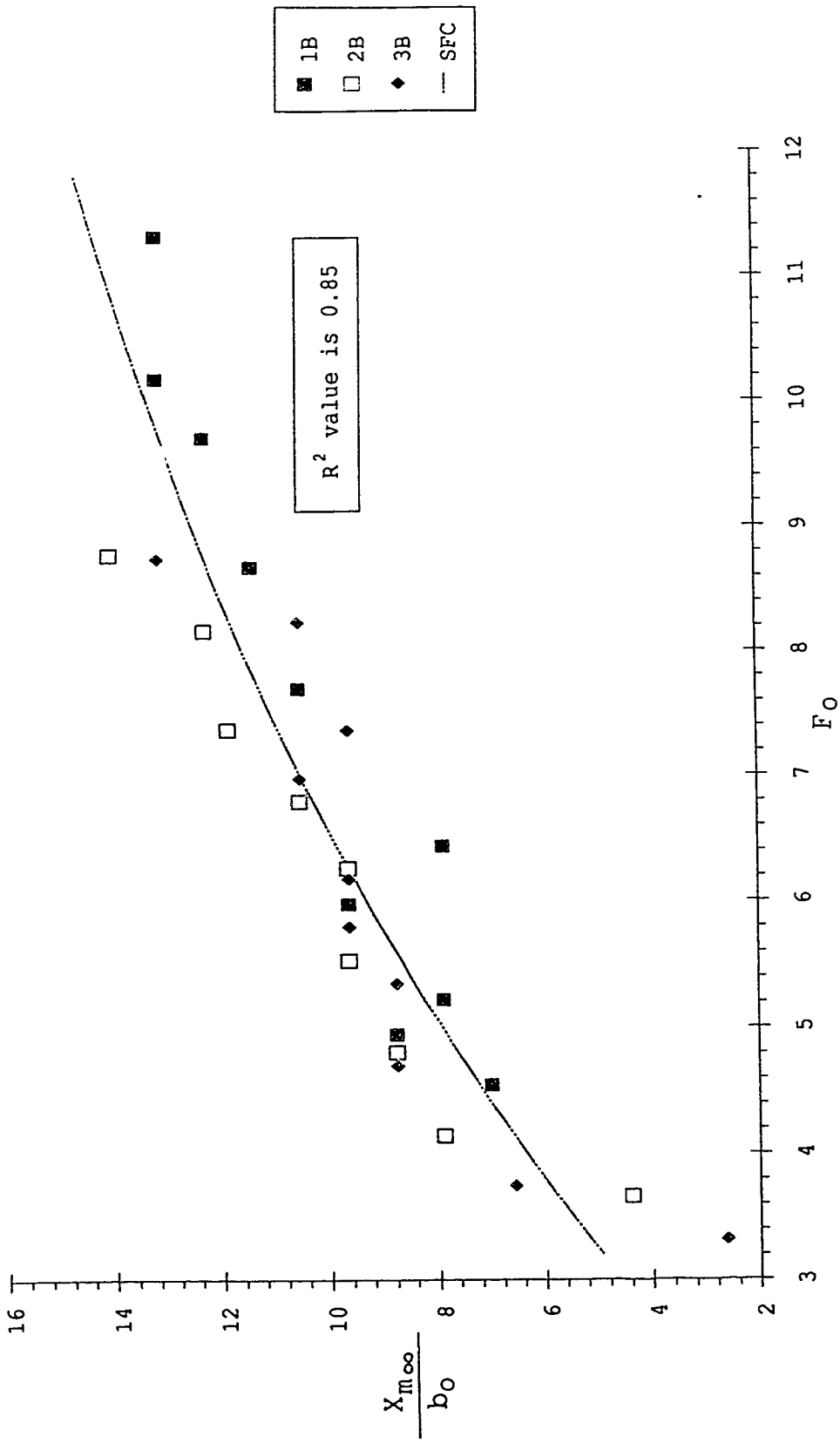

Figure 19 Screen B: Variation of Location of Maximum Scour with Fo

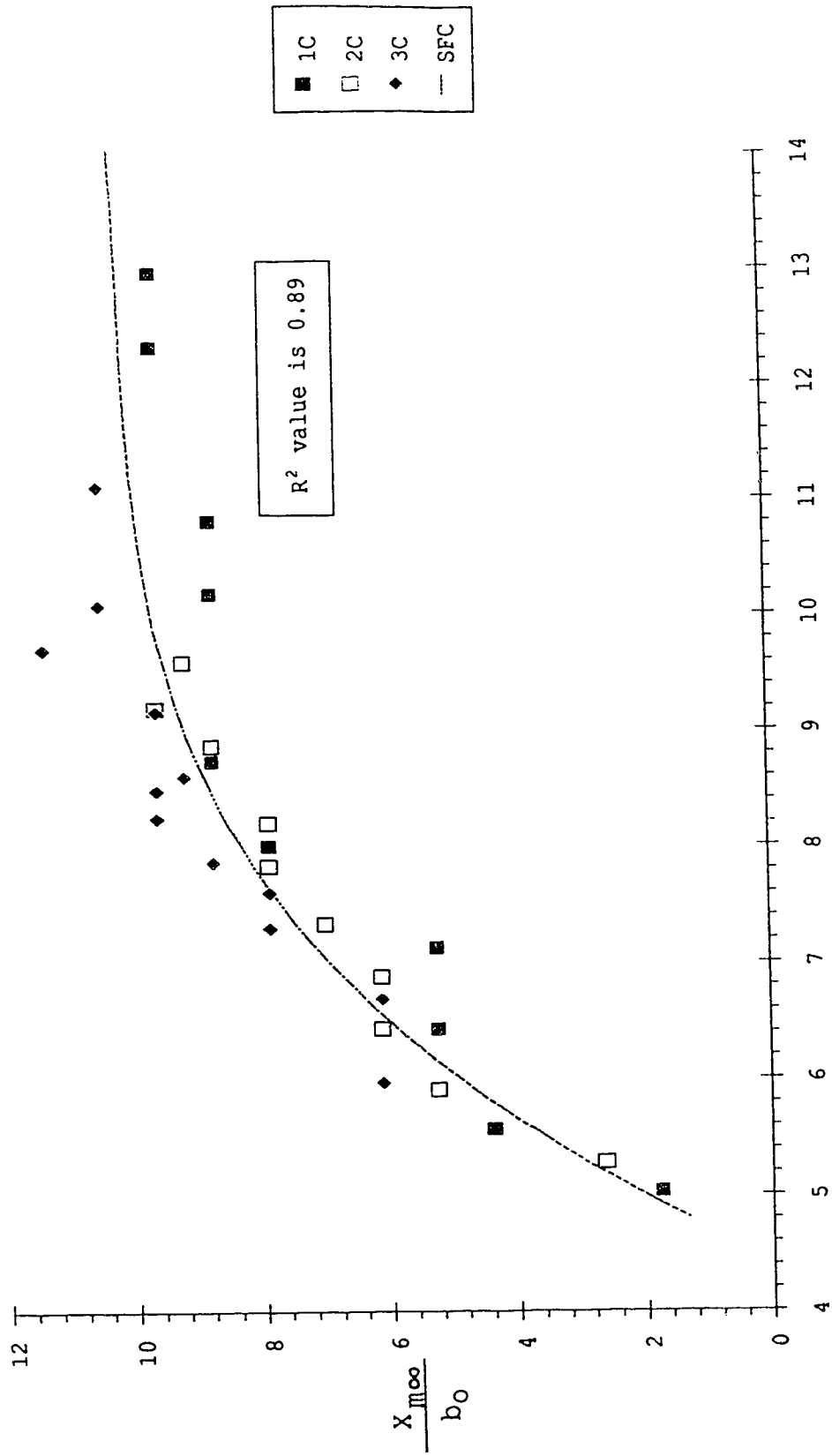

Figure 20 Screen C: Variation of Location of Maximum Scour with Fo

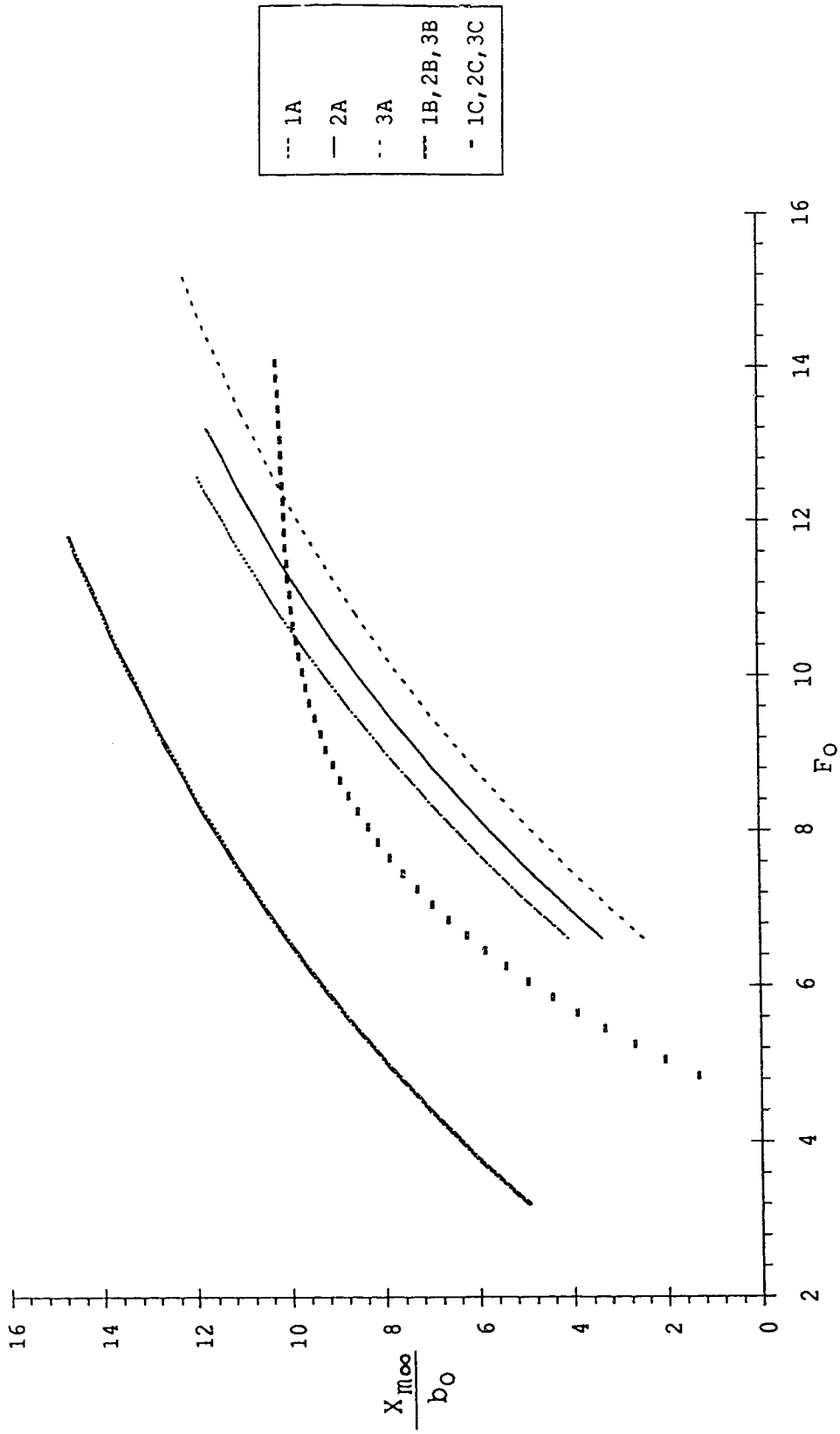

Figure 21
Variation of Location of Maximum Scour with Fo for all Screens

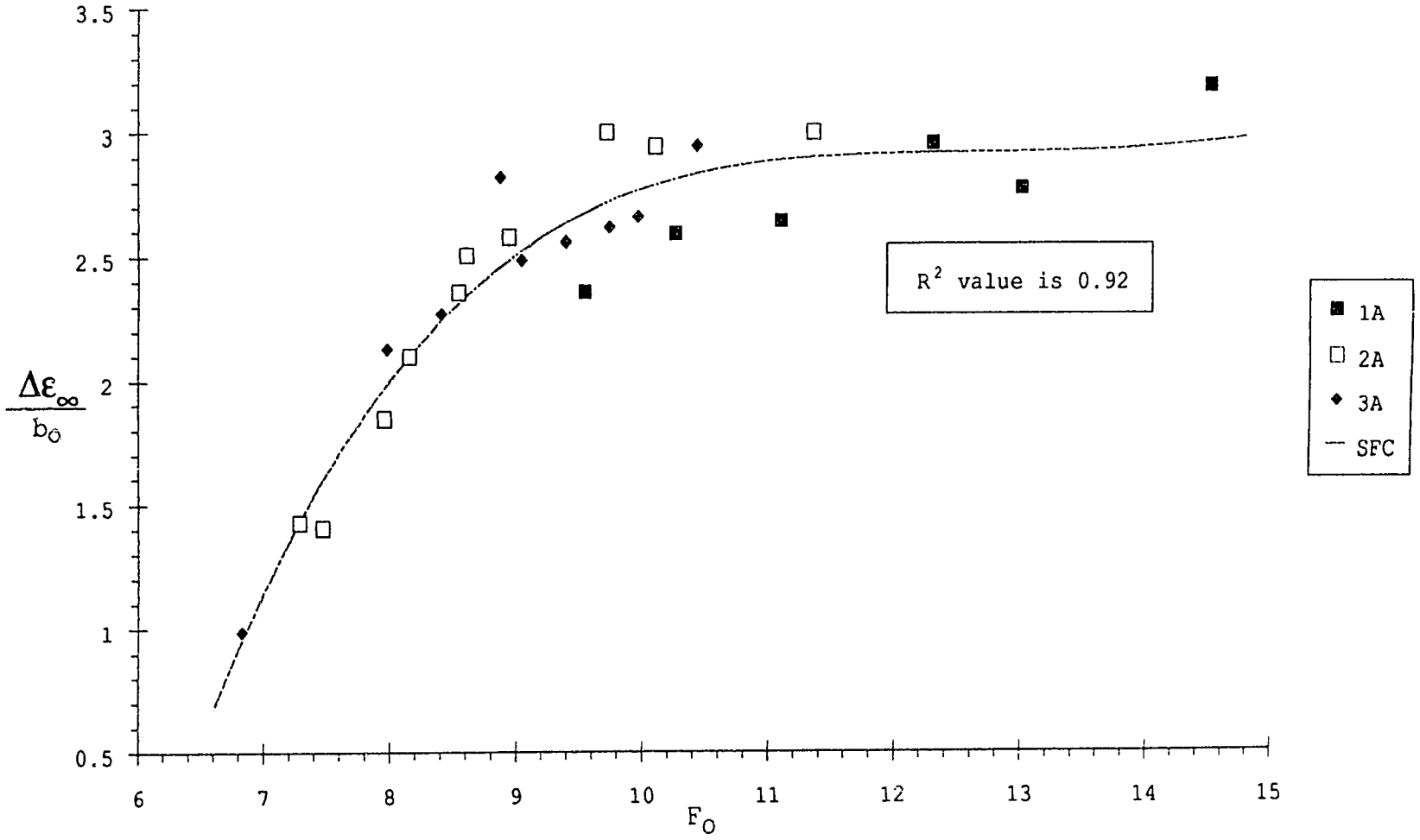

Figure 22 Screen A: Variation of Ridge Height with Fo

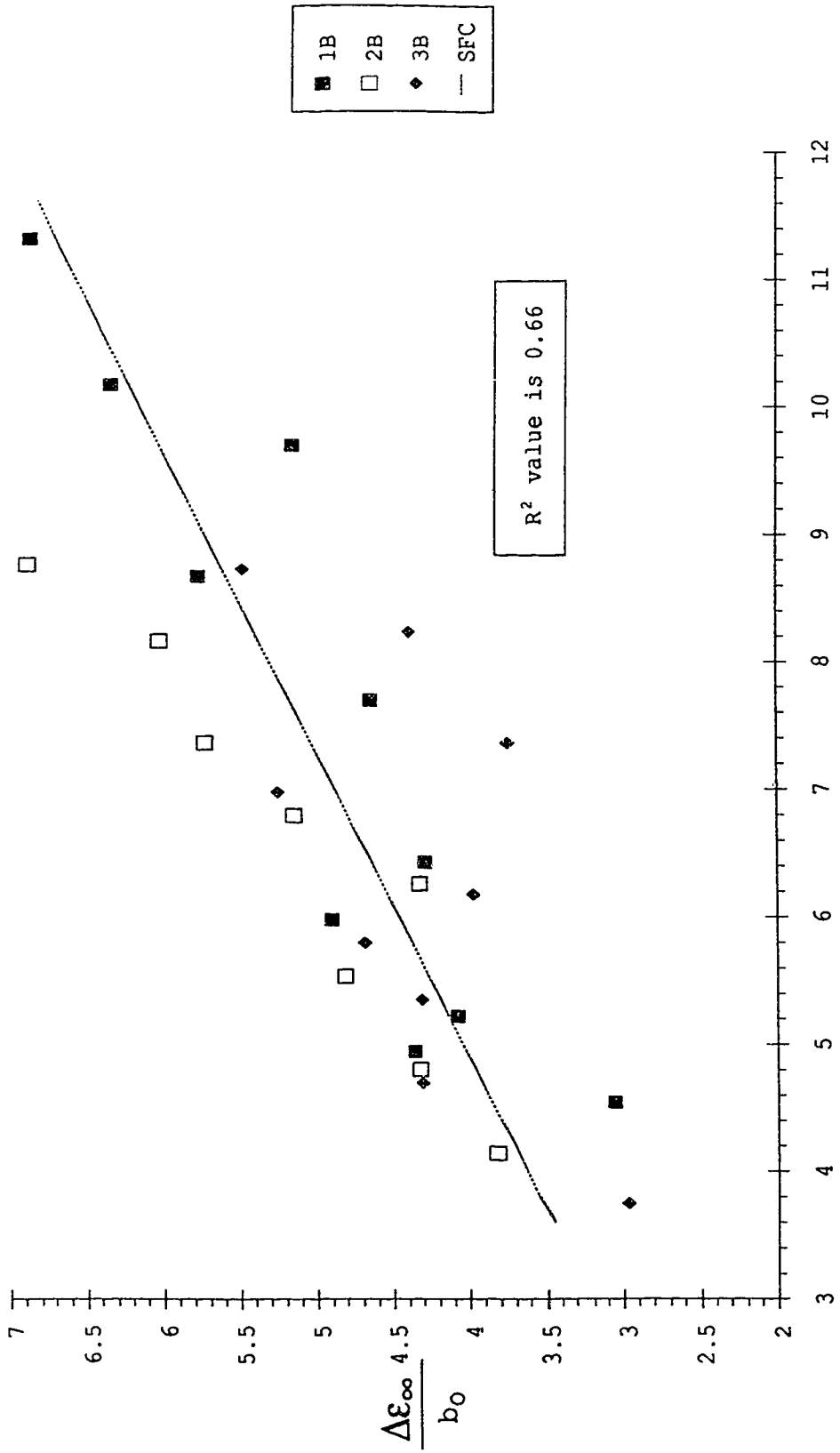

Figure 23 Screen B: Variation of Ridge Height with Fo

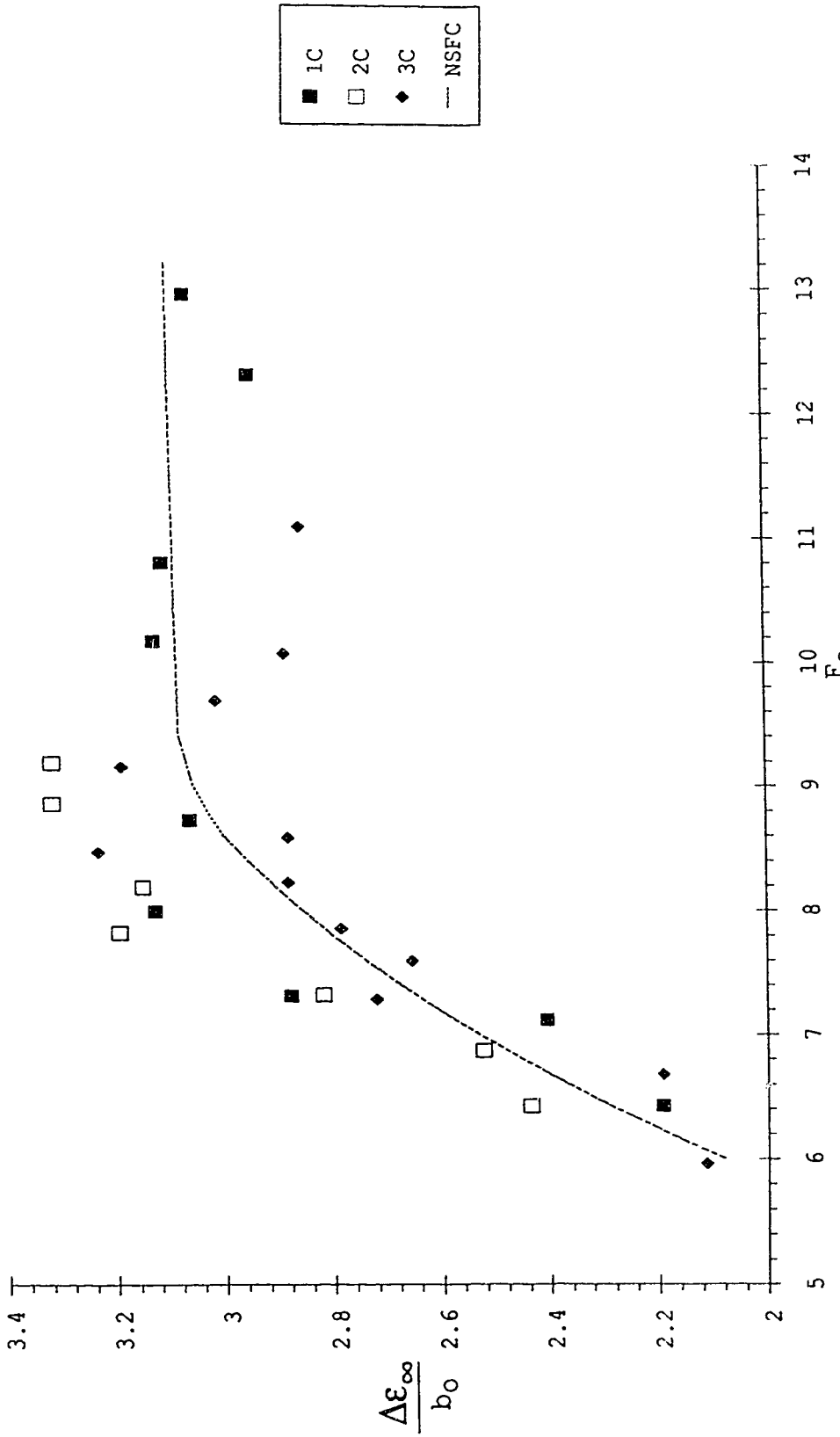

Figure 24 Screen C: Variation of Ridge Height with Fo

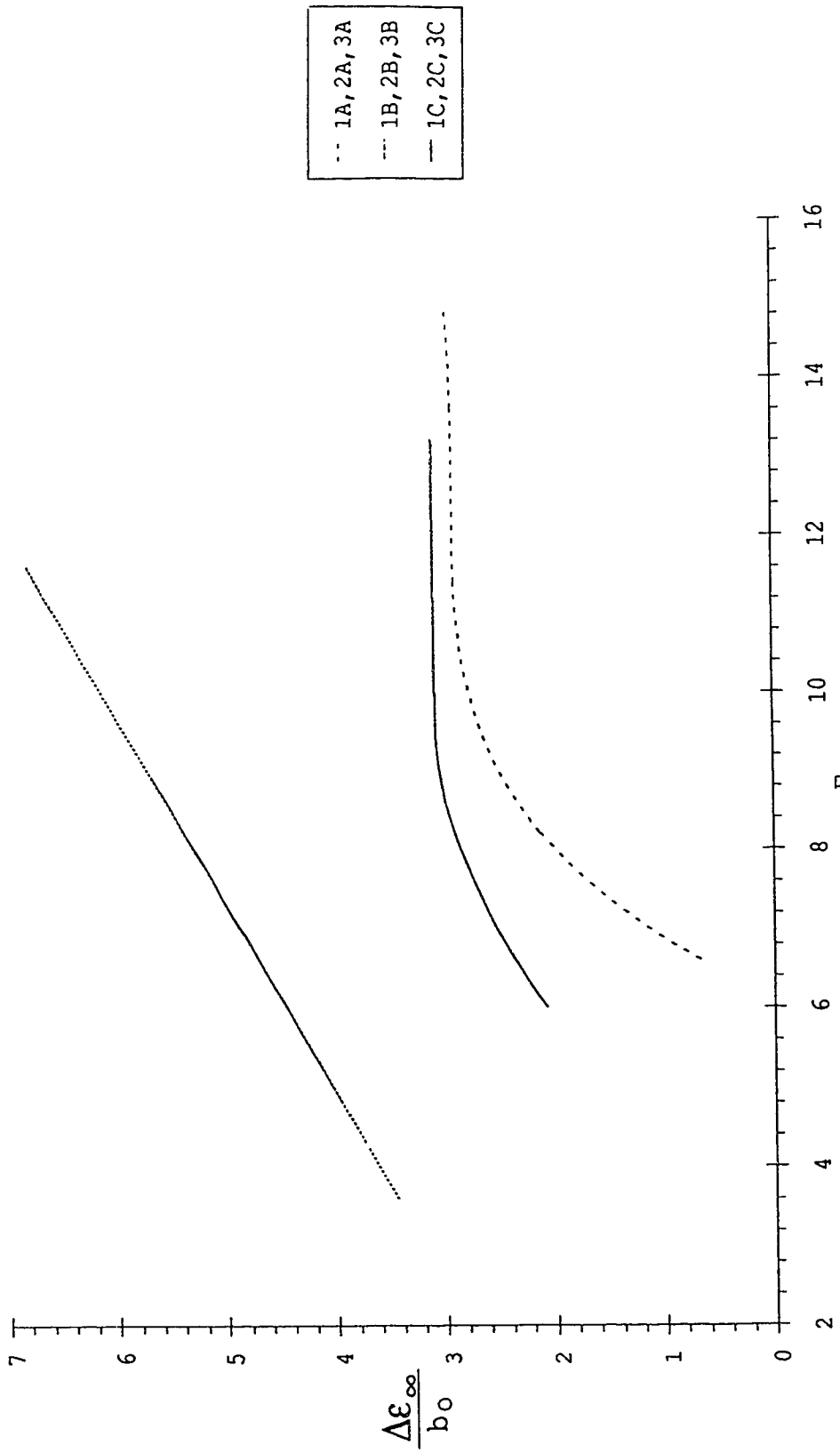

Figure 25 Variation of Ridge Height with Fo for all Screens

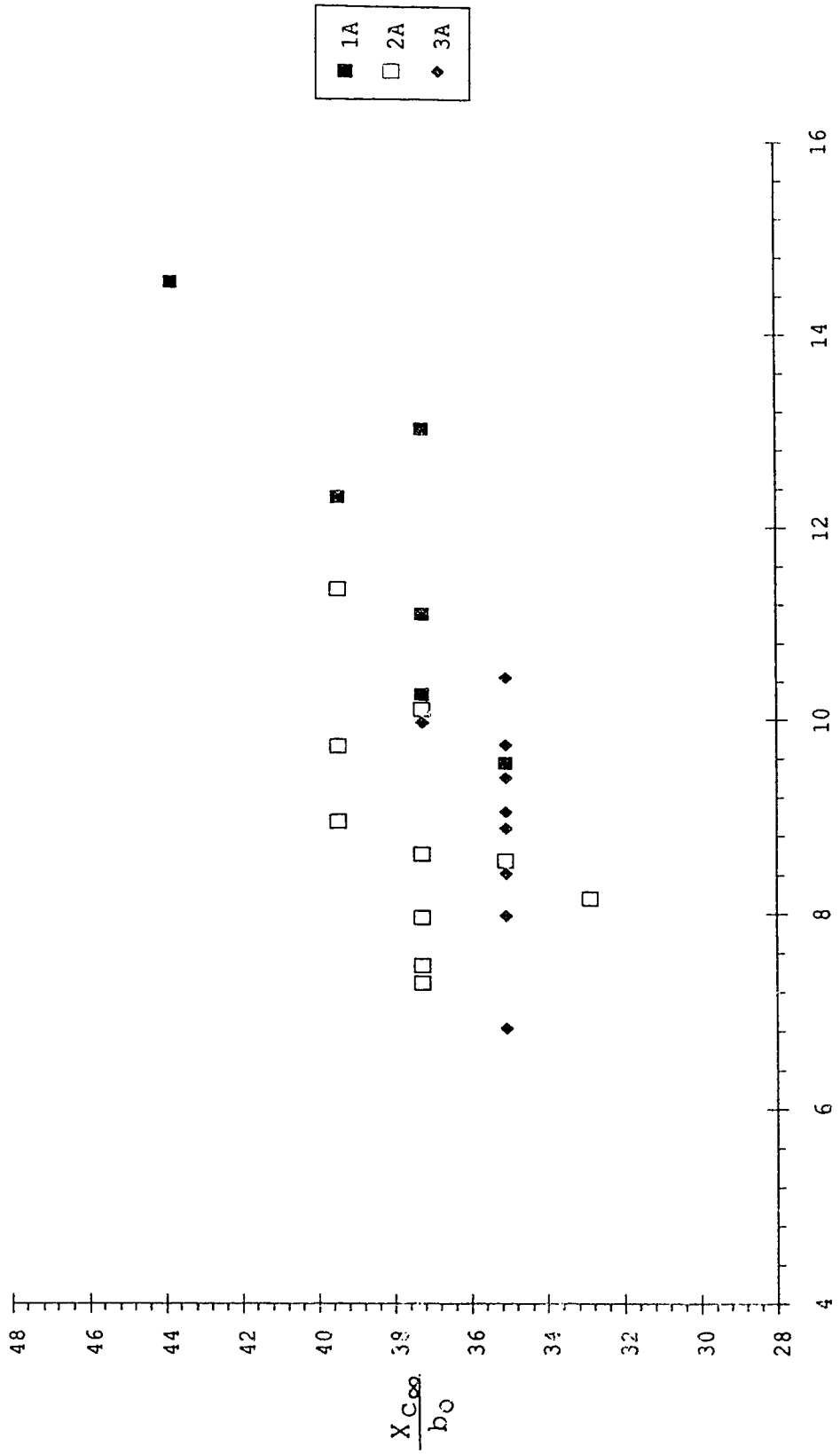

Figure 26 Screen A: Variation of Ridge Location with Fo

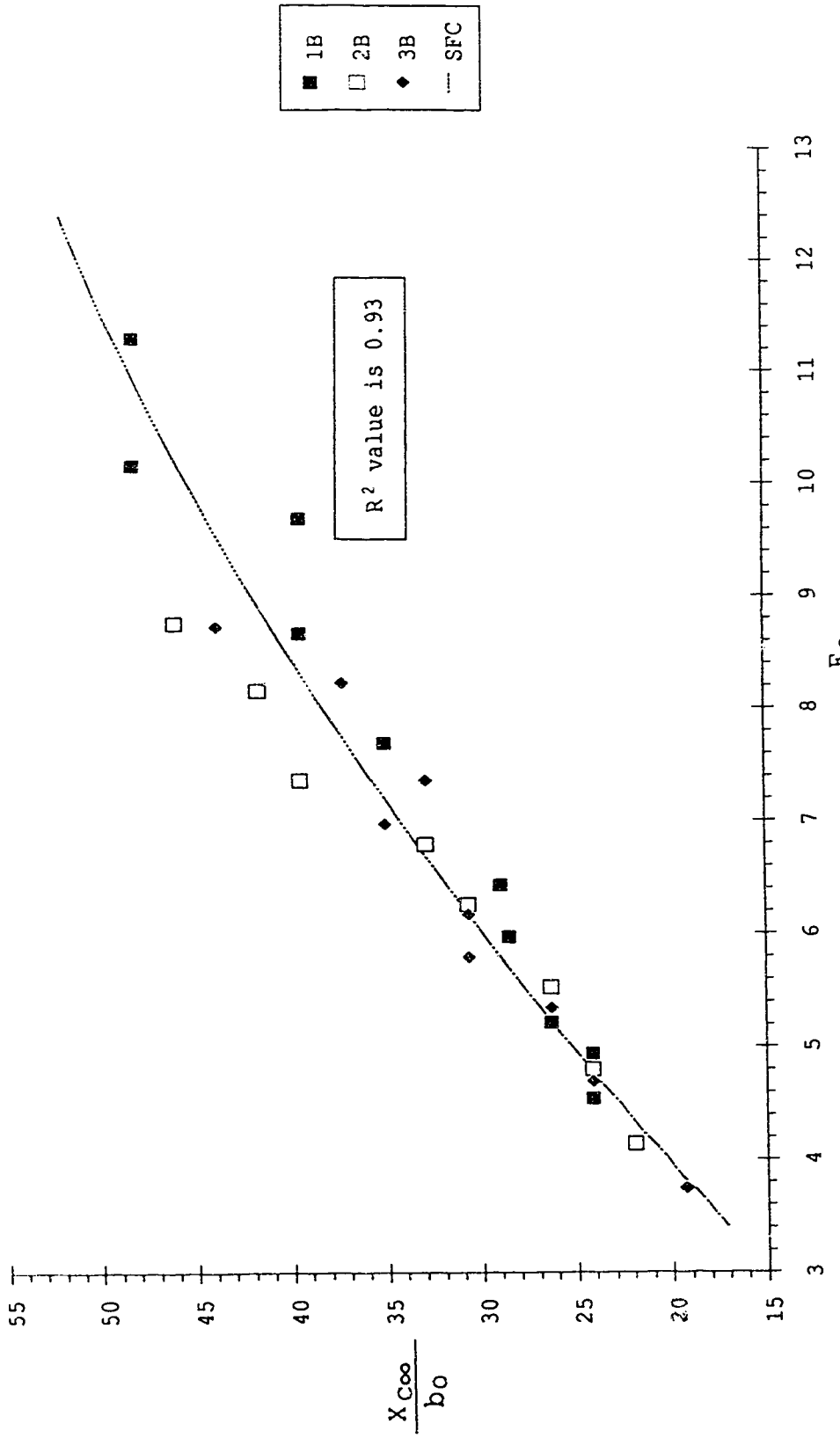

Figure 27 Screen B: Variation of Ridge Location with Fo

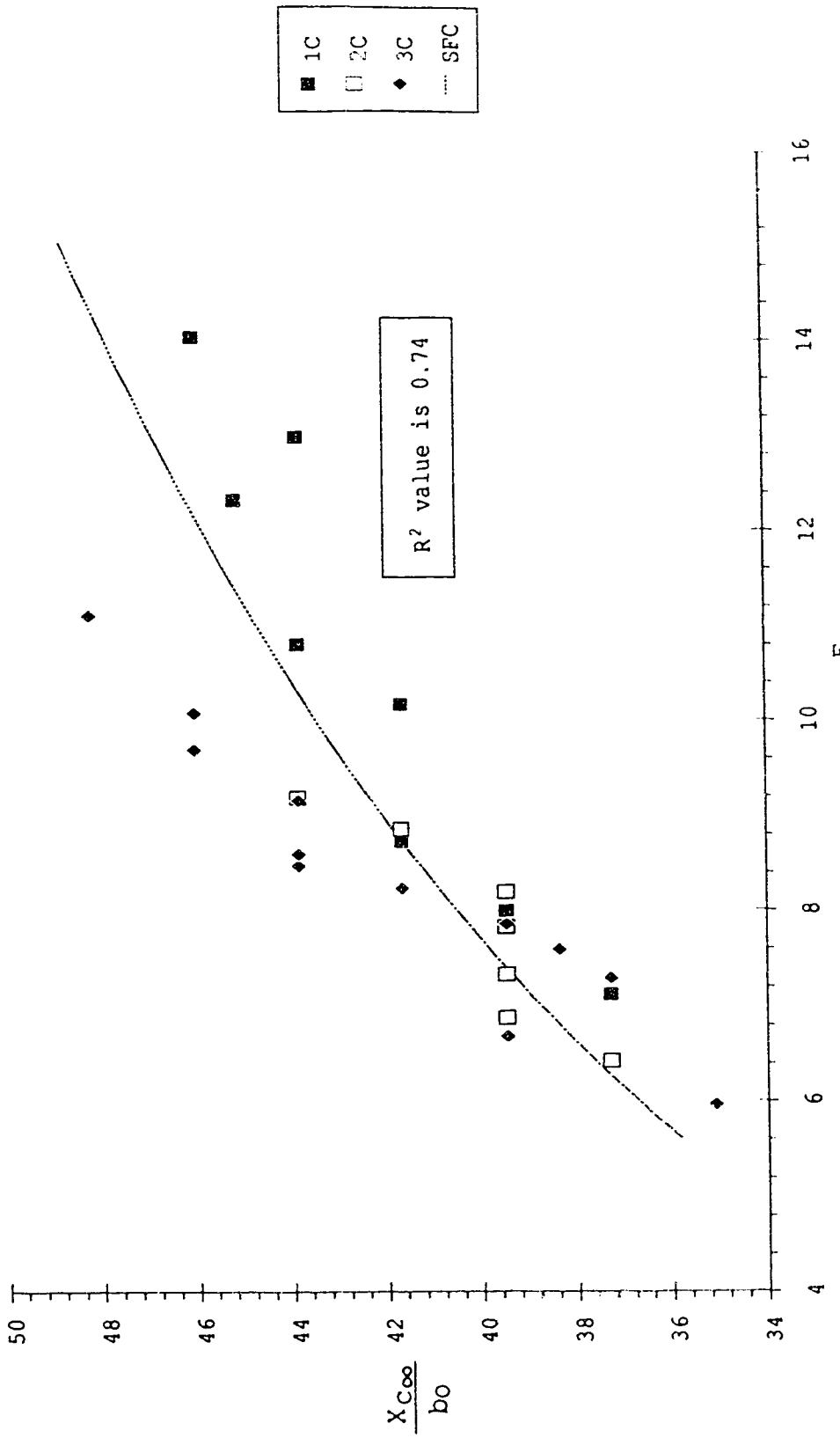

Figure 28 Screen C: Variation of Ridge Location with Fo

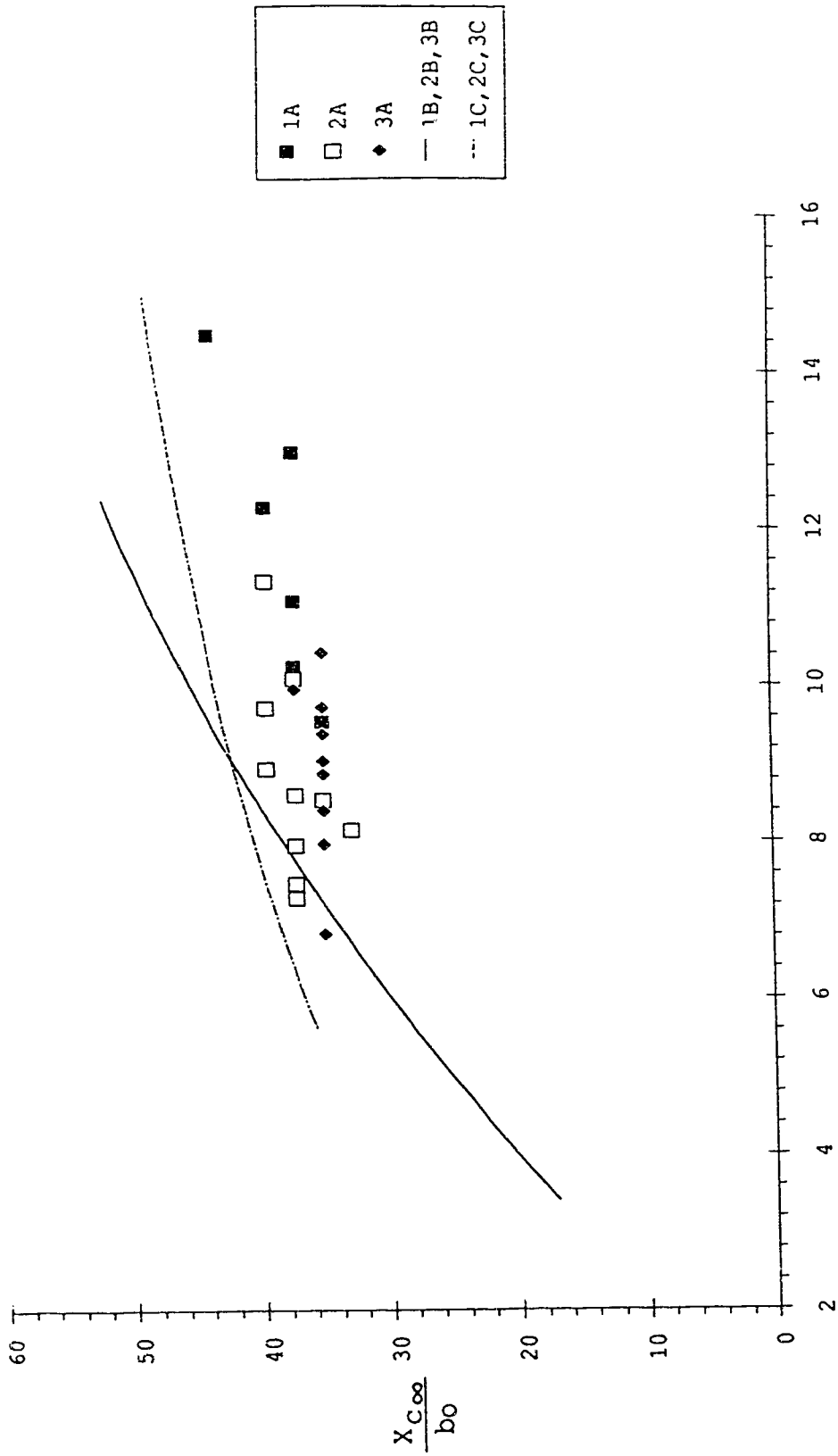

Figure 29 Variation of Ridge Location with Fo for all the Screens

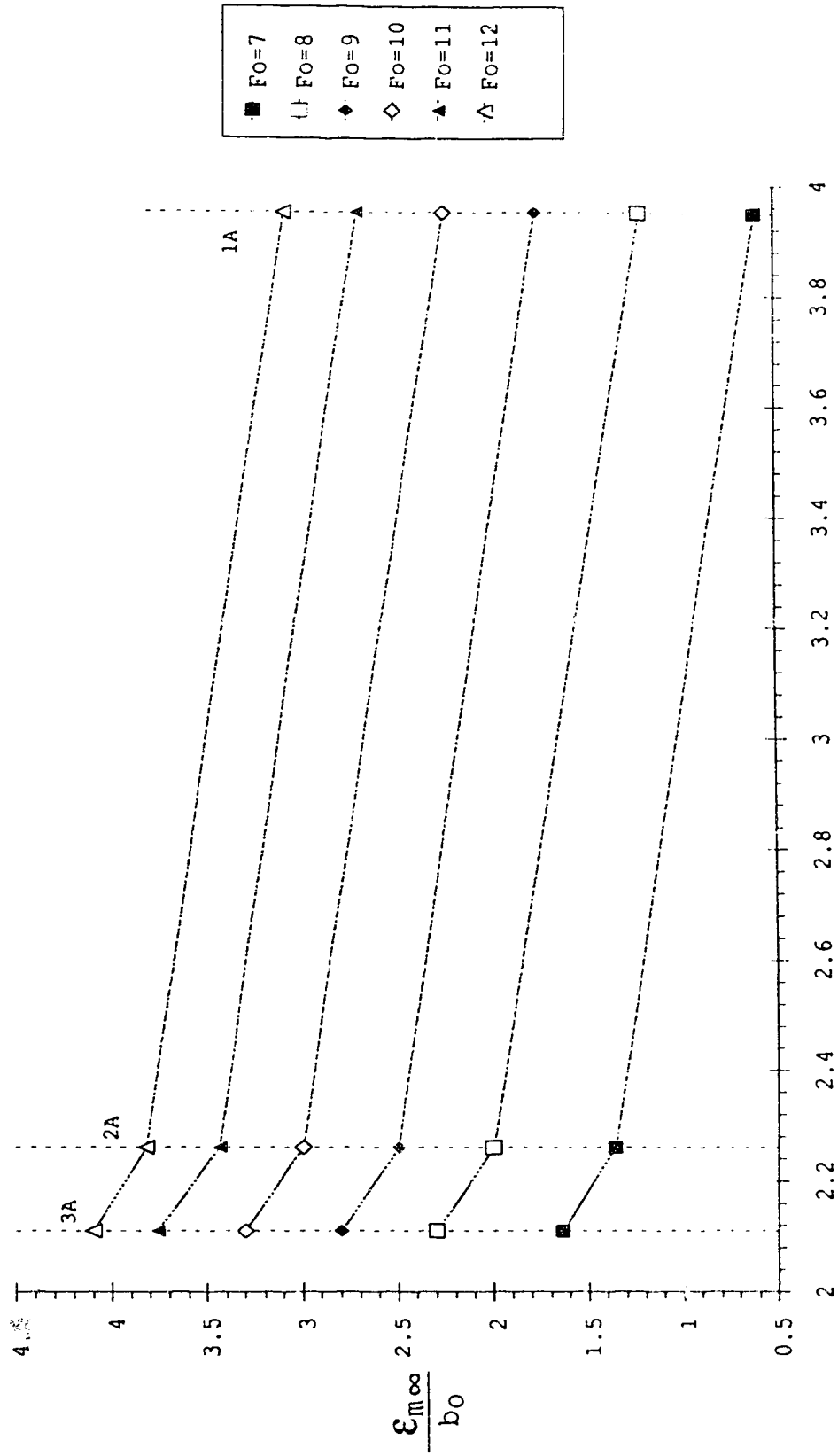

Figure 30 Screen A: Variation of Maximum Scour with Screen Size

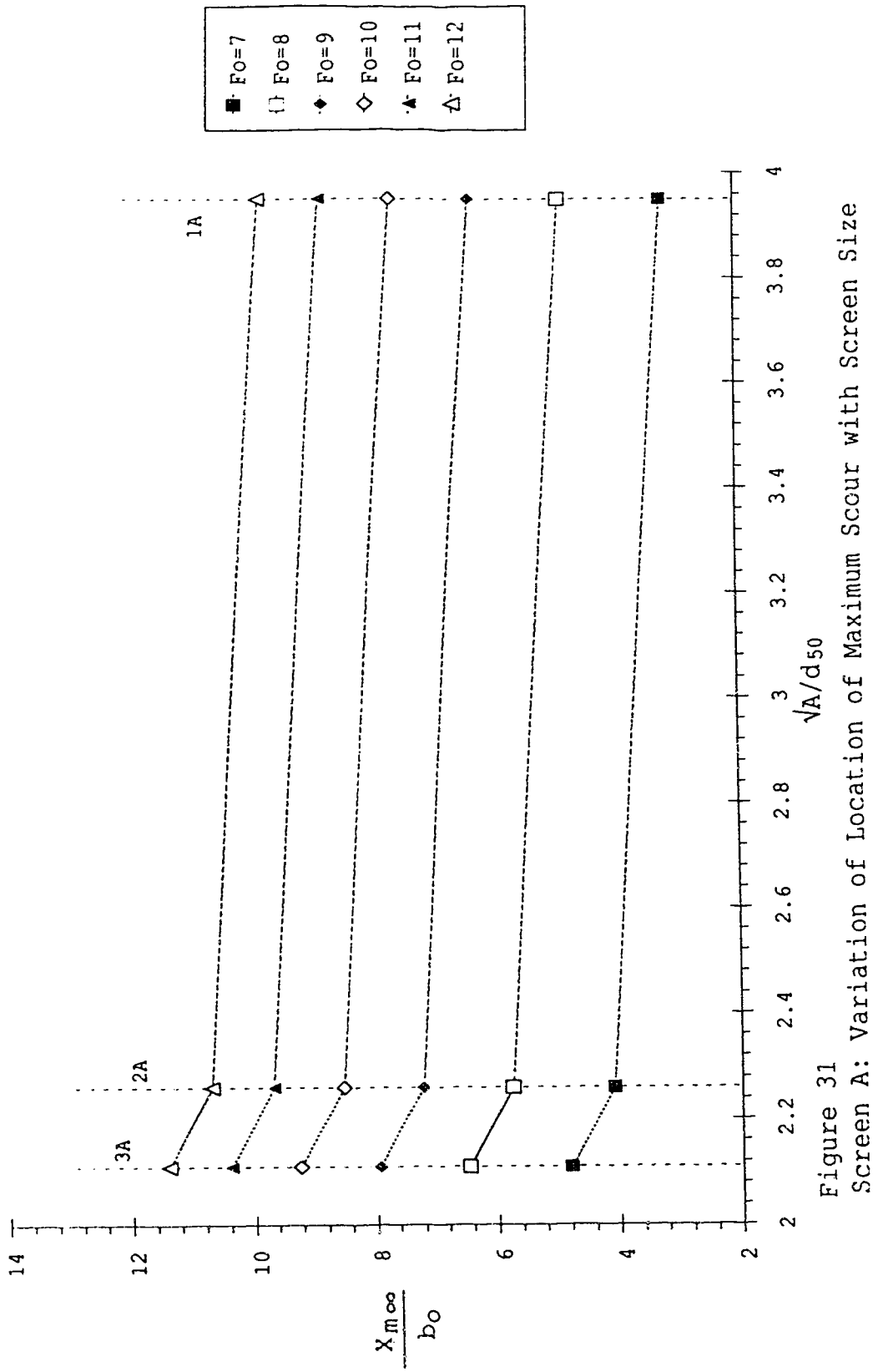

Figure 31
Screen A: Variation of Location of Maximum Scour with Screen Size

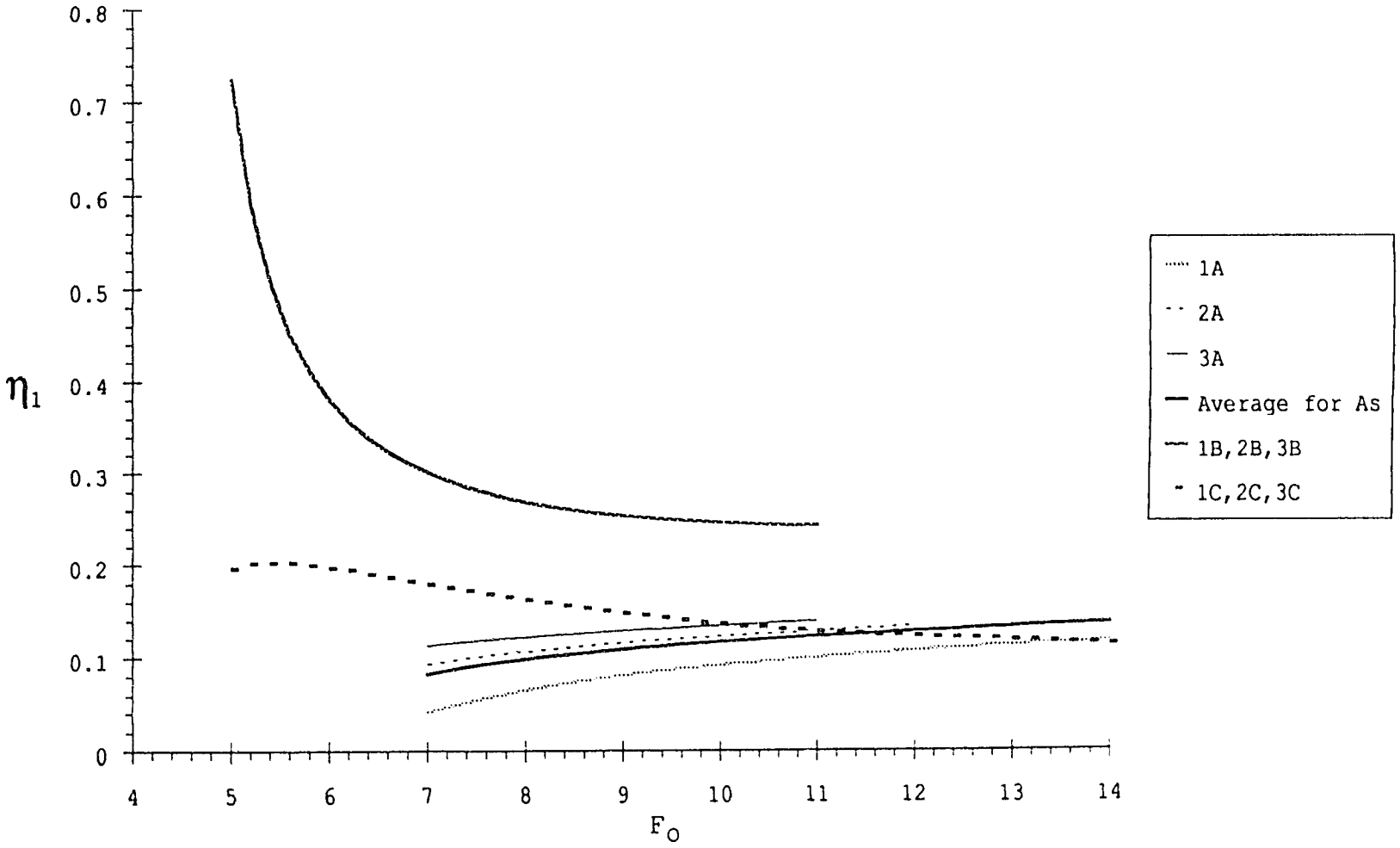

Figure 32 Variation of Maximum Scour Reduction Ratio with Fo

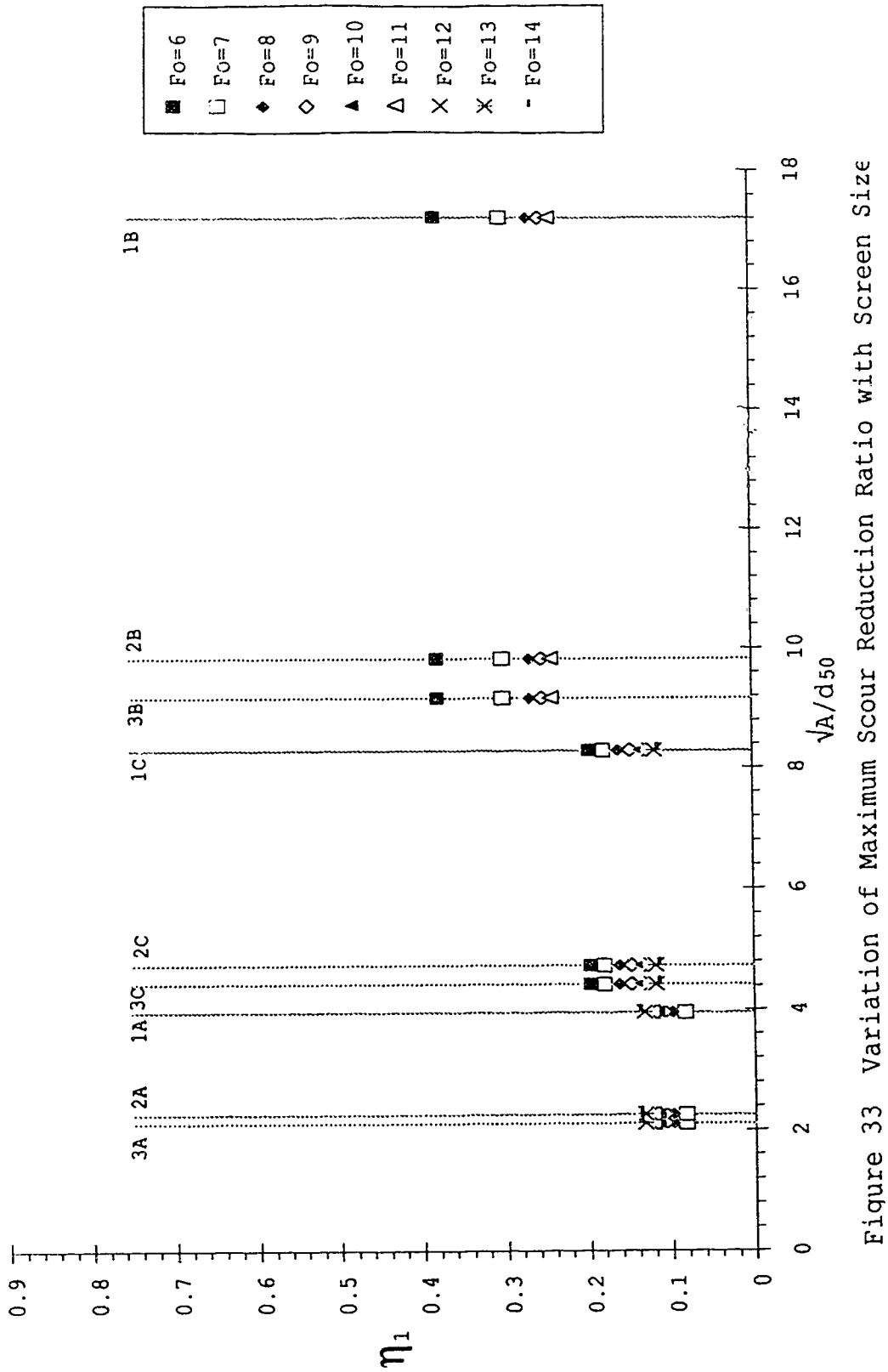

Figure 33 Variation of Maximum Scour Reduction Ratio with Screen Size

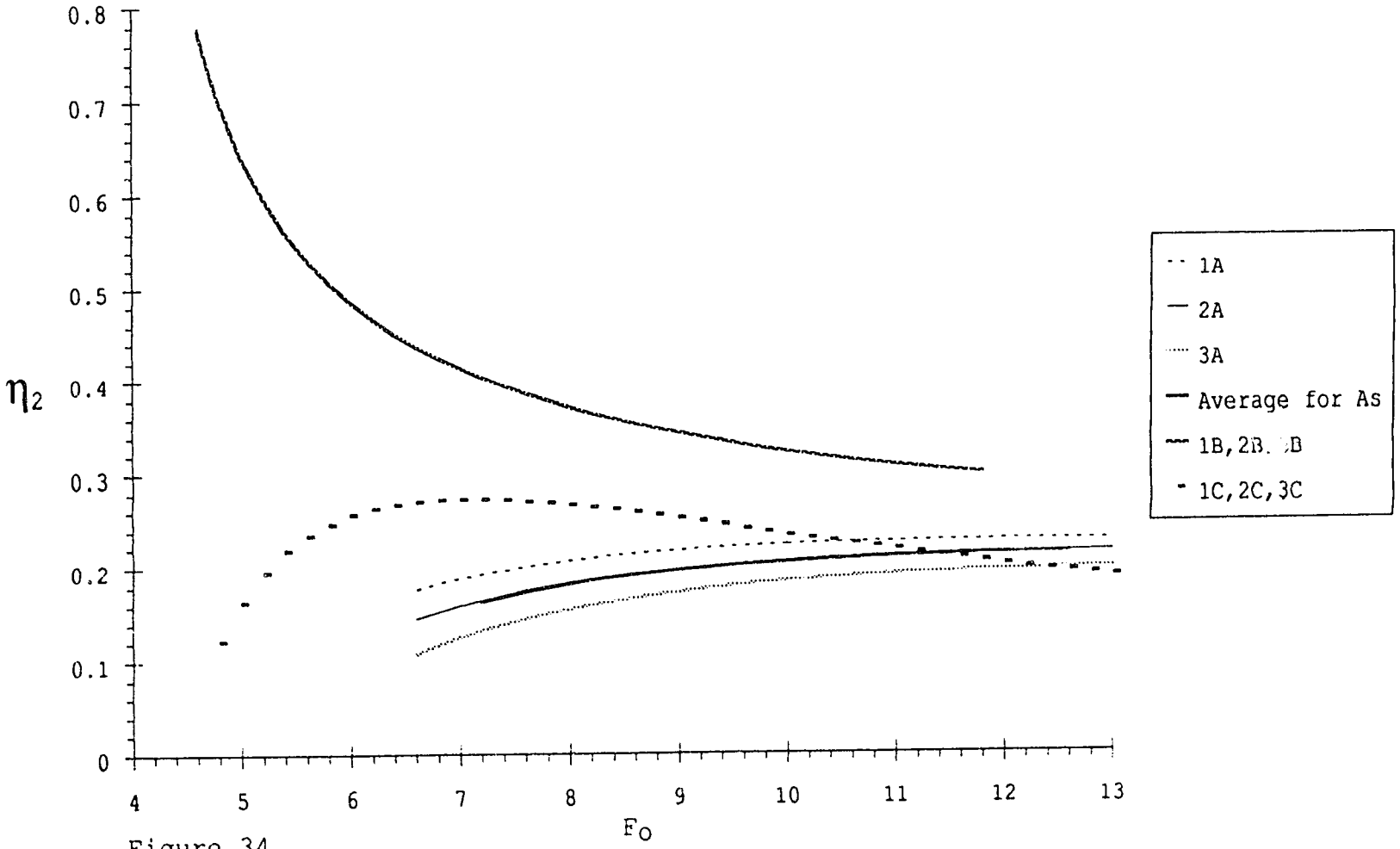

Figure 34
Variation of Reduction Ratio for Maximum Scour Location with Fo

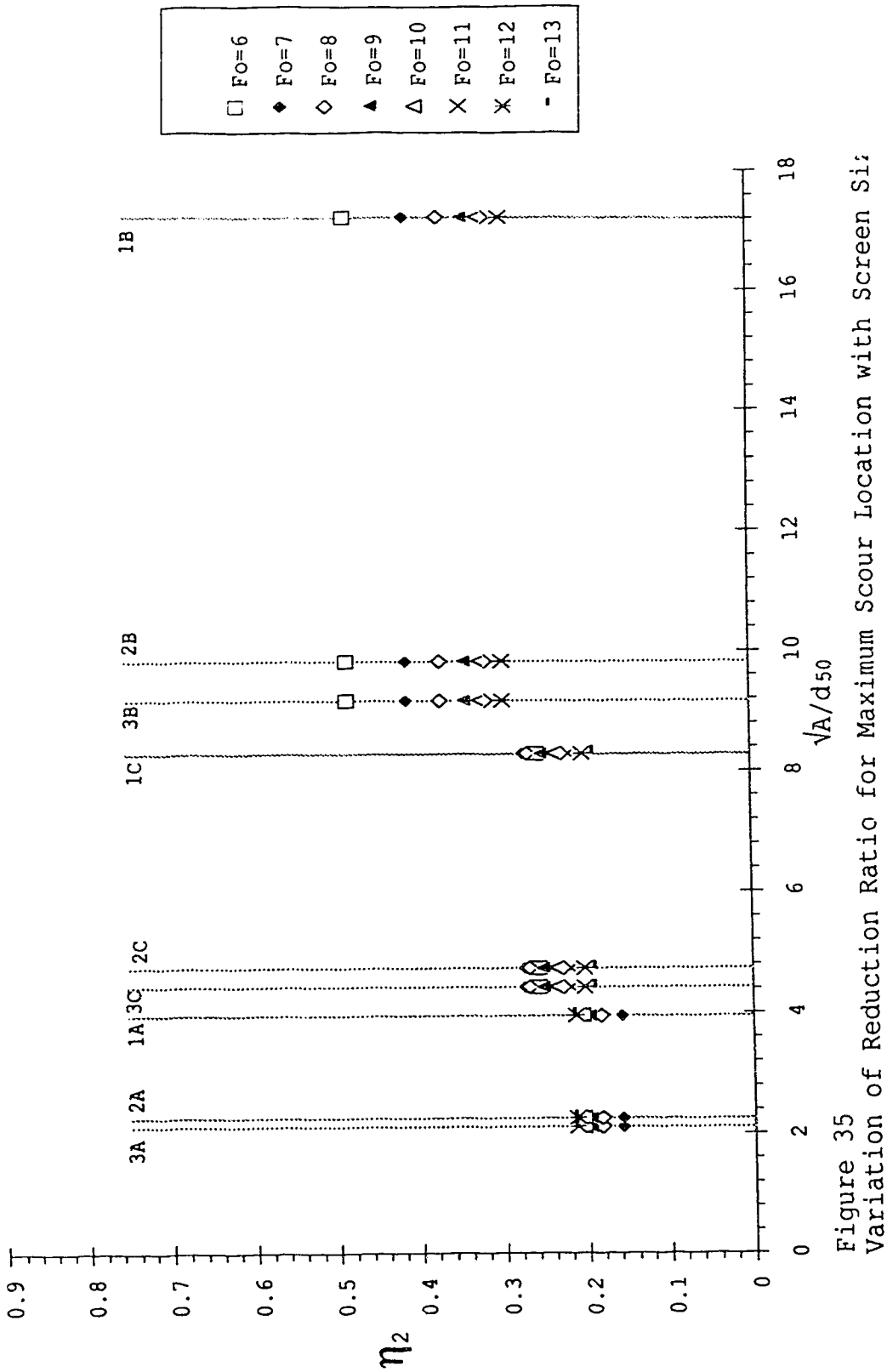

Figure 35
Variation of Reduction Ratio for Maximum Scour Location with Screen Si

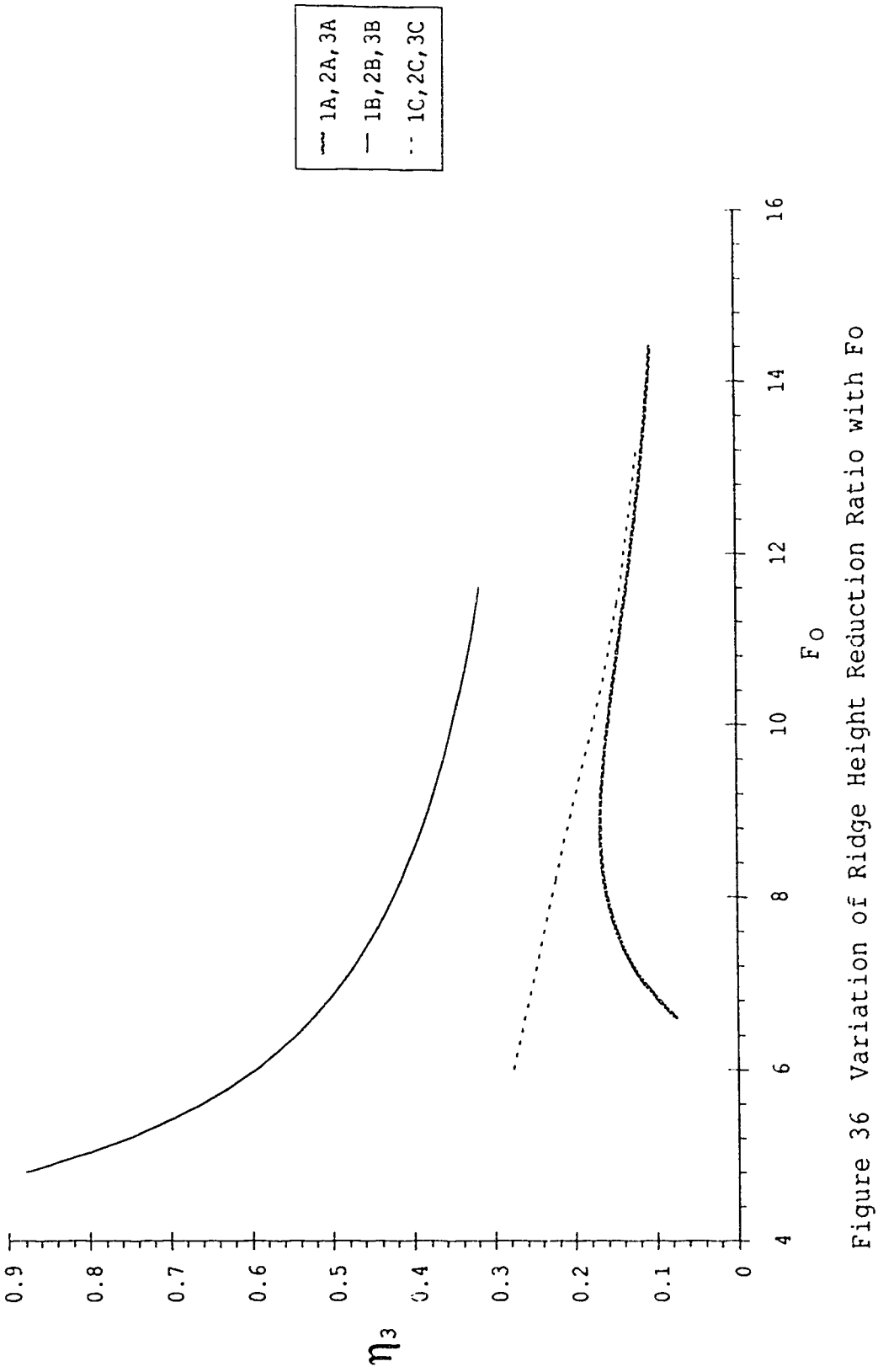

Figure 36 Variation of Ridge Height Reduction Ratio with Fo

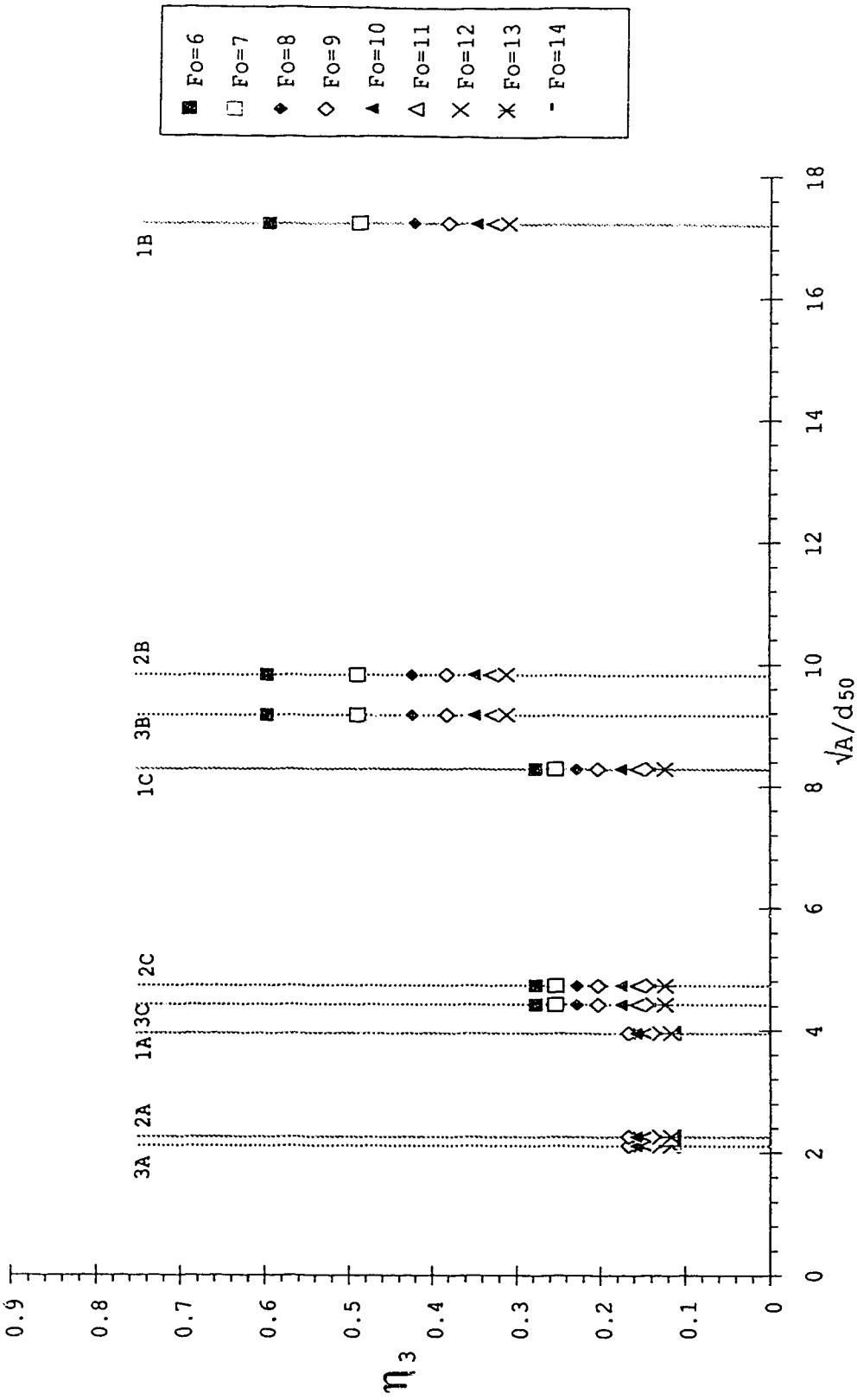

Figure 37 Variation of Ridge Height Reduction Ratio with Screen Size

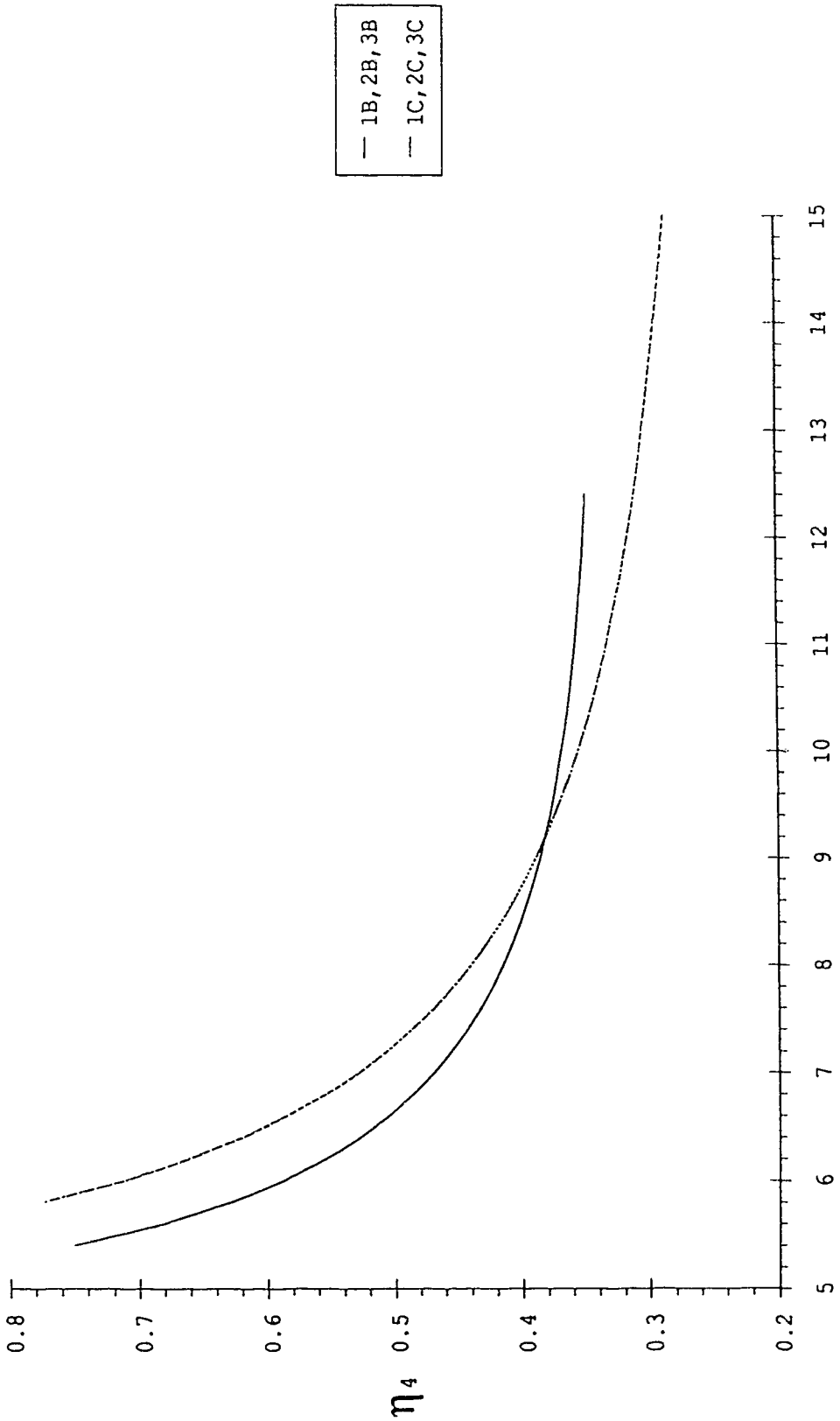

Figure 38 Variation of Reduction Ratio for Ridge Location with F(

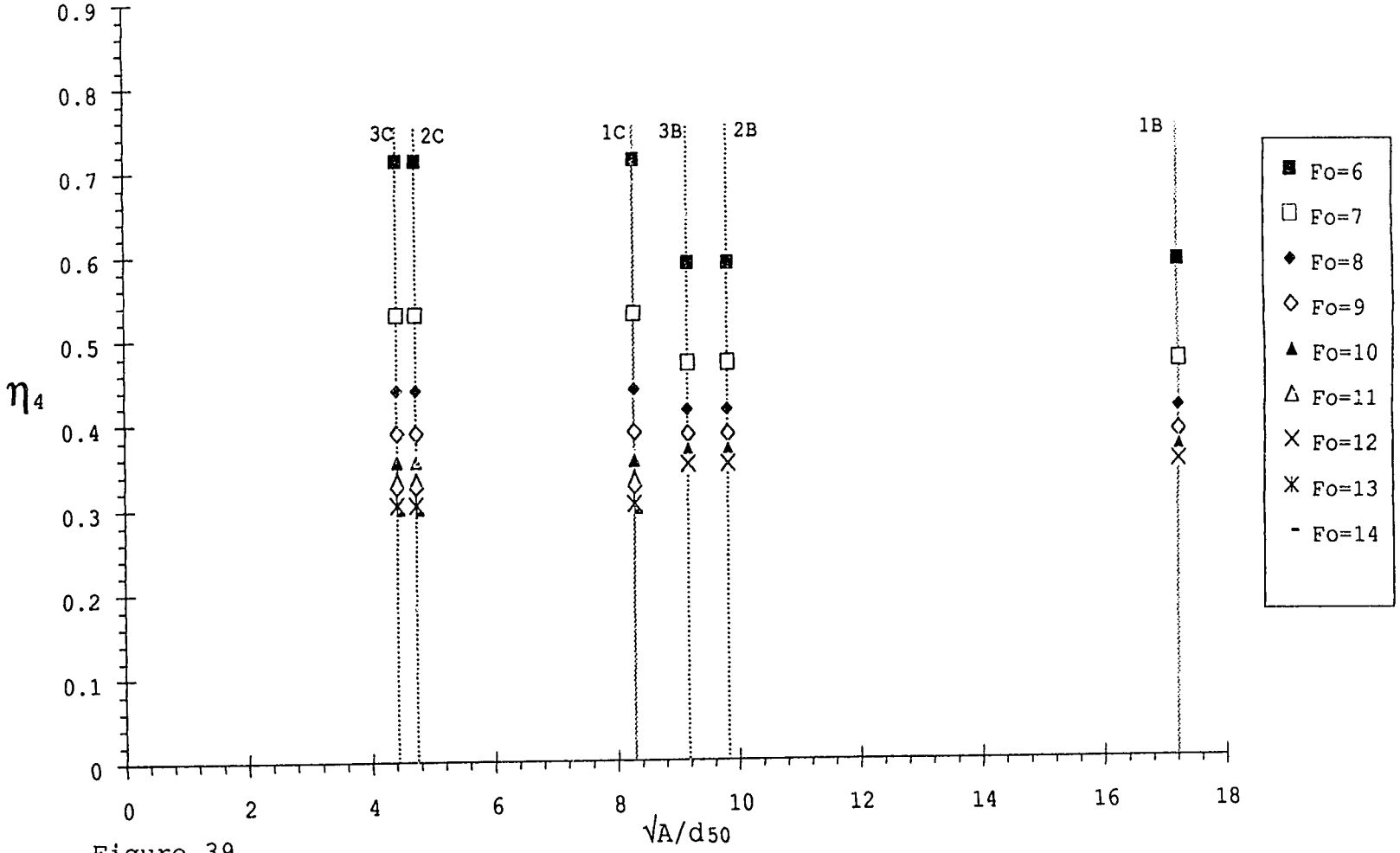

Figure 39
Variation of Reduction Ratio for Ridge Location with Screen Size

4. CONCLUSIONS AND RECOMMENDATIONS

4.1 Conclusions

This study is a purely experimental investigation to look at the use of screens to reduce scour caused by plane turbulent submerged wall jets. Three sizes of sand and three screens of different design were used, that is, nine combinations of sand and screen. With the help of dimensional analysis, the experimental results provided the necessary information to analyze the characteristic lengths of the scoured bed. Similarity of erosion profiles was checked and reduction ratios for quantifying the reductions in the characteristic lengths of the eroded bed profile were defined and evaluated. The following conclusions could be drawn based on the small number of combinations tried.

As noticed by some previous investigators, the eroded bed profile changed with time and eventually attained an asymptotic state. It was quite noticeable in one of the preliminary experiments that a significant reduction in maximum scour can be achieved when the bed is protected with a screen.

The screen design parameter, ϕ, which is difficult to quantify, was found to be a very important factor in

determining the eroded bed profile. Screen C is a very good example for this. Fairly good similarity of erosion profiles was found for each screen using maximum depth of erosion, $\varepsilon_{m\infty}$, and distance of scour hole end from the gate, X_o, as the length scales. Best results were obtained from Screen B. Comparing the best fit profiles from the screens' results indicates some differences and difference in screen design is responsible for this.

Variation of characteristic lengths of the scoured bed in terms of gate opening with densimetric particle Froude number, F_o, were studied and each screen produced a different relationship. Results from Screens B and C were independent of dimensionless screen hole size, α, but this was not the case for the results from Screen A when characteristic lengths $\varepsilon_{m\infty}$ and $x_{m\infty}$ were studied. It is presumed at this stage that for each screen, there is a range of α values within which all the results are independent of α, that is, all results are represented by a curve and outside this range as α tends to lower values, the results become dependent and every α value has to be represented by a curve. More experiments will have to be performed to check this.

Parameters for quantifying the reductions in the characteristic lengths of the eroded bed profile due to the use of a protective screen were defined and referred to as scour reduction ratios. Their relationships with densimetric

particle Froude number, F_o, and dimensionless screen size, α, were studied. It was found that at high F_o values, these ratios tend towards asymptotic values and their relationships with dimensionless screen size show less dependency on F_o as F_o increases.

4.2 Recommendations

In this study, it was not possible to bring all the screens' results togetner because the screens had different designs. Evaluation of the screen design parameter, ϕ, which is difficult to evaluate at this stage, could be what is needed to bring all the screens' results together. Before this can be evaluated, it is recommended that further study should be carried out with a particular screen design but different screen hole sizes so that its behavior can be well understood for a wide range of α values. This can be done for other screens and evaluating ϕ can then be attempted.

This study can be extended to screen protection for scour due to impinging jets. Shallow tail water conditions can also be investigated.

REFERENCES

Ali, H.M. and Lim, Y., "Local Scour caused by Submerged Wall Jet," Journal of Institution of Civil Engineers, Part 2, Vol. 81, December 1986.

Ali Uyumaz, "Scour Downstream of Vertical Gate," Journal of Hydraulic Engineering, Vol. 114, No. 7, July, 1988.

Arumugam, K. and Mason, J.P., "Free Jet Scour below Dams and Flip Buckets," Journal of Hydraulic Engineering, Vol.111, No. 2, February, 1985.

Chatterjee, S.S. and Ghosh, S.N., "Submerged Horizontal Jet over Erodible Bed," Journal of Hydraulics Division, ASCE, Vol. 106, No. HY11, November, 1980.

Doddiah, D., Albertson, M., and Thomas, R., "Scour from Jets ," Proceedings Minnesota International Hydraulics Convention, Minneapolis, 1953, pp 161-169.

Farhoudi, J. and Smith, K.V.H., "Local Scour Profiles Downstream of Hydraulic Jump," Journal of Hydraulic Research, Vol.23, No. 4, 1985.

Johnston, A.J. and Halliwell, A.R., "Jet Behavior in Shallow

Receiving Water," Journal of Institution of Civil Engineers, Part 2, Vol. 81, December 1986.

Johnston, A.J., "Scour hole Developments in Shallow Tailwater," Journal of Hydraulic Research, Vol. 28, No. 3, 1990.

Laursen, E.M., "Observations on the Nature of Scour," Proceedings of Fifth Hydraulic Conference, Bulletin 34, University of Iowa, Iowa City, Iowa, 1952, pp 179-197.

Narayanan, R. and Nik Hassan, N.M.K., "Local Scour Downstream of an Apron," Journal of Hydraulic Engineering, Vol 111, No. 11, November 1985.

Rajaratnam, N., "Flow below a Submerged Sluice Gate as a Wall Jet Problem," Proceedings, Second Australasian Conference on Hydraulics and Fluid Mechanics, Auckland, New Zealand, December 1965, pp. B131 - 136.

Rajaratnam, N., "Erosion by Plane Turbulent Jets," Journal of Hydraulic Research, Vol. 19, No. 4, 1981.

Rajaratnam, N., "Erosion by Unsubmerged Plane Water Jets," Proceedings of the Conference Applying Research to

Hydraulic Practice ASCE, Jackson, Mississippi, August 17-20, 1982.

Rajaratnam, N. and Macdougall, R.K., "Erosion of Sand Beds by Plane Turbulent Water Jets with Minimum Tailwater," Journal of Hydraulics Division, ASCE, Vol. 109, No. HY7, 1983.

Rajaratnam, N., "Turbulent Jets," Developments in Water Science 5, Elvesier Scientific Publishing Company, Amsterdam, Holland, 1976.

Raudkivi, A.J., "Loose Boundary Hydraulics," 3rd Edition, Pergamon Press, 1990.

Rossinskki, K.I., "Hydraulics of Scouring Pits," Problems of river runoff control. Academy of Science of the U.S.S.R., Moscow, 1961, chapter 2.

Rouse, H., "Criteria for Similarity in the Transportation of Sediment," Proceedings of the 1st Hydraulic Conference, Bulletin 20, State University of Iowa, Iowa City, Iowa, 1940, pp 33-49.

Tarapore, Z.S., "Scour Below a Submerged Sluice Gate," Thesis presented to the University of Minnesota, at Minneapolis, Minnesota, in 1956, in partial

fulfillment of the requirements for the degree of Master of Science.

Vanoni, V.A. (Editor), "Sedimentation Engineering," ASCE - Manuals and Reports on Engineering Practice - No. 54, 1975.

APPENDIX A
Summary of Experiments

TABLE A-1: FLOW MEASUREMENTS

Gate Opening = 22.8 mm

No	Date	Expt. #	Time (hrs)	Delta H (m)	Uo (m/s)	Fo	TW/bo
1	27-Dec	1A1	12	0.224	2.1	14.53	16.54
2	28-Dec	1A2	14.5	0.18	1.88	13.01	16.23
3	29-Dec	1A3	16.5	0.112	1.48	10.24	15.79
4	29-Dec	1A4	9	0.161	1.78	12.32	16.1
5	30-Dec	1A5	12.5	0.131	1.6	11.07	15.92
6	3-Jan	1A6	10.5	0.051	1	6.92	15.09
7	3-Jan	1A7	10.5	0.079	1.24	8.58	15.53
8	4-Jan	1A8	14	0.061	1.09	7.54	15.26
9	28-Jan	1A9	12	0.097	1.38	9.55	15.7
10	20-Nov	1B1	10	0.044	0.93	6.43	15.26
11	19-Dec	1B2	10	0.08	1.25	8.65	15.7
12	21-Dec	1B3	10	0.022	0.66	4.57	14.61
13	22-Dec	1B4	10	0.038	0.86	5.95	15
14	23-Dec	1B5	10	0.063	1.11	7.68	15.44
15	24-Dec	1B6	12	0.1	1.4	9.69	15.53
16	27-Dec	1B7	15	0.136	1.63	11.28	15.79
17	20-Jan	1B8	15	0.029	0.75	5.19	14.82
18	21-Jan	1B9	14	0.026	0.71	4.91	14.69
19	27-Jan	1B10	22	0.11	1.47	10.17	15.79
20	11-Jan	1C5	14	0.124	1.56	10.79	15.83
21	12-Jan	1C6	10.5	0.068	1.16	8.03	15.39
22	13-Jan	1C7	11	0.161	1.78	12.32	16.18
23	14-Jan	1C8	11	0.081	1.26	8.72	15.66
24	15-Jan	1C9	10.5	0.057	1.06	7.33	15.31
25	16-Jan	1C10	11	0.033	0.8	5.54	14.96
26	17-Jan	1C11	10.75	0.11	1.47	10.17	15.79
27	18-Jan	1C12	14.5	0.179	1.87	12.94	16.27
28	22-Jan	1C13	14	0.209	2.02	13.98	16.45
29	24-Jan	1C14	10.5	0.054	1.03	7.13	15.22
30	24-Jan	1C15	15	0.044	0.93	6.43	15.09

No	Date	Expt. #	Time (hrs)	Delta H (m)	Uo (m/s)	Fo	TW/bo
31	25-Jan	1C16	16.5	0.215	2.05	14.18	16.49
32	26-Jan	1C17	12	0.027	0.73	5.05	14.74
33	30-Jan	2B1	12	0.032	0.79	4.13	14.87
34	31-Jan	2B2	12	0.025	0.7	3.66	14.74
35	31-Jan	2B3	10	0.057	1.06	5.54	15.31
36	1-Feb	2B4	13	0.086	1.3	6.80	15.57
37	2-Feb	2B5	12.5	0.043	0.92	4.81	15.04
38	2-Feb	2B6	13.5	0.124	1.56	8.16	15.92
39	3-Feb	2B7	14.5	0.143	1.68	8.79	16.05
40	4-Feb	2B8	14	0.101	1.41	7.37	15.7
41	5-Feb	2B9	12	0.073	1.2	6.28	15.48
42	6-Feb	2A1	15	0.124	1.56	8.16	15.92
43	7-Feb	2A2	11	0.165	1.8	9.41	16.18
44	8-Feb	2A3	12	0.136	1.63	8.52	15.92
45	9-Feb	2A4	12	0.104	1.43	7.48	15.66
46	9-Feb	2A5	12.5	0.087	1.31	6.85	15.53
47	10-Feb	2A6	15	0.138	1.65	8.63	15.92
48	11-Feb	2A7	14	0.176	1.86	9.73	16.18
49	14-Feb	2A8	13.5	0.24	2.17	11.35	16.54
50	15-Feb	2A9	12	0.15	1.71	8.94	16.05
51	16-Feb	2A10	14	0.19	1.93	10.09	16.32
52	16-Feb	2A11	14	0.12	1.52	7.95	15.83
53	17-Feb	2A12	14	0.10	1.39	7.27	15.66
54	18-Feb	2C1	13	0.16	1.76	9.20	16.14
55	19-Feb	2C2	13.5	0.077	1.23	6.43	15.44
56	19-Feb	2C3	11	0.065	1.13	5.91	15.39
57	20-Feb	2C4	12.5	0.052	1.01	5.28	15.18
58	21-Feb	2C5	12	0.146	1.69	8.84	15.96
59	22-Feb	2C6	13	0.1	1.4	7.32	15.7
60	23-Feb	2C7	14	0.171	1.83	9.57	16.23
61	24-Feb	2C8	12	0.088	1.31	6.85	15.53
62	25-Feb	2C9	12	0.114	1.5	7.84	15.79
63	26-Feb	2C10	11	0.125	1.57	8.21	15.83
64	27-Feb	3B1	14	0.057	1.06	5.36	15.22

No	Date	Expt. #	Time (hrs)	Delta H (m)	Uo (m/s)	Fo	TW/bo
65	28-Feb	3B2	14	0.044	0.93	4.70	15
66	1-Mar	3B3	12	0.028	0.74	3.74	14.74
67	2-Mar	3B4	13	0.076	1.22	6.17	15.44
68	3-Mar	3B5	12	0.097	1.38	6.98	15.66
69	3-Mar	3B6	13.5	0.022	0.66	3.34	14.61
70	4-Mar	3B7	14	0.067	1.15	5.81	15.39
71	5-Mar	3B8	12	0.108	1.46	7.38	15.79
72	6-Mar	3B9	12	0.135	1.63	8.24	15.92
73	7-Mar	3B10	15	0.152	1.73	8.75	16.14
74	8-Mar	3A1	16	0.093	1.35	6.83	15.61
75	9-Mar	3A2	12	0.141	1.66	8.39	16.01
76	10-Mar	3A3	12	0.109	1.46	7.38	15.83
77	11-Mar	3A4	11	0.217	2.06	10.41	16.27
78	12-Mar	3A5	14	0.163	1.79	9.05	16.05
79	13-Mar	3A6	14	0.198	1.97	9.96	16.23
80	14-Mar	3A7	12	0.189	1.93	9.76	16.18
81	15-Mar	3A8	12	0.176	1.86	9.40	16.1
82	16-Mar	3A9	14	0.127	1.58	7.99	15.79
83	17-Mar	3A10	13	0.157	1.76	8.90	16.01
84	18-Mar	3C1	14	0.071	1.18	5.97	15.26
85	19-Mar	3C2	14	0.187	1.92	9.71	16.1
86	20-Mar	3C3	14.5	0.106	1.44	7.28	15.61
87	21-Mar	3C4	12	0.167	1.81	9.15	16.05
88	22-Mar	3C5	12	0.123	1.55	7.84	15.75
89	23-Mar	3C6	13	0.143	1.678	8.48	15.92
90	24-Mar	3C7	13.5	0.147	1.7	8.59	16.18
91	29-Mar	3C8	12	0.089	1.32	6.67	15.48
92	30-Mar	3C9	12	0.202	1.99	10.06	16.36
93	30-Mar	3C10	12	0.245	2.19	11.07	16.54
94	31-Mar	3C11	12	0.135	1.63	8.24	15.88
95	31-Mar	3C12	12	0.115	1.5	7.58	15.7

TABLE A-2: SCOURED BED MEASUREMENTS

Gate Opening = 22.8 mm

No	Expt. #	Fo	Max. Scour (m)	Xm (m)	Δε (m)	Xc (m)	Xo (m)	Remarks
1	1A1	14.53	.085	0.28	.073	1	0.53	GSPR
2	1A2	13.01	.076	0.24	.063	0.88	0.47	GSPR
3	1A3	10.24	.060	0.22	.059	0.86	0.50	GSPR
4	1A4	12.32	.072	0.24	.067	0.9	0.51	GSPR
5	1A5	11.07	.064	0.24	.060	0.85	0.46	GSPR
6	1A6	6.92	.016	0.1	.015	0.95	0.51	PSPR
7	1A7*	8.58	.031	0.12	.037	0.85	0.46	PSPR
8	1A8*	7.54	.019	0.1	.029	0.9	0.50	PSPR
9	1A9	9.55	.045	0.14	.054	0.82	0.40	GSPR
10	1B1	6.43	.076	0.18	.098	0.66	0.42	GSGR
11	1B2	8.65	.110	0.26	.132	0.88	0.55	GSGR
12	1B3	4.57	.056	0.16	.070	0.52	0.33	GSGR
13	1B4	5.95	.083	0.22	.112	0.66	0.43	GSGR
14	1B5	7.68	.106	0.24	.106	0.8	0.50	GSGR
15	1B6	9.69	.114	0.28	.117	0.91	0.56	GSFR
16	1B7	11.28	.145	0.3	.157	1.1	0.67	GSGR
17	1B8	5.19	.070	0.18	.093	0.59	0.37	GSGR
18	1B9	4.91	.068	0.2	.099	0.57	0.36	GSGR
19	1B10	10.17	.140	0.3	.144	1.1	0.64	GSFR
20	1C5	10.79	.081	0.2	.071	1.03	0.60	GSPR
21	1C6	8.03	.065	0.18	.071	0.9	0.52	GSPR
22	1C7	12.32	.082	0.22	.067	1.03	0.58	GSPR
23	1C8	8.72	.072	0.2	.070	0.93	0.55	GSPR
24	1C9	7.33	.062	0.16	.066	0.88	0.55	GSFR
25	1C10*	5.54	.040	0.1	.038	0.85	0.41	GSPR
26	1C11	10.17	.072	0.2	.071	0.97	0.55	GSPR
27	1C12	12.94	.083	0.22	.070	1	0.58	GSPR
28	1C13	13.98	.079	0.2	.059	1.05	0.60	GSPR
29	1C14	7.13	.045	0.12	.055	0.85	0.48	GSPR
30	1C15	6.43	.043	0.12	.050	0.83	0.44	GSPR

No	Expt. #	Fo	Max. Scour (m)	Xm (m)	Δε (m)	Xc (m)	Xo (m)	Remarks
31	1C16*	14.18	.074	0.18	.061	1	0.58	GSPR
32	1C17	5.05	.020	0.04	.016	1	0.37	PSPR
33	2B1	4.13	.059	0.18	.087	0.5	0.32	GSGR
34	2B2*	3.66	.029	0.1	.013	0.6	0.21	FSPR
35	2B3	5.54	.078	0.22	.110	0.62	0.40	GSGR
36	2B4	6.80	.100	0.24	.117	0.77	0.47	GSGR
37	2B5	4.81	.074	0.2	.099	0.57	0.37	GSGR
38	2B6	8.1	.127	0.28	.137	0.96	0.59	GSGR
39	2B7	8.7	.145	0.32	.157	1.05	0.64	GSGR
40	2B8	7.37	.113	0.27	.131	0.9	0.54	GSGR
41	2B9	6.28	.088	0.22	.099	0.68	0.41	GSGR
42	2A1	8.16	.051	0.14	.048	0.77	0.39	PSPR
43	2A2*	9.41	.064	0.18	.054	0.85	0.45	GSFR
44	2A3	8.52	.055	0.16	.054	0.82	0.42	GSPR
45	2A4	7.48	.036	0.1	.032	0.85	0.38	GSPR
46	2A5*	6.85	.025	0.08	.020	0.85	0.39	PSPR
47	2A6	8.63	.051	0.14	.057	0.85	0.47	GSPR
48	2A7	9.73	.061	0.18	.068	0.9	0.46	GSPR
49	2A8	11.35	.077	0.22	.068	0.9	0.47	GSPR
50	2A9	8.94	.054	0.14	.059	0.9	0.46	GSPR
51	2A10	10.09	.072	0.22	.067	0.86	0.44	GSPR
52	2A11	7.95	.046	0.12	.042	0.85	0.45	GSPR
53	2A12	7.27	.035	0.1	.033	0.87	0.36	GSPR
54	2C1	9.20	.078	0.22	.076	1	0.56	GSPR
55	2C2	6.43	.048	0.14	.056	0.85	0.52	GSPR
56	2C3*	5.91	.048	0.12	.038	0.95	0.43	GSPR
57	2C4*	5.28	.022	0.06	.016	1.05	0.45	FSPR
58	2C5	8.84	.076	0.2	.076	0.97	0.53	GSFR
59	2C6	7.32	.059	0.16	.064	0.9	0.55	GSFR
60	2C7*	9.57	.070	0.21	.070	1	0.60	GSFR
61	2C8	6.85	.048	0.14	.058	0.9	0.57	GSFR
62	2C9	7.84	.073	0.18	.073	0.92	0.53	GSFR
63	2C10	8.21	.074	0.18	.072	0.92	0.54	GSFR
64	3B1	5.36	.076	0.2	.098	0.58	0.37	GSGR

No	Expt. #	Fo	Max. Scour (m)	Xm (m)	Δε (m)	Xc (m)	Xo (m)	Remarks
65	3B2	4.70	.075	0.2	.098	0.57	0.38	GSGR
66	3B3	3.74	.048	0.15	.068	0.44	0.27	GSGR
67	3B4	6.17	.084	0.22	.091	0.7	0.41	GSGR
68	3B5	6.98	.108	0.24	.120	0.82	0.50	GSGR
69	3B6*	3.34	.024	0.06	.010	0.55	0.18	GSPR
70	3B7	5.81	.091	0.22	.107	0.72	0.44	GSGR
71	3B8	7.38	.093	0.22	.086	0.77	0.45	GSGR
72	3B9	8.24	.111	0.24	.100	0.85	0.50	GSFR
73	3B10	8.75	.125	0.3	.125	1.01	0.58	GSGR
74	3A1	6.83	.036	0.1	.023	0.82	0.36	FSPR
75	3A2	8.39	.058	0.16	.052	0.81	0.45	GSPR
76	3A3*	7.38	.044	0.1	-	-	-	-
77	3A4	10.41	.075	0.22	.067	0.81	0.44	GSPR
78	3A5	9.05	.065	0.18	.057	0.8	0.45	GSPR
79	3A6	9.96	.074	0.22	.061	0.85	0.45	GSPR
80	3A7	9.76	.071	0.2	.060	0.8	0.45	GSPR
81	3A8	9.40	.069	0.2	.058	0.8	0.44	GSPR
82	3A9	7.99	.050	0.14	.049	0.82	0.43	GSPR
83	3A10	8.90	.074	0.18	.064	0.82	0.45	GSPR
84	3C1	5.97	.053	0.14	.048	0.8	0.50	GSPR
85	3C2	9.71	.077	0.26	.069	1.07	0.62	GSPR
86	3C3	7.28	.066	0.18	.062	0.85	0.55	GSPR
87	3C4	9.15	.073	0.22	.073	1	0.60	GSPR
88	3C5	7.84	.066	0.2	.064	0.9	0.54	GSPR
89	3C6	8.48	.075	0.22	.074	1	0.58	GSPR
90	3C7	8.59	.071	0.21	.066	1	0.57	GSPR
91	3C8	6.67	.056	0.14	.050	0.92	0.49	GSGR
92	3C9	10.06	.074	0.24	.066	1.08	0.60	GSFR
93	3C10	11.07	.074	0.24	.065	1.1	0.65	GSPR
94	3C11	8.24	.073	0.22	.066	0.97	0.58	GSPR
95	3C12	7.58	.069	0.18	.061	0.875	0.53	GSPR

* Scoured Bed Profile was Bad

APPENDIX B
Plates